2013

The Synthesis And Characterization Of 3-Nitro-2-Styrenyl Benzoic Acid Amide Derivatives As Potential Cancer Chemopreventives

Brittany Lynn Nichols
North Carolina Agricultural and Technical State University

The Synthesis and Characterization of 3-Nitro-2-Styrenyl Benzoic Acid Amide Derivatives as Potential Cancer Chemopreventives

Brittany Lynn Bass Nichols

North Carolina A&T State University

A thesis submitted to the graduate faculty

in partial fulfillment of the requirements for the degree of

MASTER OF SCIENCE

Department: Chemistry

Major: Chemistry

Major Professor: Marion A. Franks, PhD

Greensboro, North Carolina

2013

The Graduate School
North Carolina Agricultural and Technical State University
This is to certify that the Master's Thesis of

Brittany Lynn Bass Nichols

has met the thesis requirements of
North Carolina Agricultural and Technical State University

Greensboro, North Carolina
2013

Approved by:

Marion A. Franks, PhD Major Professor	Mufeed Basti, PhD Committee Member
Margaret Kanipes-Spinks, PhD Department Chair	Claude Lamb, PhD Committee Member

Dr. Sanjiv Sarin
Dean, The Graduate School

Biographical Sketch

Brittany Lynn Bass Nichols was born on December 1st, 1987 in Greensboro, NC. She is the daughter of Harold A. Nichols and Gaynelle E.B. Nichols. Brittany spent most of her childhood in the small rural town of Gibsonville, NC. She completed her undergraduate degree in chemistry at the University of North Carolina at Chapel Hill in the fall of 2010. She entered the North Carolina Agricultural & Technical State University master's in chemistry program in 2011. Her thesis research in the organic synthesis of nitrostyrenyl amides was conducted under Dr. Marion Franks. She plans to continue her study of chemistry in a doctorate program upon completion of her master's degree.

Dedication

This thesis is dedicated to my grandmother Bessie Mills Bass. It is also dedicated to my grandfathers William McDuffy Bass and Vangus Temason Nichols, who both lost their battles with cancer this past year. I appreciate the examples that these three people set for me and cherish the memories they left behind. They continue to inspire me daily and will forever be missed.

Acknowledgements

I would like to first acknowledge my advisor, Dr. Marion Franks. I will never be able to repay him or thank him enough for his all that he has taught me. I am so grateful to have had the opportunity to work with him and the training I received will undoubtedly benefit me for years to come. His dedication to helping students realize their goals is truly remarkable. My research group members (Davia McKoy, Rhashanda Haywood, Courtney Peace, Shaina Richardson, Jonathan Mosley, Jeramie Stamps, and Sharla Gadson) have also been a great help to me by providing encouragement and feedback whenever needed. I would like to acknowledge my committee members, Dr. Claude Lamb and Dr. Mufeed Basti for their time and patience in helping me put forth my best efforts. I would like to thank the chemistry department chair, Dr. Margaret Kanipes-Spinks for her encouragement. Mr. James King has also been essential in completing this work by training me on all of the instruments I needed to utilize. The faculty and staff of the North Carolina Agricultural & Technical State University have been amazing. I also thank my family and friends for their support during the completion of this master's program.

Table of Contents

List of Figures

List of Tables

Abstract

Chemopreventives are natural or synthetic compounds that are used to stop or reverse the processes of carcinogenesis or tumorigenesis. Resveratrol (3, 5, 4'-trihydroxy-trans-stilbene) is a stilbenoid and natural phenol that is found in fruits such as grapes. In addition to antioxidant and anti-inflammatory properties, resveratrol can inhibit D-type cyclins and cyclin-dependent kinase CDK4 expression. This can also lead to inducing tumor suppressors p53 and Cdk inhibitor p21. The p53 protein is encoded by the TP53 gene and responds to cellular stresses by regulating target genes that induce cell cycle arrest, apoptosis, and DNA repair among other functions. 3-nitro-2-styryl amide derivatives contain the stilbene structure similar to resveratrol and due to this similarity will be effective chemopreventives. We have synthesized five 3-nitrostyrylamides to be tested for their chemopreventive efficacy. These compounds were synthesized using a base catalyzed condensation reaction that utilized substituted benzaldehydes and methyl 2-methyl 3 nitrobenzoate to form 3-nitro-2-styrl benzoic acids to give percent yields of 35.1-90.2%. The conversion of the 3-nitro-2-styryl benzoic acids to acid chlorides was completed using an N, N-dimethylformamide catalyzed reaction with thionyl chloride. The acid chlorides were converted to amides using N-butylamine and sodium hydroxide to give percent yields of 15.9-87.7%. The synthesized amide compounds were characterized using ^{1}H NMR, ^{13}C NMR, FT-IR, and HPLC.

CHAPTER 1

Introduction

According to the American Cancer Society, a total of 1,660,290 new *cancer* cases and 580,350 deaths from *cancer* were projected to occur in the United States in 2013, for all invasive cancer sites. One in every four males in the US will die from cancer, while one in every five females will die from the disease (American Cancer Society, 2013). Given the negative impact of cancer on health, there is a need to find a method to prevent the disease. One approach to preventing cancer is to prevent the onset of cancer which is called carcinogenesis. Carcinogenesis is the mechanism by which normal cells are transformed into cancerous cells. These cells are identified by uncontrolled cell growth. Chemoprevention is the use of natural and synthetic compounds to inhibit carcinogenesis(Tsao, Kim, & Hong, 2004).

1.1 **Carcinogenesis and Cancer Chemoprevention**

Cancer pathology studies led to the discovery that carcinogenesis is a multistep mechanism. Somatic mutations in a single cell accumulate to cause phenotypic change from hyperplastic (causing an abnormal increase in the number of cells) to dysplastic (causing abnormal growth and development of cells). Dysplastic phenotypes can eventually become fully malignant. When cells become malignant, there are two classes of genes, proto-oncogenes and tumor suppressor genes that play a role in carcinogenesis(Tsao et al., 2004). Tumor suppressor genes and proto-oncogenes are essential in transcription regulation, cell cycle control, and signal transduction. These three activities of the genes contribute to the three phases of carcinogenesis (initiation, promotion and progression)(Tsao et al., 2004).

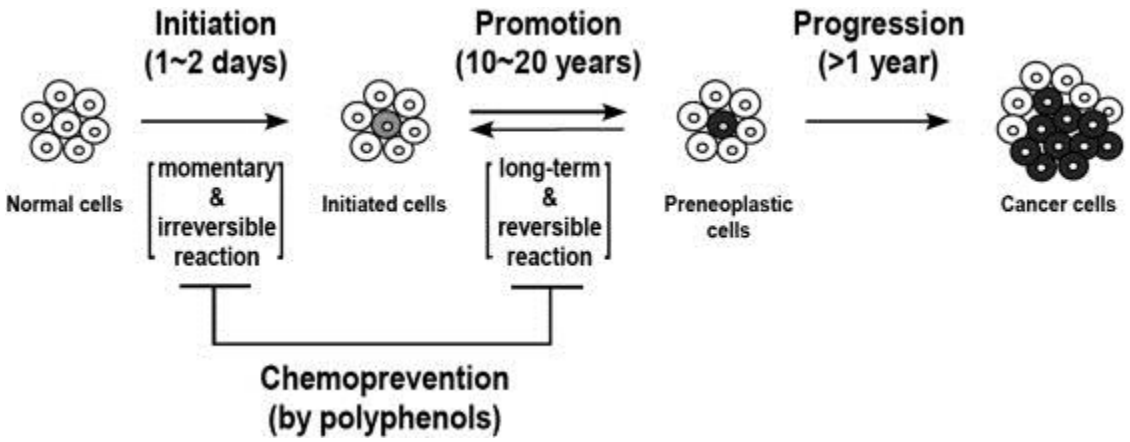

Figure 1: Three phases of carcinogenesis(Kang, Shin, Lee, & Lee, 2011)

The schematic in figure 1 shows this three phase process. Initiation is a short and irreversible process normally requiring many years before full malignancy is reached. The preneoplastic cells shown before progression are simply those preceding the development of a tumor. It is important to note that the promotion phase, while long-term, is reversible(Kang et al., 2011). This reversal is precisely the aim of chemoprevention. In figure 1, the method of chemoprevention shown is the use of polyphenols. Polyphenols are natural and synthetic molecules containing multiple phenol groups(Kuroda & Hara, 1999). They possess unique chemical and physical properties that make them of interest in chemoprevention. The compounds proposed in this study are designed to maximize these properties.

It is also essential to note the specific genes involved in carcinogenesis. One of these specific genes is KRAS(Horvath et al., 2004). This oncogene is responsible for providing instructions to make the protein K-Ras that regulates cell division(Juan, Wenzel, Daniel, & Planas, 2008). The Ras family of oncogenes also includes HRAS and NRAS which are responsible for cell proliferation and cell apoptosis (death) respectively(Juan et al., 2008). Mutations in the KRAS gene ultimately cause cancer by allowing the K-Ras protein to become overactive which accounts for the uncontrolled growth of cancerous cells. One specific pathway

to chemoprevention is to provide a detour to the multistep mechanism involving K-Ras. The nitrostyrenyl amides synthesized in this study will accomplish this detour by inducing the p53 protein that can in turn induce cell cycle arrest and apoptosis to bypass the K-Ras pathway ((Lee, Zhang, & Sanderson, 2008).

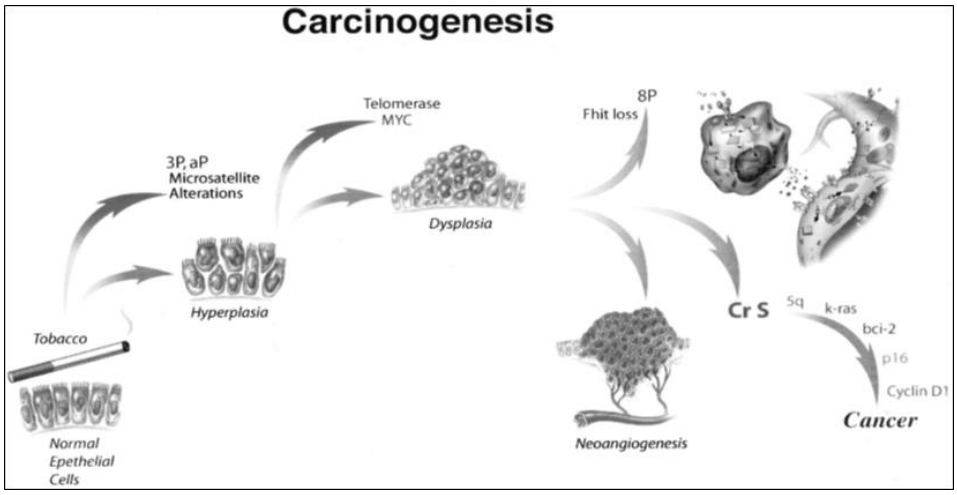

Figure 2: Multistep Carcinogenesis Model(Tsao et al., 2004)

The diagram shown in figure 3, shows a biological path to preventing cancer development using apoptotic agents. The compounds proposed in this study will be studied for their ability to initiate apoptosis. The diagram also shows the pathway by which these compounds can serve as antiangiogenic agents which prevent the growth of new blood vessels caused by carcinogens. The inhibition of the growth of these blood vessels is essential in chemoprevention.

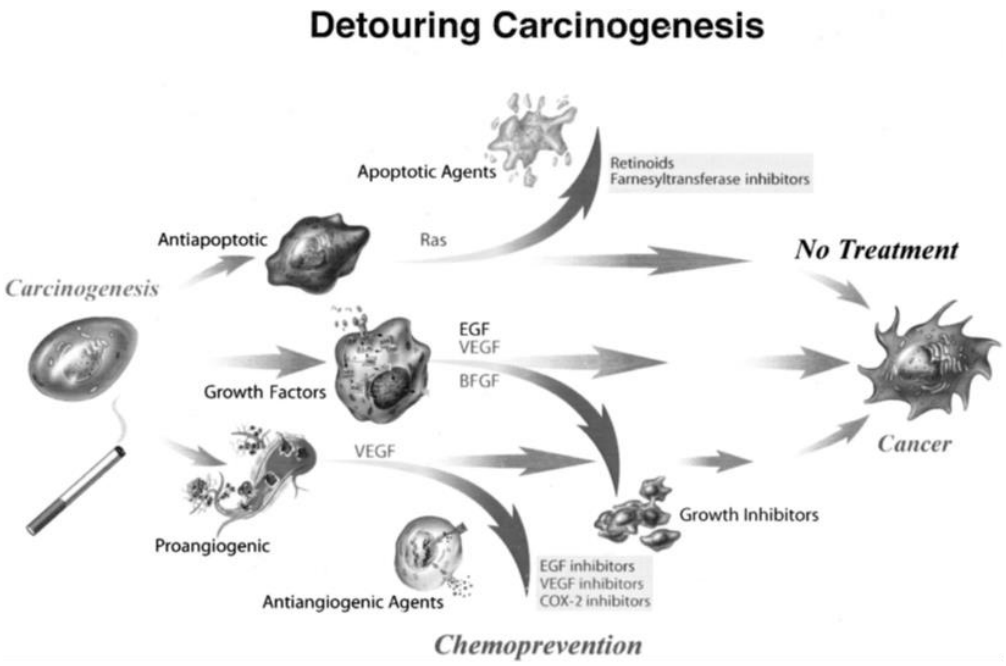

Figure 3: Biological Approaches to Preventing Cancer Development(Tsao et al., 2004)

1.2 Types of Chemopreventives

Cancer chemopreventives are natural or synthetic compounds with the ability to prevent the process of carcinogenesis. Dietary components such as ascorbic acid, β-carotene, folic acid and vitamin E are examples of compounds that have been studied in cancer chemoprevention (Sporn & Lippman, 2003). There exists the need for a wide range of potent agents in cancer chemoprevention. Chemopreventives have to be potent while maintaining low cytotoxicity. The compounds synthesized in this study seek to add to the knowledge base of what structural functionalities are ideal for chemopreventive drug design.

1.2.1 Blocking Agents and Suppressing Agents. Chemopreventives can be described by two major categories; blocking agents or suppressing agents. Blocking agents prevent the initiation of carcinogenesis, while suppressing agents prevent further progression of cancer (Sporn & Lippman, 2003).

1.2.1.1 Blocking Agents.

1.2.1.1.1 Hormonal Antagonists: Some chemopreventives mode of action involves interaction with hormone receptors. One of the well-known hormonal antagonists is tamoxifen. Tamoxifen is a non-steroidal triphenylethylene derivative that is believed to bind to the estrogen receptor to prevent mammary cell proliferation (Sporn & Lippman, 2003).

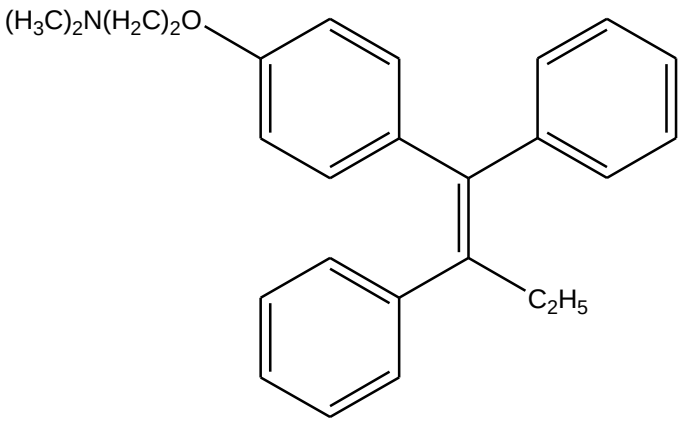

Figure 4: Structure of Tamoxifen

Another possibility is that, similar to fetal fibroblast cells, tamoxifen could induce production of the transforming growth factor-β, which is a negative autocrine regulator. In breast cancer patients, tamoxifen has also been shown to lower an insulin-like growth factor which enhances their growth. A disadvantage to using tamoxifen is that it has estrogenic effects on the epithelium of the uterus that increase the risk of developing uterine cancer (Sporn & Lippman, 2003).

Raloxifene (Figure 4) is a drug said to have a similar mode of action to tamoxifen, while also inhibiting the proliferation of uterine epithelia.

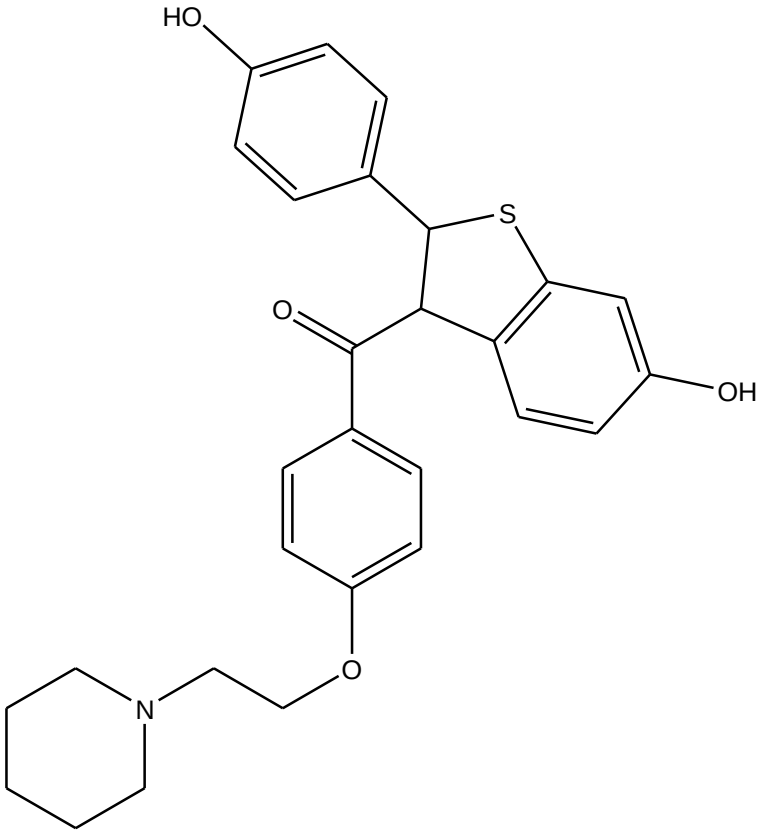

Figure 5: Structure of Raloxifene

The pharmacological activity of raloxifen is unique in that its estrogenic effect also has a positive effect on bone and serum lipids (Sporn & Lippman, 2003). For this reason, it is commonly used to treat osteoporosis and is being evaluated as a chemopreventive agent.

1.2.1.1.2 Nonsteroidal Anti-inflammatory Drugs: Nonsteroidal anti-inflammatory drugs (NSAIDs) include aspirin, ibuprofen, sulindac and piroxicam. These drugs have been studied in chemoprevention due to their ability to block prostaglandin synthesis by inhibiting cyclooxygenase (Sporn & Lippman, 2003). Since they are commonly used, researchers have been able to utilize already established dosage data in ongoing chemoprevention studies. In

animal studies NSAIDs are believed to act as blocking agents and may be particularly effective for prevention of carcinogenesis in the colon.

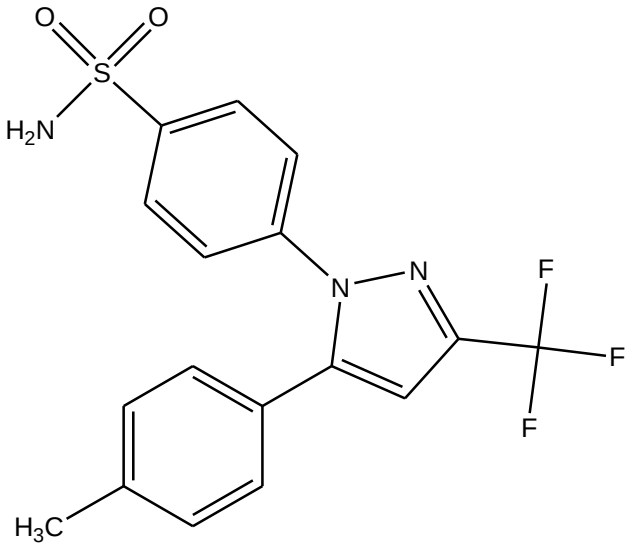

Figure 6: Structure of celecoxib

Within the NSAID category, cyclooxygenase-2 (COX-2) inhibitors are of increased interest. The COX-2 inhibitor, celecoxib is believed to be an effective chemopreventive for lung cancer (Mao et al., 2011).

1.2.1.2 Suppressing Agents

1.2.1.2.1 Retinoids: Retinoids are natural and synthetic and natural analogues of retinol (Figure 1), Vitamin A. This class of molecules has been shown to regulate the growth of epithelial cells. They interact with receptors that are active in the regulation of transcription of the genes that control cell differentiation and proliferation of epithelia. Retinoid deficiency leads to failure of stem cells to mature correctly and cell proliferation causing the formation of premalignant tissue (Sporn & Lippman, 2003). Animal studies of retinoids have shown efficacy in epithelial sites including breasts, pancreas, liver, prostate and the lungs. These agents have also been studied in combination with the preventative, tamoxifen.

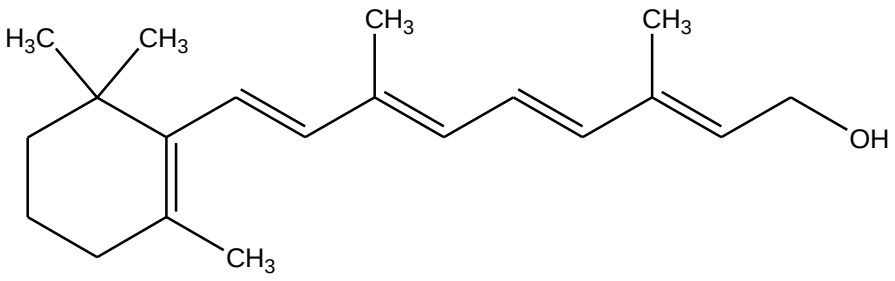

Figure 7: Structure of Retinol

1.2.1.2.2 Deltanoids: Another group in the steroid receptor family, like retinoids, is deltanoids. These include vitamin D and synthetic molecules of structural similarity.

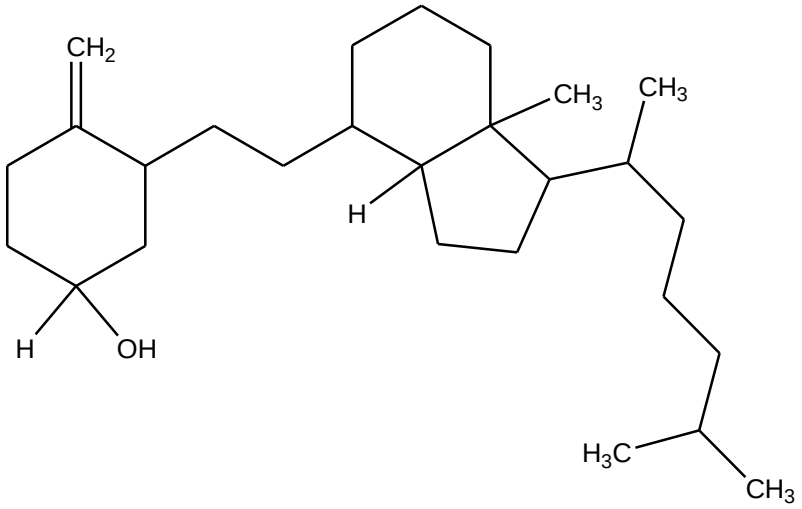

Figure 8: Structure of Vitamin D

The mode of actions for this class of molecules is the controlled expression of genes that induce cell differentiation. Newer deltanoid analogues are sought to reduce the calcemic nature of these drugs. In animal studies, they have been shown to have preventative affects for breast cancer (Sporn & Lippman, 2003).

CHAPTER 2

Literature Review

2.1 Stilbene

Stilbene based molecules are widely found in nature and are of particular interest in chemoprevention due to their biological function. Because stilbenes have been shown to prevent the growth of cancerous cells of the colon, prostate, breast, pancreas, ovaries, skin, head and neck(Rimando & Suh, 2008), we envisage that they would make effective chemopreventives.

2.1.1 Synthesis of Trans Stilbene: A common approach to the synthesis of trans stilbene is the Wittig reaction. The Wittig reaction easily converts a ketone or aldehyde to an alkene using a phosphorus ylide without producing side products that must be removed. The phosphorus ylide is generated from a phosphonium salt such as benzyltriphenyl-phosphonium chloride shown below.

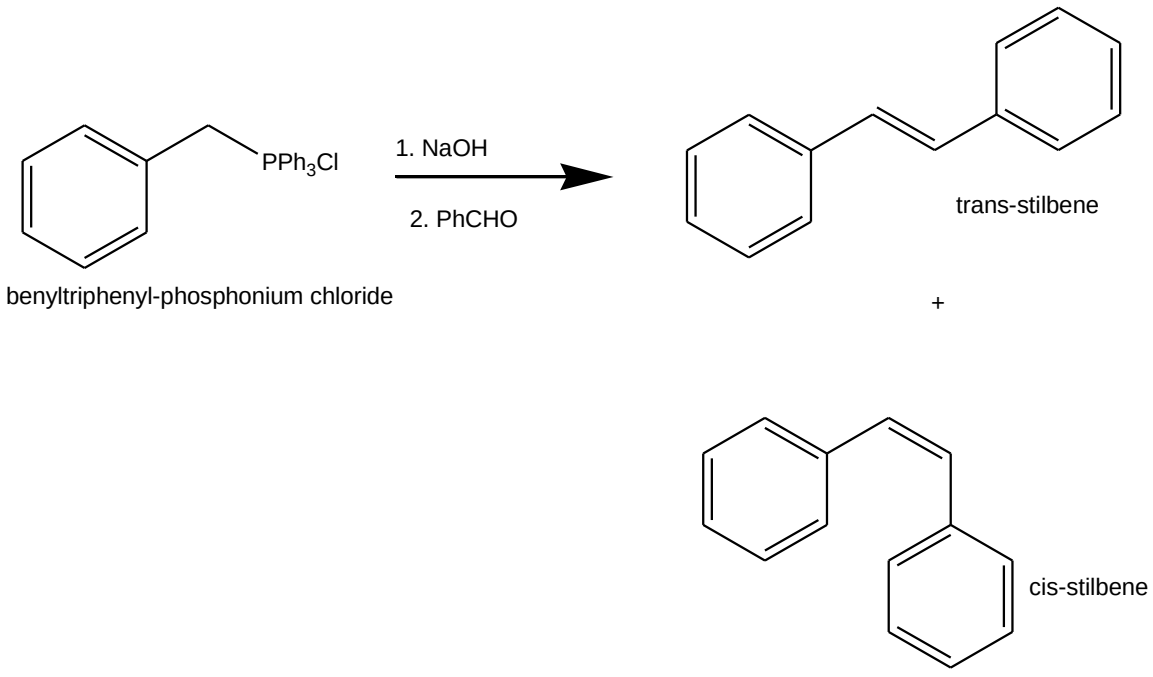

Figure 9: Wittig Reaction Synthesis of Stilbene

The reaction, Figure 9, yields both the cis and trans products. The mechanism is the cis-stilbene can then be converted to the favored trans-stilbene using crystalline iodine(Chang, Na, Shin, Choi, & Jeong, 2002).

2.1.2 Stilbenoids: Hydroxlated derivatives of stilbene, stilbenoids, are byproducts of heartwood formation in trees (Likhtenshtein, 2010). Growth inhibition of cancer cells is caused by cell cycle arrest from proteins p21, p27 and p53. This cell cycle arrest can also occur through a protein dependent mechanism called Fas-associated Death Domain (FADD), which involves this protein connecting the Fas-receptor (apoptosis antigen-1) to form a signaling complex necessary for apoptosis (Rimando & Suh, 2008). A major benefit of stilbenoids is their ability to induce apoptosis in a highly selective manner through the activation of Fas. Stilbenoids can target a wide variety of cancerous biological targets(Lion, Matthews, Stevens, & Westwell, 2005).

2.2 Resveratrol

Resveratrol (3, 5, 4'-trihydroxy-trans-stilbene) is a stilbenoid and natural phenol that is found in fruits such as grapes (Horvath et al., 2004; Lion et al., 2005). It is an important structure to use as a building block for new chemopreventives due to its proven effectiveness in biological function (Figure 10) (Juan, Wenzel, Daniel, & Planas, 2008). Resveratrol, as a phytoalexin, exhibits prominent effects on the cellular processes responsible for cancer initiation, promotion and progression(Lee et al., 2008). The polyphenol structure attributes to antioxidant behavior. As an antioxidant, resveratrol can reduce the formation of reactive oxygen species in blood platelet to effect oxidant-induced apoptosis (programmed cell death). Anti-inflammatory behavior of resveratrol is due to the inhibition of prostaglandin production. In addition to antioxidant and anti-inflammatory properties, resveratrol can inhibit D-type cyclins and cyclin-dependent kinase

CDK4 expression (Lee, Zhang, & Sanderson, 2008; Liang, Tajmir-Riahi, & Subirade, 2007). This can also lead to inducing tumor suppressors p53 and Cdk inhibitor p21. The p53 protein is encoded by the TP53 gene and responds to cellular stresses by regulating target genes that induce cell cycle arrest, apoptosis, and DNA repair among other functions (Juan, Wenzel, Daniel, & Planas, 2008). Inducing p53 is a goal of the compounds to be synthesized in this study.

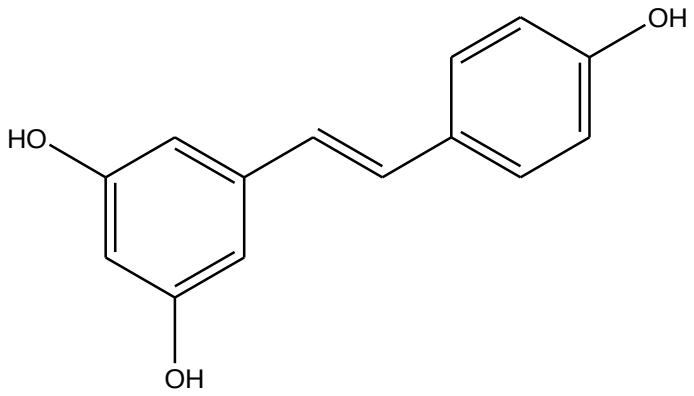

Figure 10: Structure of Resveratrol (3, 5, 4'-trihydroxy-trans-stilbene)

In order for chemopreventives to be effective and useful, they must exhibit low cytotoxicity. This means that they have very minimalized effects on normal, healthy cells. Resveratrol has exhibited selective cytotoxicity toward malignant cells with minimal cytotoxicity toward normal cells in some studies. However, other studies have shown that depending upon concentration, resveratrol can affect the proliferation of nonmalignant cells(Liang et al., 2007). This study seeks to produce compounds that retain resveratrol's chemopreventive properties through structural similarity, while minimizing cytotoxic effects on normal cells. The 3-nitro-2-styrenyl benzoic acids and their amide derivatives will utilize functional groups that are naturally occurring in the body to minimize cytotoxic effects leaving nonmalignant cell proliferation unaffected.

2.2.1 Synthesis of Resveratrol: In plants, the natural biosynthesis of resveratrol is achieved by the enzyme resveratrol synthase. However, the compound can also be achieved synthetically utilizing the Wittig reaction.

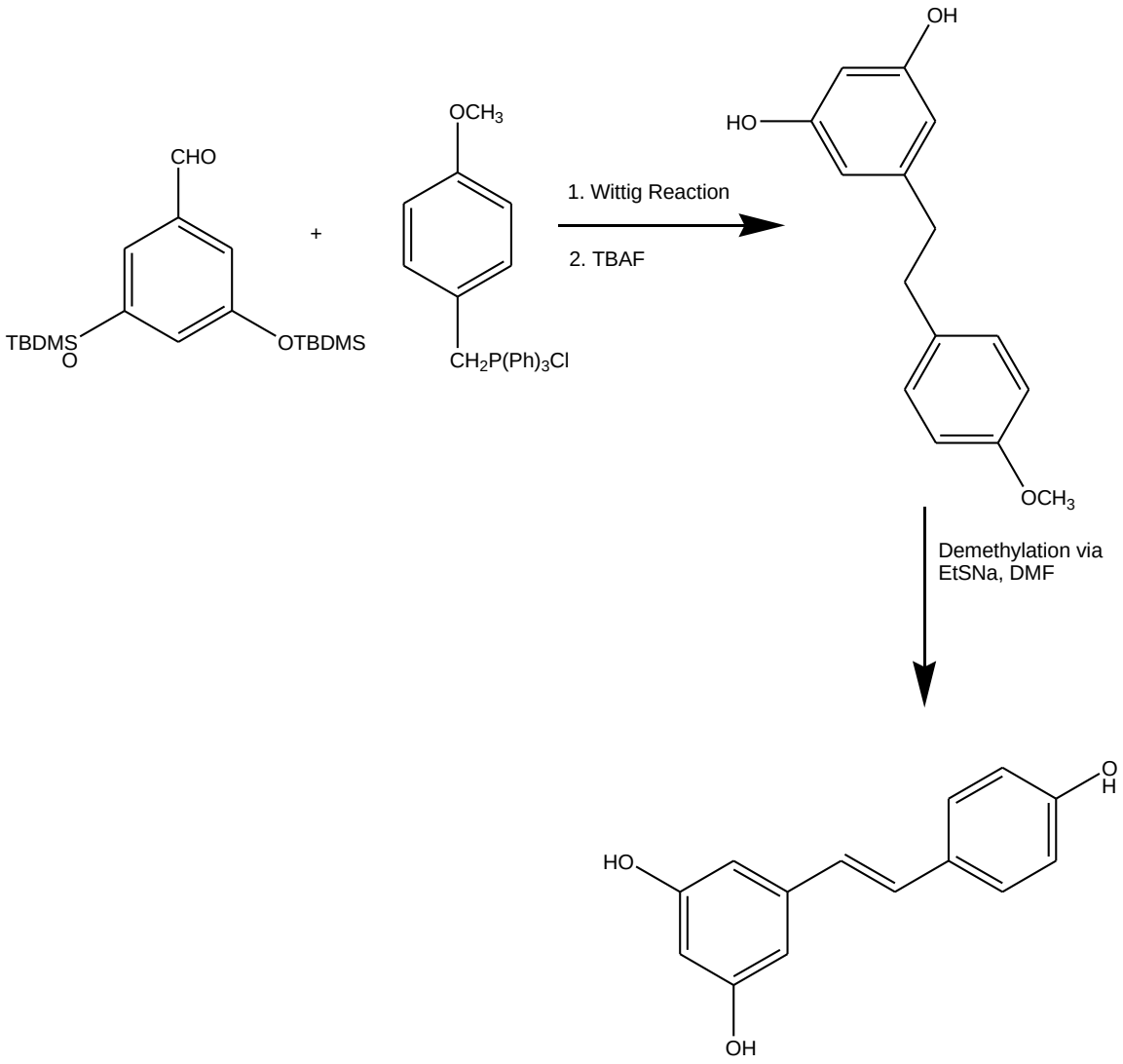

Figure 11: Synthesis of trans-resveratrol via Wittig reaction

The Wittig reaction occurs between the phosphonium salt of 4-methoxybenzyl chloride and 3,5-bis[tertbutyl(dimethylsilyl)oxy]benzaldehyde. The tertbutyldimethylsilyl groups are used to protect the hydroxyl groups on the benzaldehyde. Note that this reaction yields both the cis and trans isomers of resveratrol. The cis isomer can be separated using column chromatography before deprotection of the hydroxyl groups. The desilylation is achieved with tertbutylammonium fluoride to give the final product of (E)-resveratrol. This reaction can be carried out using any of these three organic solvents: ethanol, dichloromethane or hexanes. This

particular synthetic route has been patented by Thomas Christian Lines in the study of resveratrol as a treatment for mental disorders, including depression (Thomas Christian Lines, 2006).

2.3 Significance of 3-nitro-2-styrenyl benzoic acids in Chemoprevention

The compounds in this study are stilbene based derivatives with substituents aimed to enhance biological activity. 3-nitro-2-styrlbenzoic acid derivatives share the same structural motif as the known chemopreventive, resveratrol. Resveratrol (3, 5, 4'-trihydroxy-trans-stilbene) is a stilbenoid and natural phenol that is found in fruits such as grapes(Horvath et al., 2004; Lion et al., 2005) As shown in figure 1, phenols are of particular interest in the development of chemopreventives. Due to the structural similarities between resveratrol and 3-nitro-2-styrlbenzoic acid derivatives with substituents at the ortho and para positions, we believe that the 3-nitro-2-styrl benzoic acid derivatives will be effective chemopreventives.

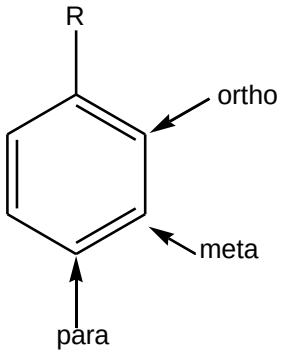

Figure 12: Relative Positions on a Benzene Ring

2.4 Amides

In its neutral state, nitrogen can form three bonds with an additional lone pair of electrons. In amides one of the bonds is to a carbonyl group. The general structure of an amide is related to that of a carboxylic acid except that the hydroxyl group is replaced by a NR_2 group. In the amide derivatives of nitrostyrenl benzoic acids, this change will reduce cytotoxicity and improve the potential for the synthesized compounds to act as chemopreventives.

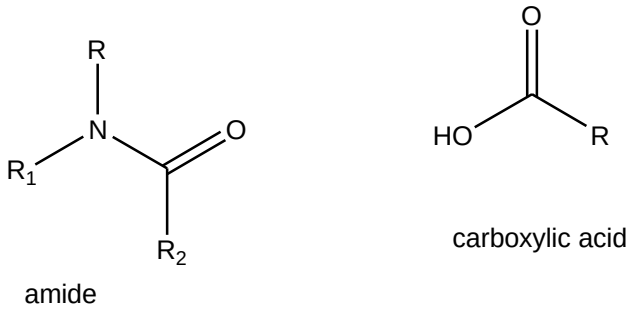

Figure 13: General Structures of an Amide and a Carboxylic Acid

2.4.1 Solubility: The solubility of amides is greatly influenced by the dipoles created by the carbonyl bond and the nitrogen-carbon bond. These dipoles allow amides to be hydrogen bond acceptors. While this property gives amides better solubility than hydrocarbons and aromatic structures, they are not generally as soluble as carboxylic acids and amines. The low water solubility of amides poses a challenge to their use in drug discovery, however with the appropriate functional groups on the starting benzaldehydes, the compounds solubility can improve.

2.4.2 Reactivity: Amides are non-basic and non-acidic at physiological pH due to the electron withdrawing nature of the carbonyl attached to the nitrogen. They are also less likely to act as nucleophiles and to be attacked by nucleophiles during hydrolysis due to resonance. Amides that are sterically hindered with large substituents will exhibit slower hydrolysis. The fact that amides are less reactive than other groups at physiological pH can aid in lowering the compounds cytotoxicity and improve dosage tolerance.

2.5 Amide Derivatives of 3-nitro-2-styrenyl benzoic acids

The amide derivatives of 3-nitro-2-styrenyl benzoic acids have a trans-stilbene structure with biologically active amide and nitro groups. Equally important is the electron withdrawing substituents on ring 2 located at the ortho and para positions (as labeled in figure 12). In our compounds, ring 1 has a nitro group at the ortho position and the amide at the meta position. The

substituents on ring 2 will be electron donating groups, such as methoxy and chloro groups. A push-pull mechanism will result from the placement of these groups in order to observe the reactivity of various structural motiffs. We believe that amide derivatives will maximize biological activity without increasing cytotoxicity.

2.5.1 Amide Derivatives Improve Biological Activity of Ibuprofen: The known anti-inflammatory (NSAID) ibuprofen is widely used to treat the symptoms of pain, joint disease and rheumatoid arthritis. The mechanism of action is the inhibition of the COX enzyme and the production of prostaglandins. Ibuprofen and other NSAIDs exhibit negative side effects such as development of ulcers and dyspepsia(Mehta et al., 2010). These adverse effects are associated most of all with NSAIDs containing a free carboxylic acid group(Mehta et al., 2010). In a 2010 study, it was shown that amide derivatives of ibuprofen (prodrugs) were able to retain the anti-inflammatory activity while providing gastro protection, reducing the occurrence of adverse effects like ulcerogenicity.

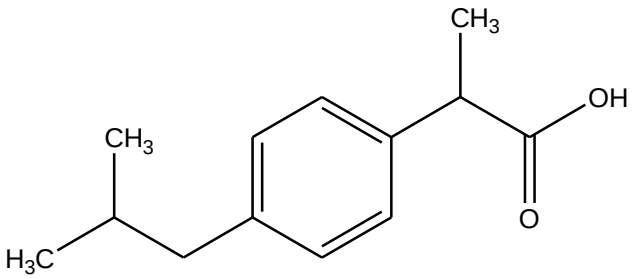

Figure 14: Structure of Ibuprofen

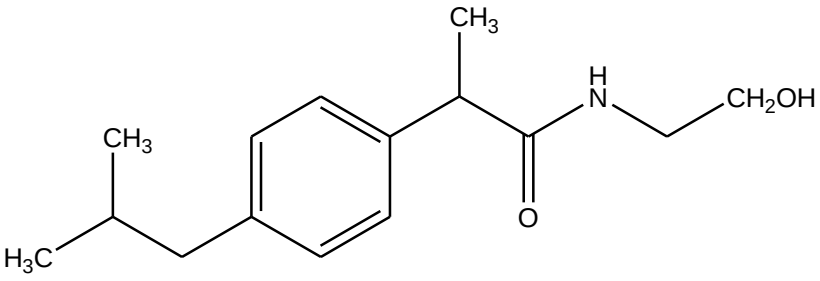

Figure 15: Structure of aminoprofen prodrug

2.5.1.1 Biological Activity Studies: Biological tests of the amide derivatives were done on Wistar rats in blind studies. The rats were treated for paw edema (painful swelling that can lead to infection) with a control, ibuprofen or the prodrug. All doses were administered at the molar equivalent basis of ibuprofen. The results showed a drastic decrease in ulcer index resulting from the aryl acetic moiety to the amides. The ulcer index for ibuprofen was measured at 4.0, while the amide prodrugs had ulcer indexes ranging from 0.5 to 1.0 (Mehta et al., 2010). All prodrugs tested showed comparable pharmacological activity to the parent drug with some even exhibiting improvement.

2.5.2 Sulindac Sulfide Amide Studies: In another carboxylic acid to amide drug conversion study, the drug Sulindac was studied. Sulindac is a NSAID prodrug derived from sulfinylindene(Piazza et al., 2009). Sulindac, like other NSAIDs has negative side effects stemming from the mechanism of COX enzyme and prostaglandin inhibition. While sulindac has shown promise as a chemopreventive, the toxicity to the gastrointestinal, renal and cardiovascular systems is too great for it to be effective(Piazza et al., 2009). Researchers were able to synthesize an amide derivative using an N, N-dimethylethyl amine substitution. This amide derivative did not exhibit inhibition to the COX enzyme, but was highly effective in inhibition of colon tumor cell growth(Piazza et al., 2009). In the HT-29 colon tumor cell line, the amide derivative was 40 times as potent against the cancer.

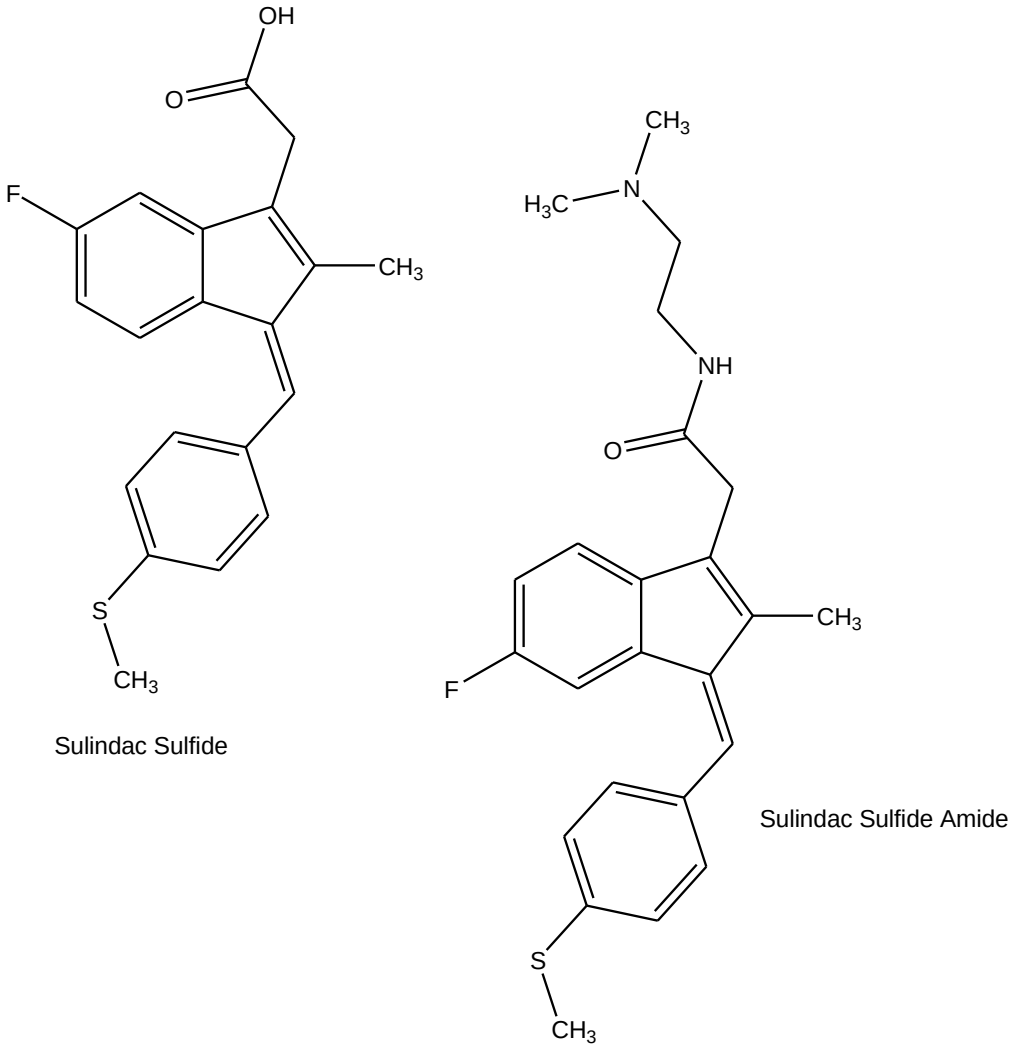

Figure 16: Structures of Sulindac Sulfide and Sulindac Sulfide Amide

According to the study, the amide derivative also showed greater bioavailability than the sulindac sulfide. In addition to the colon tumor cell line studies, SSA was also studied on lung tumor cell lines (Gurpinar, 2013).

CHAPTER 3

Methodology

3.1 General Procedure

All chemical reagents used were purchased from Sigma-Aldrich, Fischer-Scientific and Acros Chemicals. The nitro Styrenyl benzoic acids were synthesized using a base catalyzed condensation reaction in which 1, 8-diazobicycloundec-7-ene was the base. Nitro Styrenyl benzoic acids were then converted to the respective amide derivatives using an N, N-dimethylformamide catalyzed reaction of thionyl chloride producing an acid chloride that can then undergo substitution with a desired amine. All products were characterized using ^{1}H NMR, ^{13}C NMR and FT-IR. The NMR used was a Varian 300 MGHz utilizing VNMRJ software. The FT-IR was a Shimadzu IRPRESTIGE-21. HPLC analysis was done on a Varian ProStar. Melting point ranges for each compound were determined using a MEL TEMP apparatus and are recorded in degrees Celsius.

3.2 Synthesis of Nitro Styrenyl Benzoic Acids (1a-8a)

The appropriately substituted benzaldehyde (11.5 mmol) was added to a round bottom flask equipped with a magnetic stir bar along with 1.50g of methyl-2-methyl-3-nitrobenzoate in 10 mL of dried dimethylsulfoxide (DMSO). This reaction mixture was allowed to stir for 20 hours at room temperature before being heated to 55°C for 4 hours, allowed to cool having sodium hydroxide (20mL, 1M) added to it. The reaction mixture is then washed with washes of ethyl acetate(2X 25 mL). The aqueous layer was made acidic with concentrated hydrochloric acid and extracted with ethyl acetate. The extracted reaction mixture was dried over magnesium sulfate and the solvent was removed by rotary evaporation. The resultant crude oil product was

recrystallized using dried methanol and water. Percent yields for these reactions ranged from 35.1-90.2%.

3.2.1 2-[(E)-2-(2-chlorophenyl) ethenyl]-3-nitrobenzoic acid (1a): 1H NMR (301 MHz, ACETONITRILE-d3) □ ppm 6.87 (d, J=1.00 Hz, 1 H) 7.37 (dt, J=1.00 Hz, 3 H) 7.49 (s, 1 H) 7.58 (t, J=1.00 Hz, 1 H) 7.74 (br. d, J=1.00 Hz, 1 H) 7.97 (s, 1 H) 8.08 (br. s., 1 H) 13C NMR (101 MHz, ACETONITRILE-d3) □ ppm -0.28 (s, 1 C) -0.07 (s, 1 C) 0.14 (s, 1 C) 0.35 (s, 1 C) 0.49 (s, 1 C) 0.55 (s, 1 C) 0.76 (s, 1 C) 0.97 (s, 1 C) 117.34 (s, 1 C);MP 153-161℃

3.2.2 3-nitro-2-{(E)-2-[2-(trifluoromethyl)phenyl]ethenyl} benzoic acid (2a): ^{1}H NMR (400 MHz, *ACETONITRILE-d_3*) δ ppm 6.62 (1 H, s), 7.66 (4 H, s), 8.04 (1 H, s), 8.21 (3 H, s) ^{13}C NMR (101 MHz, ACETONITRILE-d_3) δ ppm 123.03 (s, 1 C) 125.83 (s, 1 C) 126.83 (s, 1 C) 127.73 (s, 1 C) 127.93 (s, 1 C) 128.34 (s, 1 C) 128.74 (s, 1 C) 130.07 (s, 1 C) 131.29 (s, 1 C) 132.50 (s, 1 C) 132.72 (s, 1 C) 133.20 (s, 1 C) 133.67 (s, 1 C) 135.31 (s, 1 C) 150.41 (s, 1 C) 166.68 (s, 1 C) ; MP 155-169℃

3.2.3 2-[(E)-2-(4-chlorophenyl)ethenyl]-3-nitrobenzoic acid (3a): ^{1}H NMR (301 MHz, CHLOROFORM-*d*) δ ppm 6.50 (br. d, *J*=1.00 Hz, 1 H) 7.36 (t, *J*=14.20 Hz, 5 H) 7.53 (br. d, *J*=1.00 Hz, 2 H) 7.98 (br. d, *J*=1.00 Hz, 1 H) 8.18 (br. d, *J*=1.00 Hz, 1 H) ^{13}C NMR (101 MHz, ACETONITRILE-d_3) δ ppm 117.34 (s, 1 C) 121.64 (s, 1 C) 124.30 (s, 1 C) 126.59 (s, 1 C) 127.90 (s, 1 C) 128.08 (s, 1 C) 128.42 (s, 1 C) 128.89 (s, 1 C) 131.22 (s, 1 C) 131.74 (s, 1 C) 132.42 (s, 1 C) 133.51 (s, 1 C) 135.41 (s, 1 C) 150.36 (s, 1 C) 166.86 (s, 1 C) 167.97 (s, 1 C); MP 150-162℃

3.2.4 2-[(E)-2-(4-bromophenyl) ethenyl]-3-nitrobenzoic acid (4a): ^{1}H NMR (301 MHz, CHLOROFORM-*d*) δ ppm 6.47 (d, *J*=1.00 Hz, 1 H) 7.26 (s, 1 H) 7.33 (d, *J*=1.00 Hz, 2 H) 7.48 (br. t, *J*=1.00, 1.00 Hz, 2 H) 7.55 (br. d, *J*=1.00 Hz, 1 H) 7.96 (br. d, *J*=1.00 Hz, 1 H) 8.17

(br. d, *J*=1.00 Hz, 1 H) ^{13}C NMR (101 MHz, ACETONITRILE-d_3) δ ppm 117.33 (s, 1 C) 121.73 (s, 1 C) 124.39 (s, 1 C) 126.69 (s, 1 C) 127.46 (s, 1 C) 128.35 (s, 1 C) 128.47 (s, 1 C) 131.27 (s, 1 C) 131.81 (s, 1 C) 131.88 (s, 1 C) 132.50 (s, 1 C) 133.18 (s, 1 C) 133.51 (s, 1 C) 135.79 (s, 1 C) 166.71 (s, 1 C); MP 149-162°C

3.2.5 2-[(E)-2-(4-nitrophenyl)ethenyl]-3-nitrobenzoic acid (5a): ^{1}H NMR (400 MHz, ACETONITRILE-d_3) δ ppm 6.64 (br. d, *J*=1.00 Hz, 1 H) 7.69 (tt, *J*=1.00 Hz, 4 H) 7.77 (s, 1 H) 8.04 (d, *J*=1.00 Hz, 1 H) 8.14 (d, *J*=1.00 Hz, 1 H) 8.21 (d, *J*=1.00 Hz, 2 H) ^{13}C NMR (101 MHz, ACETONITRILE-d_3) δ ppm 124.15 (s, 1 C) 126.56 (s, 1 C) 126.90 (s, 1 C) 127.05 (s, 1 C) 127.33 (s, 1 C) 128.34 (s, 1 C) 128.94 (s, 1 C) 130.55 (s, 1 C) 132.43 (s, 1 C) 132.80 (s, 1 C) 133.35 (s, 1 C) 133.84 (s, 1 C) 142.99 (s, 1 C) 147.44 (s, 1 C) 166.33 (s, 1 C); MP 135-150°C

3.3 General Procedure for Synthesis of Nitro Styrenyl Amide Derivatives (1b-5b)

Into a 2-neck round bottom flask was added 6.5 mmol of appropriately substituted 3-nitro-2-styrenyl benzoic acid along with 0.2 mL of N.N-dimethylformamide (DMF). Molecular sieves were added to this reaction mixture and the flask was equipped with a stir bar. The reaction mix was allowed to stir until a homogeneous mixture was observed and thionyl chloride was added (1:3 mole ratio with benzoic acid starting material) via syringe into a rubber septum. This mixture was then refluxed for 30minutes. To an Erlenmeyer flask was added 4 mL of 20% sodium hydroxide (NaOH) and it was cooled below room temperature in an ice bath. Once the NaOH cooled, 1 mL of N-butylamine was added. The reaction mixture was removed from reflux and added dropwise to the cooled amine/base solution. As the reaction mix was added, the flask was gently swirled. The product was extracted with ethyl ether (2x 25 mL washes) and dried over magnesium sulfate. The product was then concentrated with rotary evaporation and dried on high vacuum. The crude product was then dissolved in 10 mL of dried methanol. Distilled water

was added drop wise (30 mL) to form slurry that was allowed to stir for an hour before product was isolated by vacuum filtration. Percent yields for this reaction range from 15.9-87.7%.

3.3.1 2-(2-chlorostyryl)-N-butyl-3-nitrobenzamide (1b): ^{1}H NMR (301 MHz, ACETONITRILE-d_3) δ ppm 0.84 (t, *J*=1.00 Hz, 3 H) 1.28 (br. t, *J*=1.00, 1.00 Hz, 2 H) 1.49 (br. t, *J*=1.00, 1.00 Hz, 2 H) 2.79 (br. d, *J*=1.00 Hz, 2 H) 6.96 (d, *J*=1.00 Hz, 2 H) 7.25 - 7.34 (m, 3 H) 7.43 (br. t, *J*=1.00, 1.00 Hz, 4 H) 7.61 (br. s., 1 H) 7.75 (br. s., 1 H) 7.88 (br. s., 1 H) ^{13}C NMR (101 MHz, ACETONITRILE-d_3) δ ppm -0.28 (s, 1 C) -0.07 (s, 1 C) 0.14 (s, 1 C) 0.35 (s, 1 C) 0.49 (s, 1 C) 0.55 (s, 1 C) 0.76 (s, 1 C) 0.97 (s, 1 C) 117.34 (s, 1 C) ; MP 147-159°C

3.3.2 2-(2-(trifluoromethyl)styryl)-N-butyl-3-nitrobenzamide (2b): ^{1}H NMR (301 MHz, ACETONITRILE-d_3) δ ppm 0.76 (d, *J*=7.10 Hz, 2 H) 1.27 (br. t, *J*=1.00, 1.00 Hz, 1 H) 1.41 (br. d, *J*=1.00 Hz, 1 H) 3.26 (s, 2 H) 7.03 (br. s., 1 H) 7.40 (br. s., 1 H) 7.47 - 7.63 (m, 2 H) 7.66 - 7.77 (m, 2 H) 7.88 (br. s., 1 H) 8.00 (br. s., 1 H) ^{13}C NMR (101 MHz, ACETONITRILE-d_3) δ ppm 12.92 (s, 1 C) 19.78 (s, 1 C) 31.15 (s, 1 C) 39.14 (s, 1 C) 123.07 (s, 1 C) 124.66 (s, 1 C) 124.88 (s, 1 C) 125.79 (s, 1 C) 126.52 (s, 1 C) 126.94 (s, 1 C) 127.55 (s, 1 C) 128.44 (s, 1 C) 128.71 (s, 1 C) 129.33 (s, 1 C) 129.88 (s, 1 C) 131.63 (s, 1 C) 131.91 (s, 1 C) 132.69 (s, 1 C) 135.13 (s, 1 C) 139.85 (s, 1 C) 149.25 (s, 1 C) 167.25 (s, 1 C) ; MP 110-119°C

3.3.3 2-(4-chlorostyryl)-N-butyl-3-nitrobenzamide (3b): ^{1}H NMR (400 MHz, ACETONITRILE-d_3) δ ppm 0.76 (d, *J*=1.00 Hz, 3 H) 1.23 (br. t, *J*=1.00, 1.00 Hz, 2 H) 1.38 (br. t, *J*=1.00, 1.00 Hz, 2 H) 3.23 (br. d, *J*=1.00 Hz, 2 H) 6.72 (br. d, *J*=1.00 Hz, 1 H) 7.28 - 7.57 (m, 6 H) 7.69 (br. d, *J*=1.00 Hz, 1 H) 7.98 (br. d, *J*=1.00 Hz, 1 H) ^{13}C NMR (101 MHz, ACETONITRILE-d_3) δ ppm 12.94 (s, 1 C) 19.80 (s, 1 C) 31.24 (s, 1 C) 38.99 (s, 1 C) 39.12 (s, 1 C) 122.99 (s, 1 C) 124.82 (s, 1 C) 128.19 (s, 1 C) 128.36 (s, 1 C) 128.86 (s, 1 C) 130.03 (s, 1 C)

131.91 (s, 1 C) 132.25 (s, 1 C) 133.20 (s, 1 C) 133.57 (s, 1 C) 135.29 (s, 1 C) 139.82 (s, 1 C) 149.16 (s, 1 C) 167.49 (s, 1 C) ; MP 139-148℃

3.3.4 2-(4-bromostyryl)-N-butyl-3-nitrobenzamide (4b): ^{1}H NMR (400 MHz, ACETONITRILE-d_3) δ ppm 0.76 (d, *J*=1.00 Hz, 3 H) 1.25 (t, *J*=1.00 Hz, 2 H) 1.37 (t, *J*=1.00 Hz, 2 H) 3.23 (t, *J*=1.00 Hz, 2 H) 6.70 (br. s., 1 H) 7.35 (s, 1 H) 7.41 (d, *J*=1.00 Hz, 2 H) 7.55 (t, *J*=1.00 Hz, 3 H) 7.70 (s, 1 H) 7.97 (s, 1 H) ^{13}C NMR (101 MHz, ACETONITRILE-d_3) δ ppm 12.94 (s, 1 C) 19.81 (s, 1 C) 31.24 (s, 1 C) 39.12 (s, 1 C) 121.77 (s, 1 C) 122.58 (s, 1 C) 123.09 (s, 1 C) 124.83 (s, 1 C) 128.38 (s, 1 C) 128.45 (s, 1 C) 130.03 (s, 1 C) 130.23 (s, 1 C) 131.09 (s, 1 C) 131.84 (s, 1 C) 131.93 (s, 1 C) 133.26 (s, 1 C) 135.68 (s, 1 C) 139.81 (s, 1 C) 167.48 (s, 1 C) ; MP 168-175℃

3.3.5 2-(4-nitrostyryl)-N-butyl-3-nitrobenzamide (5b): ^{1}H NMR (400 MHz, ACETONITRILE-d_3) δ ppm 0.82 (br. d, *J*=1.00 Hz, 3 H) 1.42 (br. t, *J*=1.00, 1.00 Hz, 2 H) 2.11 (br. t, *J*=1.00, 1.00 Hz, 2 H) 3.20 (br. d, *J*=1.00 Hz, 2 H) 6.85 (br. d, *J*=1.00 Hz, 2 H) 7.47 - 7.79 (m, 6 H) 8.02 (br. s., 1 H) 8.23 (br. s, 1 H) ^{13}C NMR (101 MHz, ACETONITRILE-d_3) δ ppm 10.76 (s, 1 C) 22.30 (s, 1 C) 41.20 (s, 1 C) 55.67 (s, 1 C) 124.10 (s, 1 C) 125.04 (s, 1 C) 127.18 (s, 1 C) 127.40 (s, 1 C) 128.85 (s, 1 C) 131.87 (s, 1 C) 132.10 (s, 1 C) 139.83 (s, 1 C) 142.90 (s, 1 C) 167.37 (s, 1 C) ; MP 149-157℃

CHAPTER 4

Results and Discussion

4.1 Synthesis and Characterization of Nitro-Styrenyl Benzoic Acids

The synthesis for compounds 1a-5a is a base catalyzed condensation reaction. The base used in our case is 1,8-diazabicyclo[5.4.0]undec-7-ene (DBU). The base deprotonates the methyl group at the ortho position creating a carbanion that attacks the carbonyl on a benzaldehyde (Figure 18).

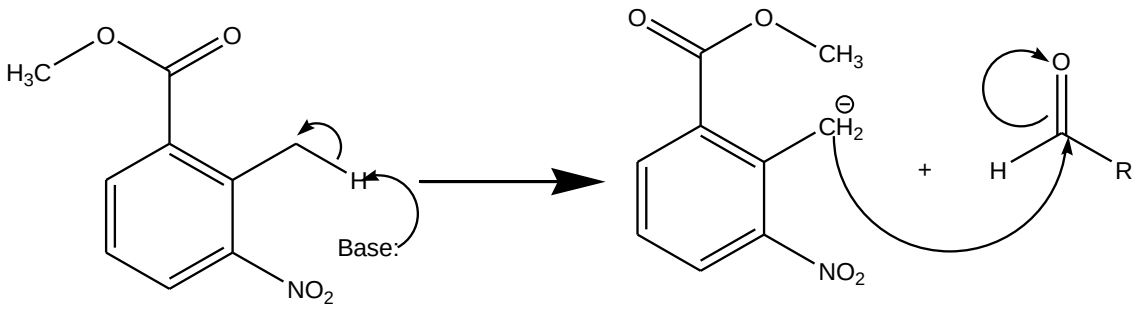

Figure 17: Synthesis of Nitro Styrenyl Benzoic Acids (Scheme A)

A ring is then formed in an intermediate structure by the alkoxide attacking the carbonyl on the nitrobenzoate. A carbonyl is reformed as a methoxy group is released, Figure 19.

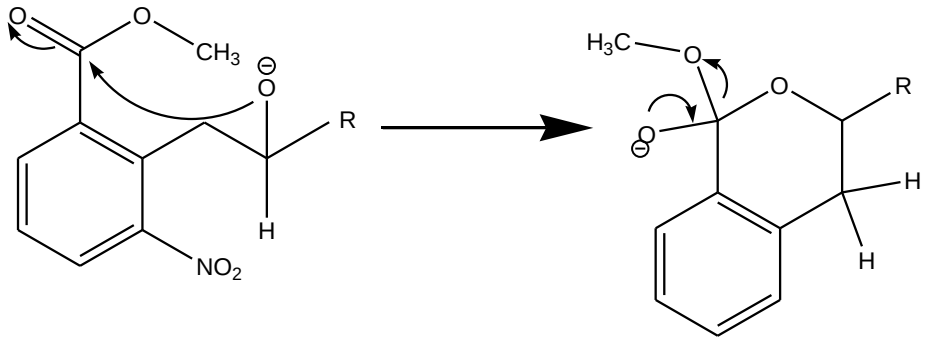

Figure 18: Synthesis of Nitro Styrenyl Benzoic Acids (Scheme B)

The base (DBU) then opens the ring, by extracting the most acidic proton and forming the alkene with heat (55°C) is applied to the reaction. Concentrated hydrochloric acid is used in the workup step to protonate the product forming the carboxylic acid (Figure 20). The reaction is specific to

the *trans*-alkene formation due to minimized unfavorable steric interactions shown in the trans product over the cis product. This is a one pot reaction and the products can be extracted in ethyl acetate.

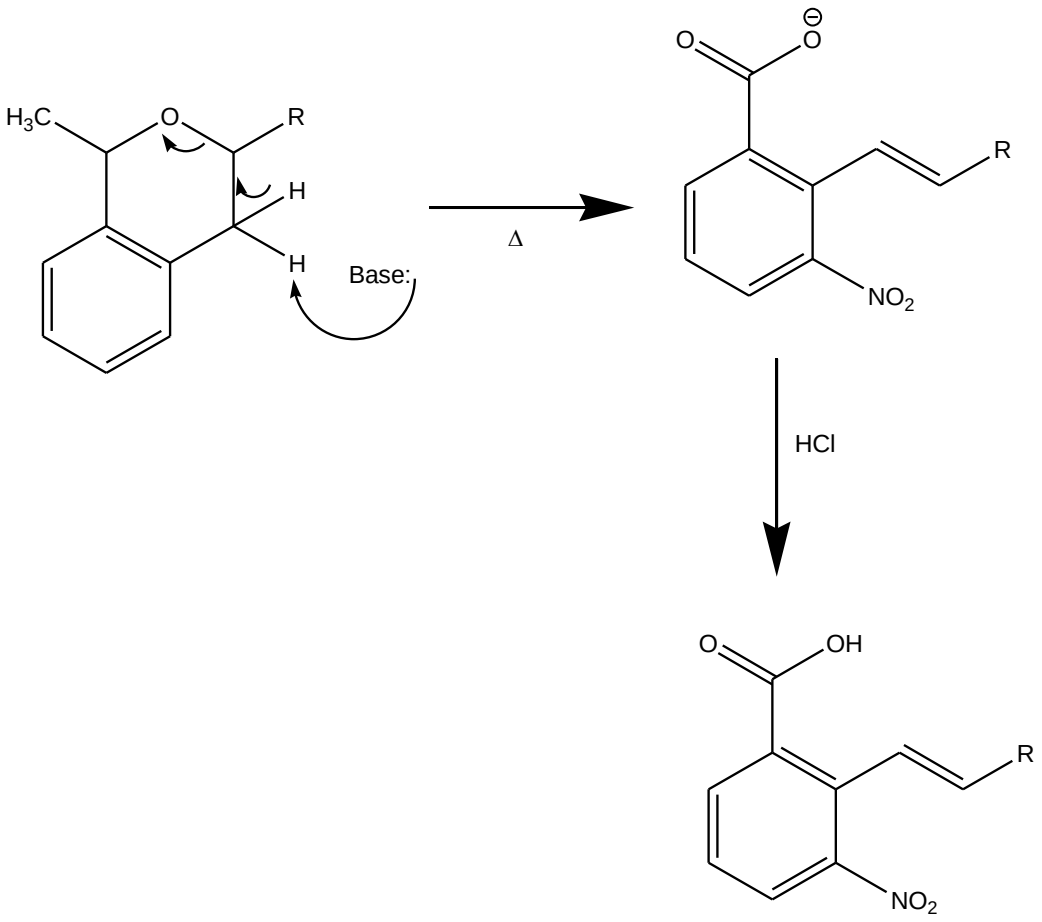

Figure 19: Synthesis of Nitro Styrenyl Benzoic Acids (Scheme C)

4.1.1 Nitro-Styrenyl Benzoic Acid Products: Compounds 1a-5a are shown in the table below with a summary of percent yields for the nitrostyrenyl benzoic acids which ranged from 35.1-90.2%. Products were all solid. All products were yellow in color with the exception of 5a, which was reddish-brown.

Table 1

Summary of NitroStyrenyl Benzoic Acids

Compound	Structure	Name	% Yield
1a	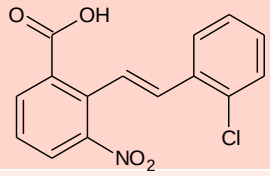	2-[(E)-2-(2-chlorophenyl) ethenyl]-3-nitrobenzoic acid	90.2
2a	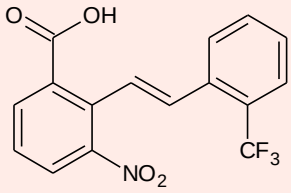	3-nitro-2-{(E)-2-[2-(trifluoromethyl)phenyl]ethenyl) benzoic acid	73.3
3a	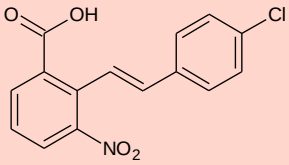	2-[(E)-2-(4-chlorophenyl)ethenyl]-3-nitrobenzoic acid	35.1
4a	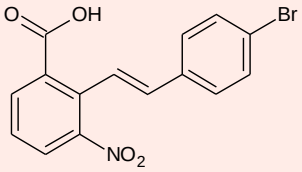	2-[(E)-2-(4-bromophenyl) ethenyl]-3-nitrobenzoic acid	78.1
5a	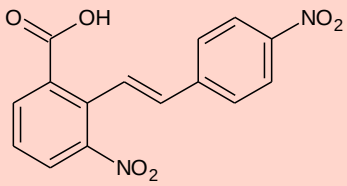	2-[(E)-2-(4-nitrophenyl) ethenyl]-3-nitrobenzoic acid	82.3

4.1.2 NMR Characterization of Nitro-Styrenyl Benzoic Acids: Nuclear Magnetic Resonance was used to characterize the structures of compounds 1a-5a. In each spectra the peaks in the aromatic region (6-8ppm) are of particular interest due to the general structure. Both proton and carbon spectra were obtained.

4.1.2.1 Discussion of Nitro-Styrenyl Benzoic Acid Proton NMR: The proton NMR for 3-nitro-2-{(E)-2-[2-(trifluoromethyl)phenyl]ethenyl} benzoic acid (2a), shows the expected peaks for the seven protons located on the rings in the aromatic region. There is significant overlapping in this region.

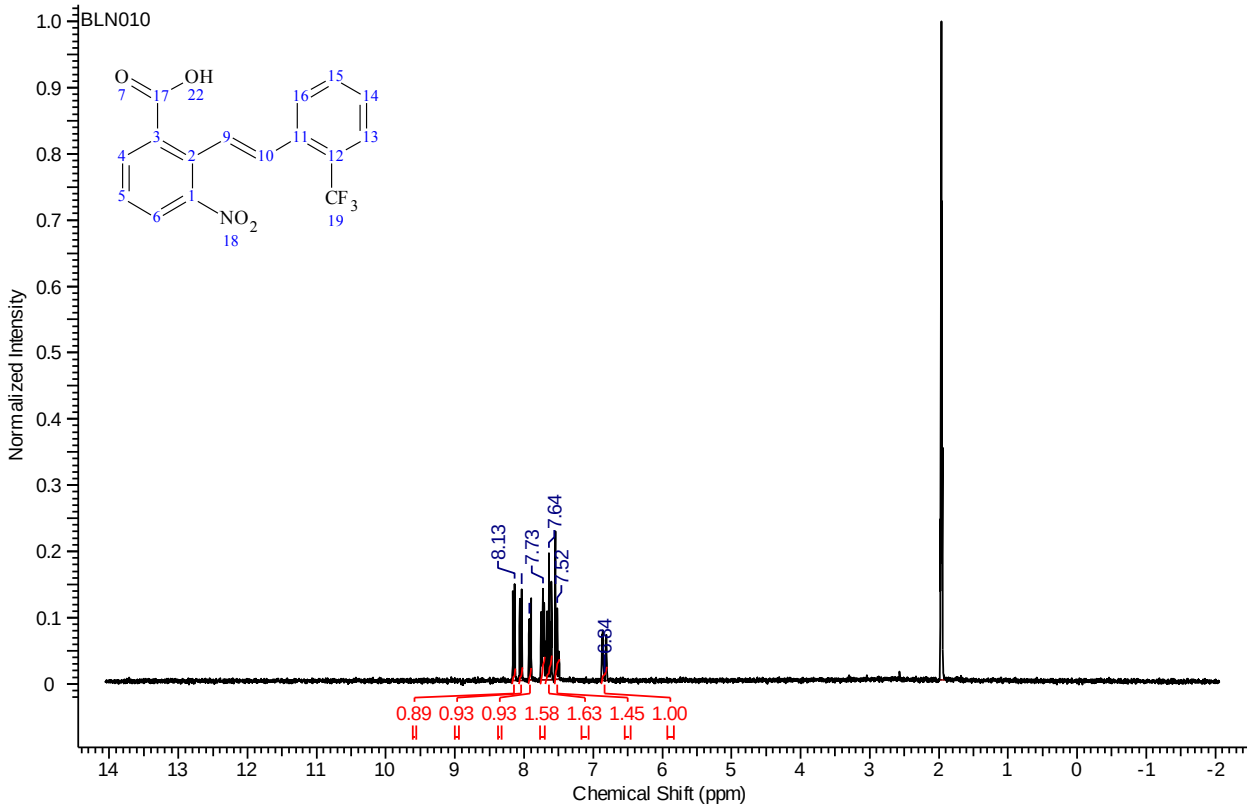

Figure 20: ^{1}H NMR Spectra for 3-nitro-2-{(E)-2-[2-(trifluoromethyl)phenyl]ethenyl}benzoic acid (2a)

The proton on the carbon number 10 in Figure 21, one of the double bond carbons of the styrene moiety, can be seen as the doublet at 6.84ppm. The proton on the other styrene carbon numbered 9 is shown within the overlapping at 7.52ppm.The styrene proton closest to the carboxylic acid containing ring will be more downfield due to electronic effects. The proton of the carboxylic acid is not seen in the spectra due to the deuterated acetonitrile NMR solvent used which can exchange with the labile hydrogen of the product.

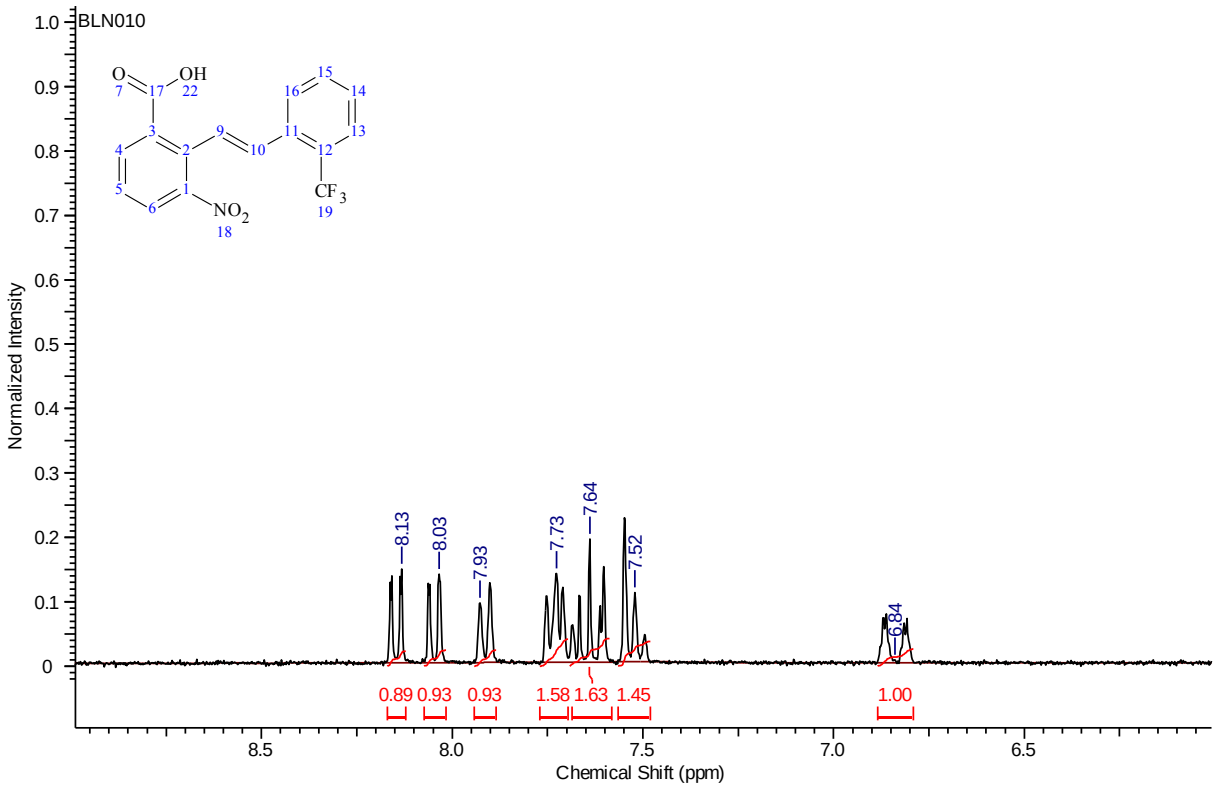

Figure 21: Aromatic Region of the 1H NMR Spectra for 3-nitro-2-{(E)-2-[2-(trifluoromethyl)phenyl]ethenyl}benzoic acid (2a)

Table 2

Chemical Shifts for 3-nitro-2-{(E)-2-[2-(trifluoromethyl)phenyl]ethenyl} benzoic acid (2a)

No.	**(ppm)**	**(Hz)**	**Height**
1	6.84	2056.7	0.0097
2	7.52	2262.0	0.1138
3	7.64	2297.5	0.1975
4	7.73	2323.5	0.1441
5	7.93	2383.8	0.0982
6	8.03	2416.4	0.1428
7	8.13	2445.9	0.1511

4.1.2.2 Discussion of Nitro-Styrenyl Benzoic Acid Carbon NMR: The carbon NMR spectra for the 3-nitro-2-{(E)-2-[2-(trifluoromethyl)phenyl]ethenyl} benzoic acid (2a) product shows the sixteen carbons including that of the trifluoromethyl group. The carboxylic acid carbon is shown at 166.68ppm and the triflouromethyl carbon at 117.35ppm.

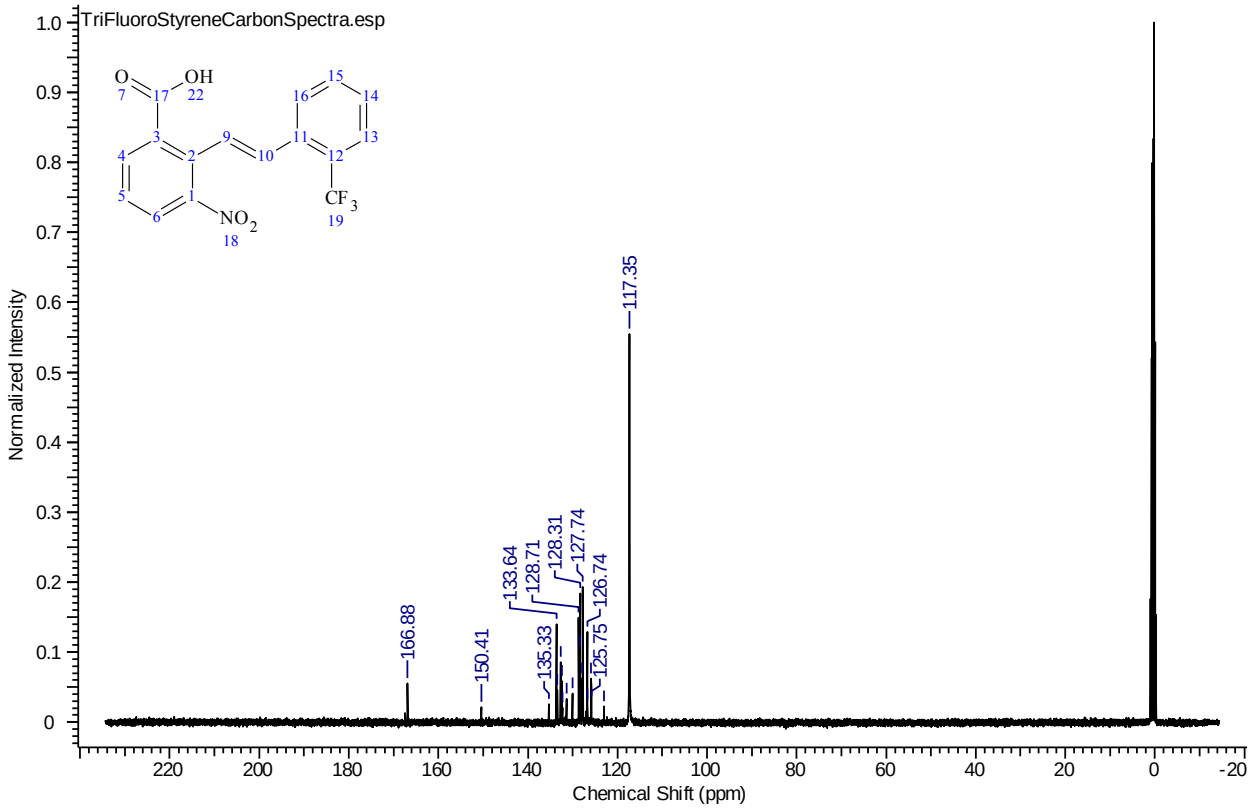

Figure 22: ^{13}C NMR Spectra for 3-nitro-2-{(E)-2-[2-(trifluoromethyl)phenyl]ethenyl} benzoic acid (2a)

The aromatic region shown in Figure 23 shows that the carbon attached to the nitro functional group is observed at 150.41ppm. The alkene carbons of the styrene are observed at 125.75ppm and 126.74ppm. The carbons associated with the two aromatic rings are observed within the range of 127-136ppm.

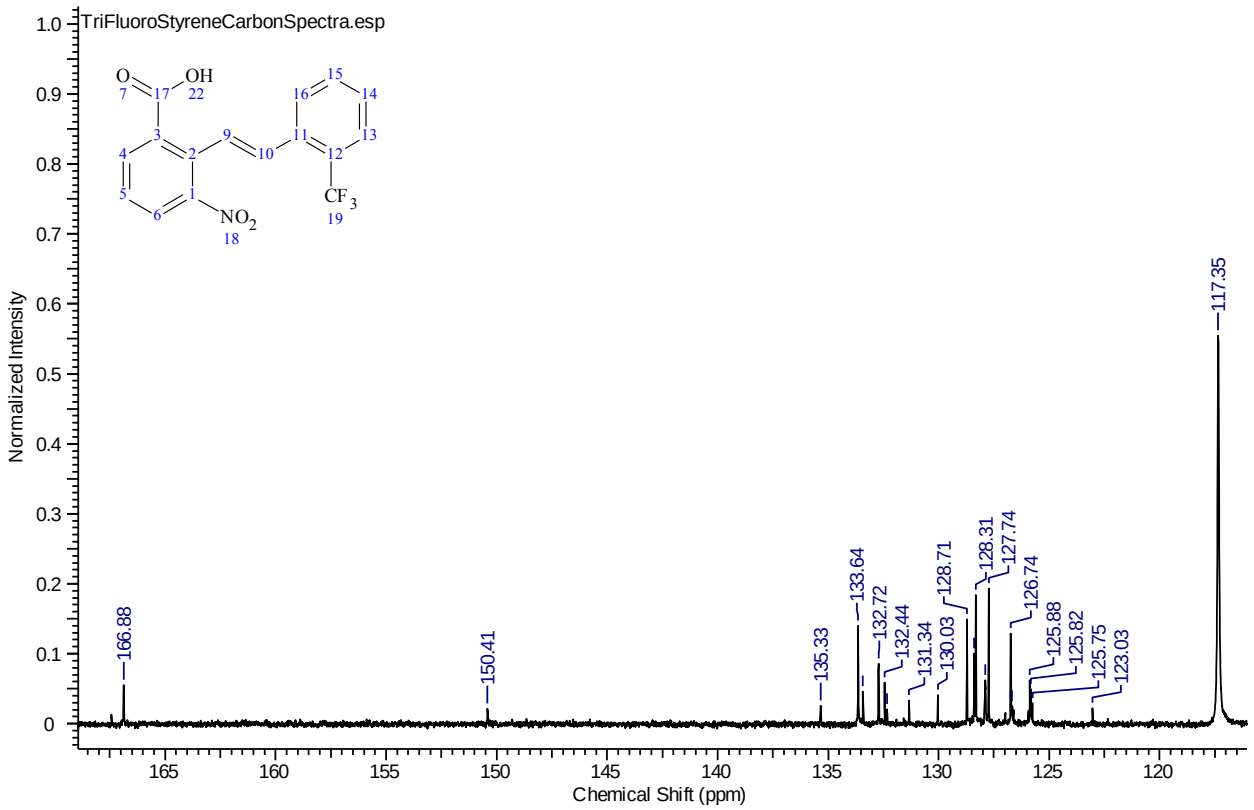

Figure 23: ^{13}C NMR Spectra for 3-nitro-2-{(E)-2-[2-(trifluoromethyl)phenyl]ethenyl} benzoic acid (2a)

Table 3

^{13}C Chemical Shifts for 3-nitro-2-{(E)-2-[2-(trifluoromethyl)phenyl]ethenyl} benzoic acid (2a)

No.	**(ppm)**	**(Hz)**	**Height**
1	117.35	11795.8	0.5547
2	123.03	12367.3	0.0221
3	125.75	12640.4	0.0286
4	125.82	12647.3	0.0494
5	125.88	12653.4	0.0618
6	126.68	12733.5	0.0251

Table 3

Cont.

7	126.74	12740.4	0.1290
8	127.74	12840.3	0.1935
9	127.88	12854.8	0.0623
10	128.31	12898.3	0.1843
11	128.39	12905.9	0.1003
12	128.71	12938.0	0.1496
13	130.03	13070.7	0.0407
14	131.34	13202.0	0.0328
15	132.33	13301.9	0.0209
16	132.44	13312.6	0.0583

4.1.3 Discussion of FT-IR of Nitro-Styrenyl Benzoic Acid: Fourier Transform Infrared Spectroscopy (FT-IR) can be used to confirm structures of organic compounds. This instrument was especially useful in this study as the conversion from a carboxylic acid to an amide was made. For the nitrostyrenyl benzoic acids, compounds 1a-5a, a large O-H stretch is expected due to the carboxylic acid. The carbonyl strectch is also a key indicator of these compounds.

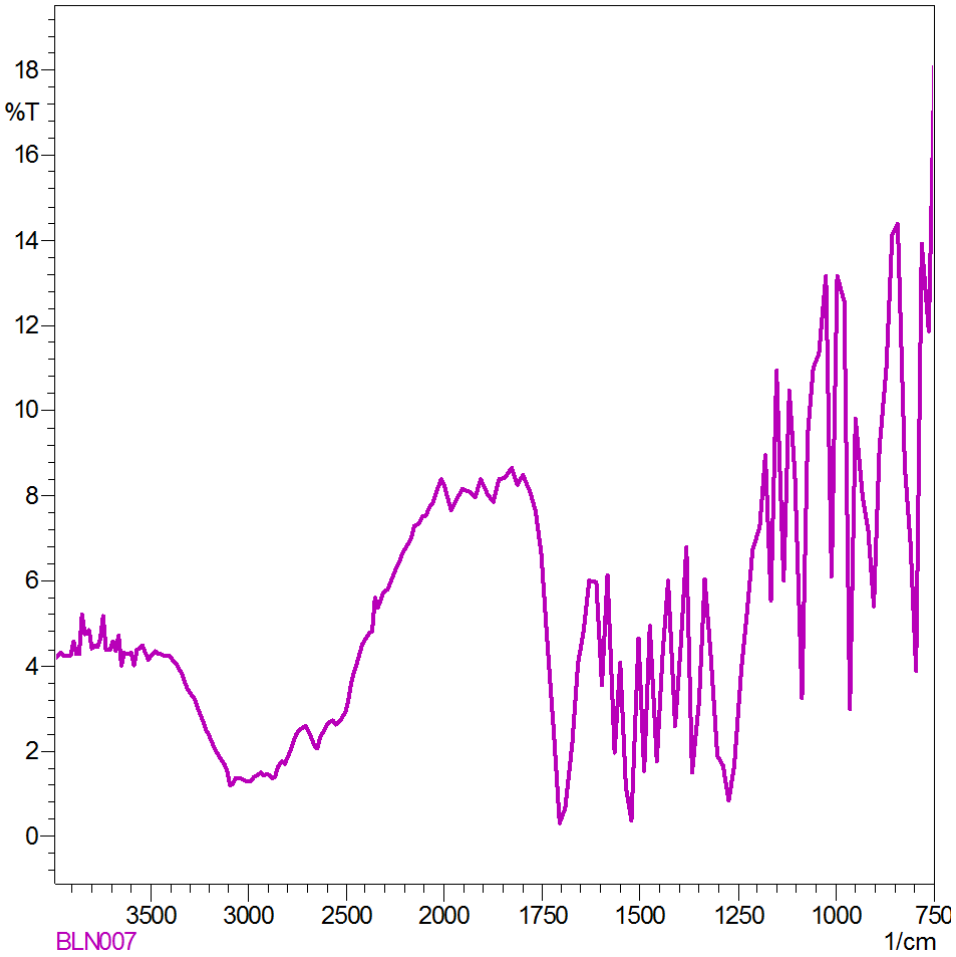

Figure 24: FT-IR Spectra of 2-[(E)-2-(4-bromophenyl) ethenyl]-3-nitrobenzoic acid (4a)

In the FT-IR spectra of 2-[(E)-2-(4-bromophenyl) ethenyl]-3-nitrobenzoic acid (4a), the large O-H stretch can be seen from 3300-2400 1/cm. The carbonyl stretch is shown at 1700 1/cm.

4.2 Synthesis and Characterization of Nitrostyrenyl Amides

The synthesis of the nitrostyrenyl amides can be broken down into two key parts. The first part is the formation of an acid chloride. The mechanism for this is shown in Figure 26. Thionyl chloride reacts with the carbonyl of the carboxylic acid of the nitrostyrenyl benzoic acids. This is followed by a [1, 2] addition of a chlorine (Figure 26) and the subsequent [1, 2] elimination (Figure 27). Chlorine then deprotonates the intermediate to achieve an acid chloride. This reaction also gives side products of $SO_{2\,(g)}$ and $HCl_{\,(g)}$.

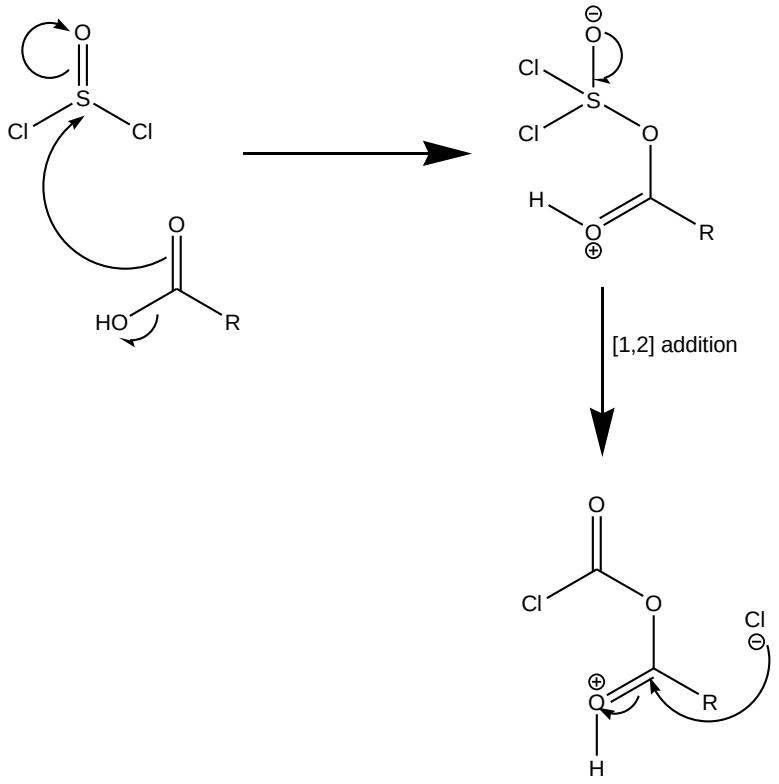

Figure 25: Formation of an Acid Chloride from a Carboxylic Acid, [1,2] addition

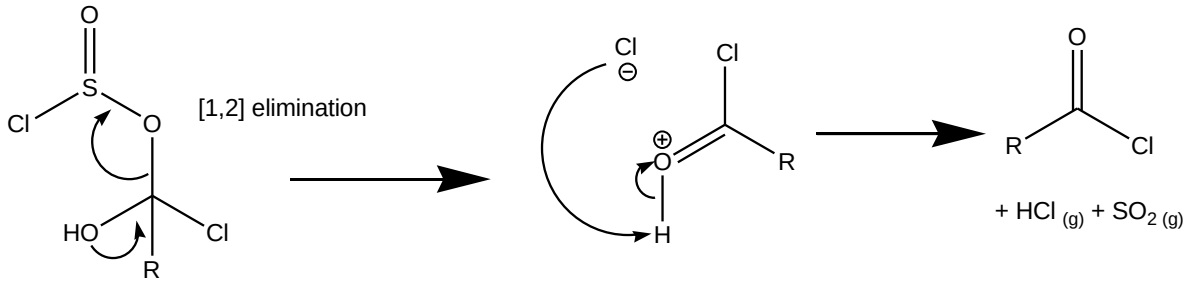

Figure 26: Formation of an Acid Chloride from a Carboxylic Acid , [1,2] elimination

The formation of the acid chloride is then followed by a simple S_N2 substitution reaction in which a base (sodium hydroxide) is used to deprotonate an amine (N-butylamine) in order to replace the chlorine on the acid chloride and form the desired amide.

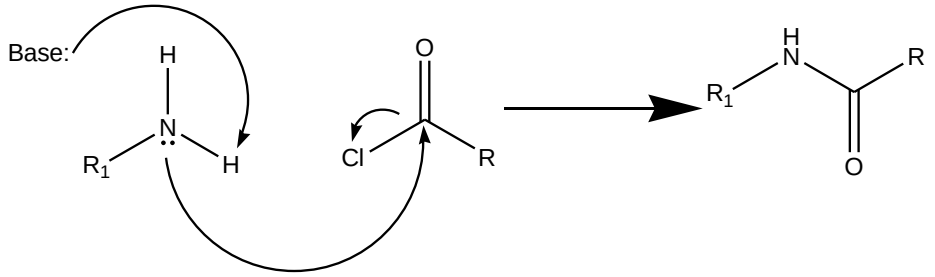

Figure 27: Formation of the Amide

The base will deprotonate the amine before the attack of the carbonyl in this case due to the fact that sodium hydroxide is a strong base.

4.2.1 Use of N,N-dimethylformamide as a Catalyst: The key step of forming the acid chloride can also be achieved by using N,N-Dimethylformamide (DMF) as a catalyst. The use of DMF allows for a quick and efficient synthesis.

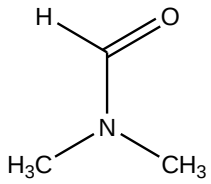

Figure 28: Structure of N,N-Dimethylformamide (DMF)

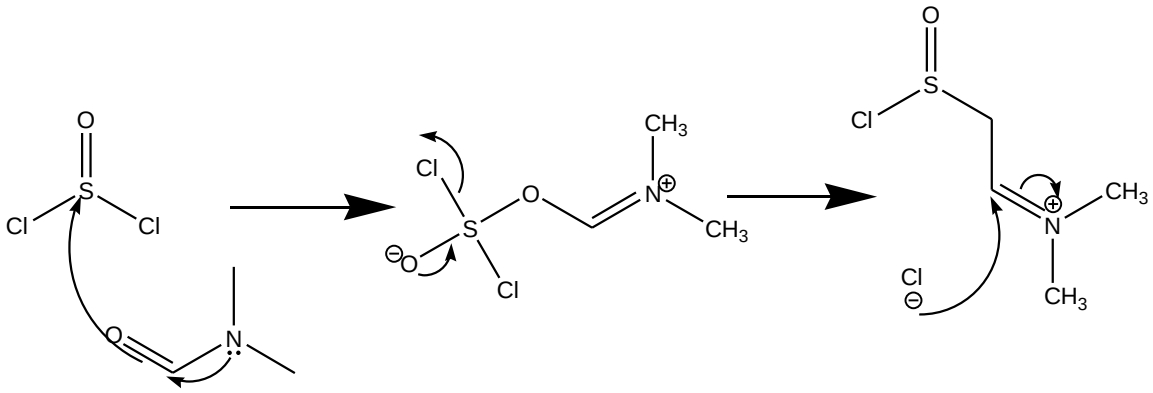

Figure 29: Formation of an Acid Chloride Using Thionyl Chloride & DMF catalyst, Scheme 1

In the mechanism shown, DMF and thionyl chloride react first and a new C=N bond is formed. An unstable chloroimide intermediate containing a carbon-nitrogen double bond is formed when

a chlorine anion is released that can then attack the carbon of the C=N bond. Sulfer dioxide gas and chloride gas are released and a chloroimide intermediate forms which can react with the nitrostyrenyl carboxylic acid compound, Figure 30.

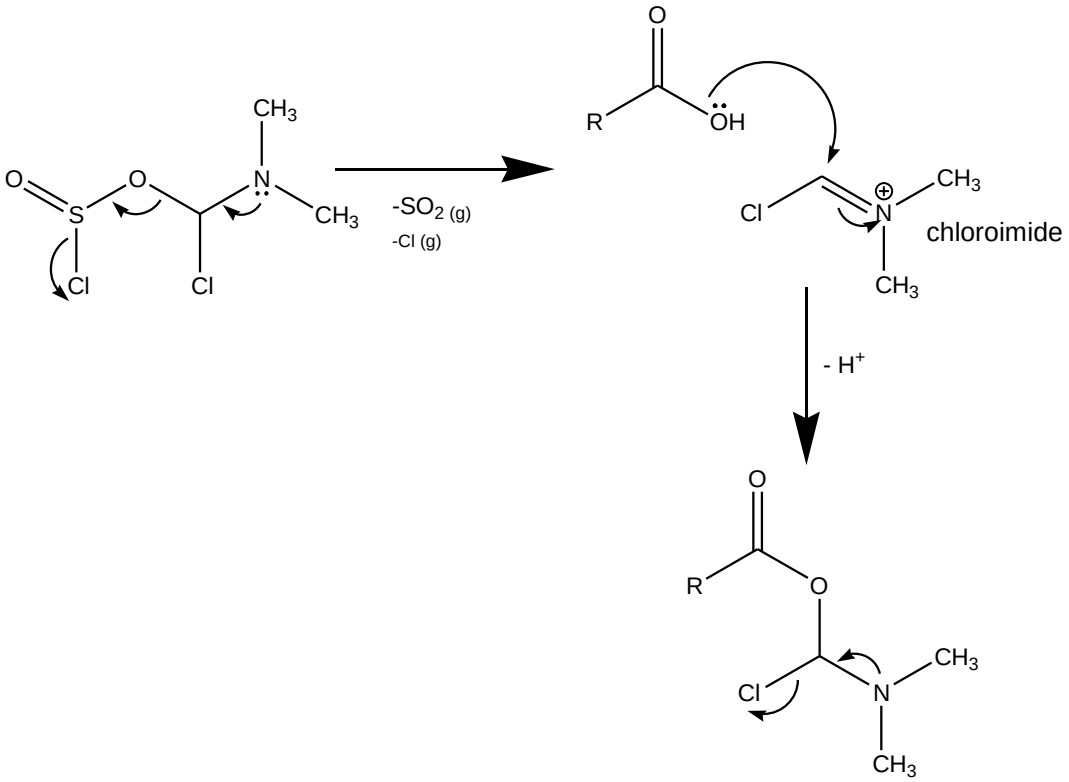

Figure 30: Formation of an Acid Chloride Using Thionyl Chloride & DMF catalyst ,Scheme 2

In the final step of the mechanism (Figure 32) the acid chloride is produced and the DMF catalyst is regenerated.

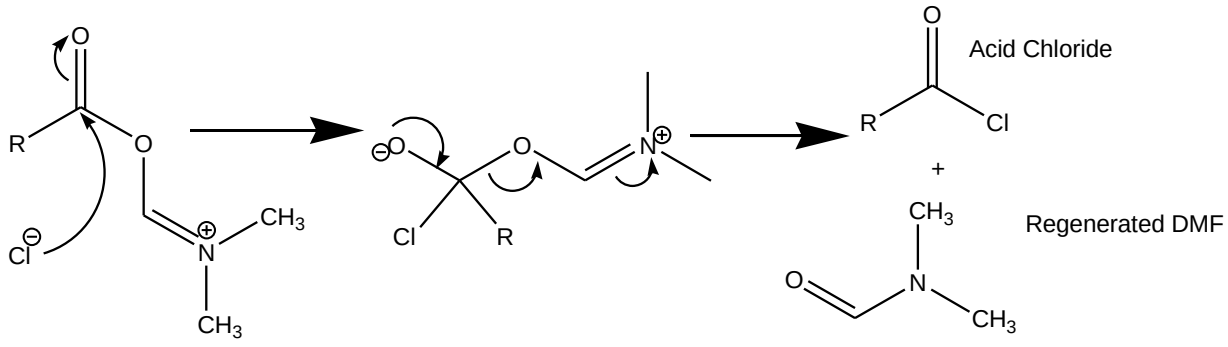

Figure 31: Formation of an Acid Chloride Using Thionyl Chloride & DMF catalyst, Scheme 3

4.2.2 Nitro Styrenyl Amide Products: The nitrostyrenyl amide products, 1b-5b, are shown in the table below with a percent yield range 15.9-87.7%.

Table 4

Summary of Nitrostyrenyl Amide Products

Compound	Structure	Name	% Yield
1b	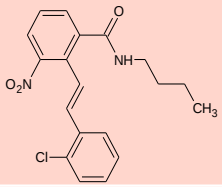	2-(2-chlorostyryl)-N-butyl-3-nitrobenzamide	87.7
2b	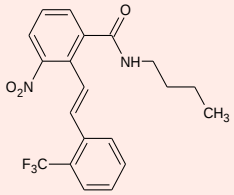	2-(2-(trifluoromethyl)styryl)-N-butyl-3-nitrobenzamide	15.9
3b	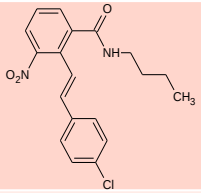	2-(4-chlorostyryl)-N-butyl-3-nitrobenzamide	57.2
4b	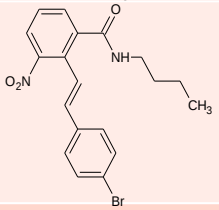	2-(4-bromostyryl)-N-butyl-3-nitrobenzamide	48.8
5b	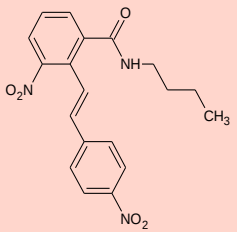	2-(4-nitrostyryl)-N-butyl-3-nitrobenzamide	61.7

4.2.3 NMR Characterization of Nitro-Styrenyl Amides: The NMR spectra for the amide derivatives show key differences from the nitrostyrenyl benzoic acids. The N-butyl chain is observed in the spectra in the region between 0.5-3.5ppm.

4.2.3.1 Discussion of Nitro-Styrenyl Amide Proton NMR: The proton NMR spectra for 2-(2-(trifluoromethyl)styryl)-N-butyl-3-nitrobenzamide (2b) shows the four peaks for the N-butyl chain at 0.76ppm, 1.27ppm, 1.41ppm and 3.26ppm. The proton on the carbon adjacent to the nitrogen shows up at 3.26ppm. The protons of the N-butyl chain are in a 2:2:2:3 ratio (-$CH_2CH_2CH_2CH_3$) in terms of integration. The nine protons on the ring structures (also including the two styrenyl protons) are shown in the aromatic region from 7.03-8.00ppm.The N-H proton does not show up in the spectra due to the acetonitrile solvent used.

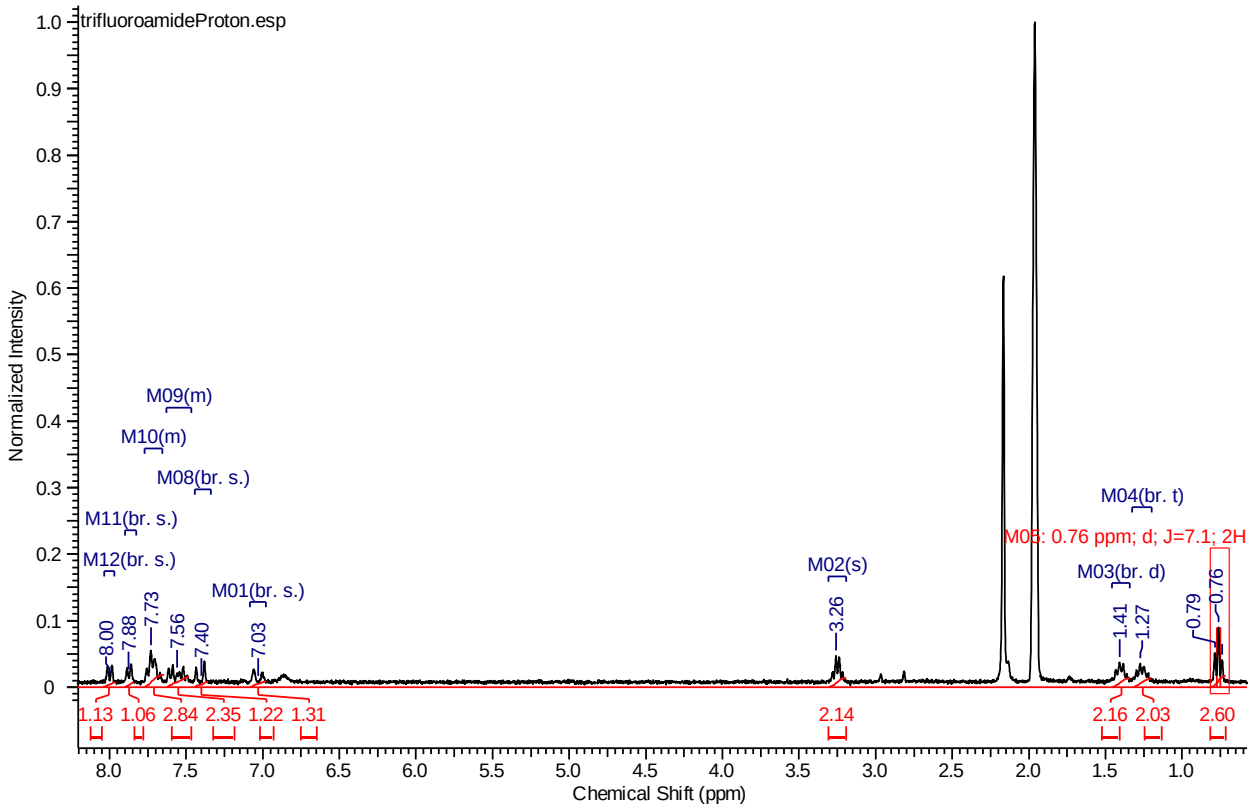

Figure 32: ^{1}H NMR of 2-(2-(trifluoromethyl)styryl)-N-butyl-3-nitrobenzamide (2b)

Table 5

Summary of Proton Chemical Shifts for 2-(2-(trifluoromethyl)styryl)-N-butyl-3-nitrobenzamide (2b)

No.	**(ppm)**	**(Hz)**	**Height**
1	0.74	222.5	0.0406
2	0.76	229.6	0.0900
3	0.79	236.7	0.0516
4	1.27	382.8	0.0353
5	1.41	423.6	0.0371
6	3.26	980.2	0.0469
7	7.03	2114.1	0.0087
8	7.40	2225.3	0.0084
9	7.56	2273.2	0.0216
10	7.73	2324.7	0.0549
11	7.88	2369.0	0.0184
12	8.00	2405.7	0.0118

4.2.3.2 Discussion of Nitro-Styrenyl Amide Carbon NMR: The carbons of the aromatic ring and Styrenyl carbons will be observed in the same region for the amide derivatives. However, the four carbons associated with the N-butyl chain will also be observed in the aliphatic region.

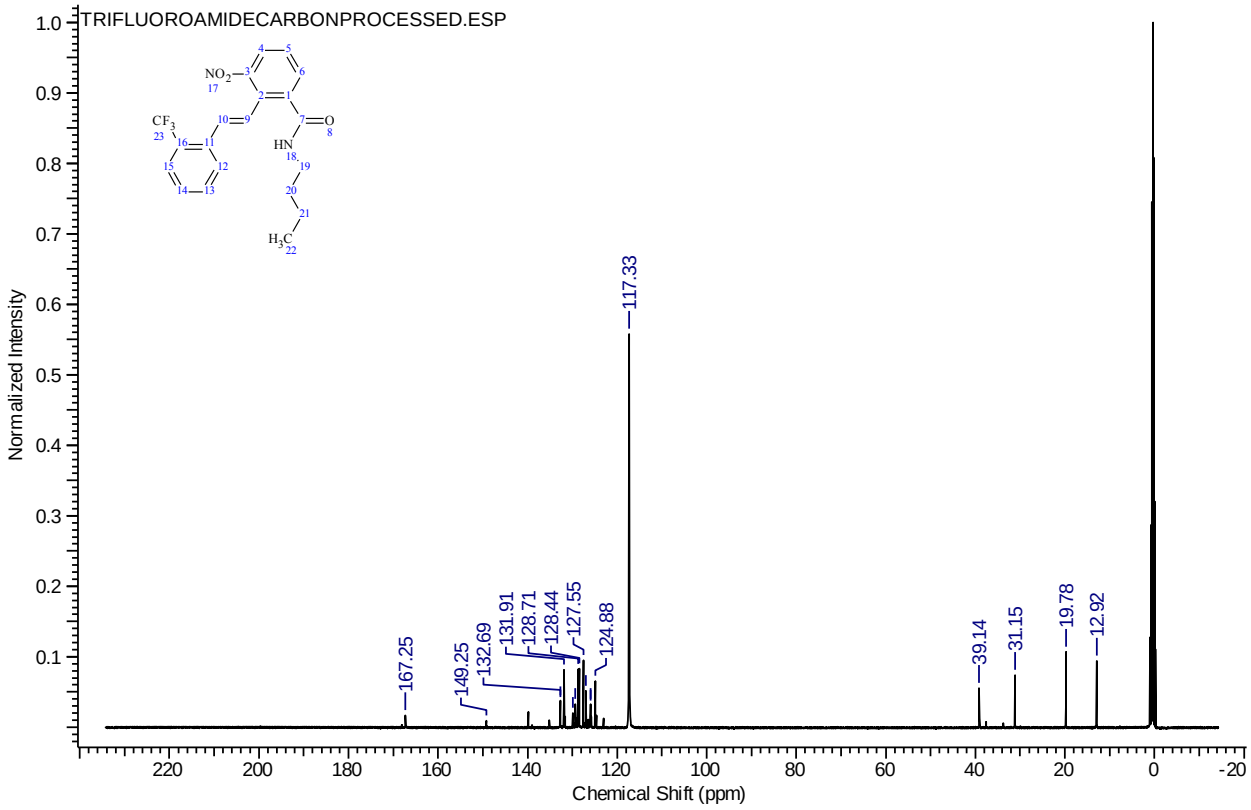

Figure 33: ^{13}C NMR Spectra for 2-(2-(trifluoromethyl)styryl)-N-butyl-3-nitrobenzamide (2b)

The chemical shifts for the twenty carbons of the 2-(2-(trifluoromethyl)styryl)-N-butyl-3-nitrobenzamide (2b) product are given in Table 8.

Table 6

^{13}C NMR Chemical Shifts for 2-(2-(trifluoromethyl)styryl)-N-butyl-3-nitrobenzamide (2b)

No.	**(ppm)**	**(Hz)**	**Height**
1	12.92	1299.0	0.0937

Table 6

Cont.

2	19.78	1987.9	0.1068
3	31.15	3130.8	0.0739
4	39.14	3934.2	0.0550
5	117.33	11794.3	0.5576
6	124.88	12553.4	0.0655
7	125.88	12653.4	0.0324
8	125.94	12659.5	0.0298
9	126.94	12760.2	0.0514
10	127.55	12821.2	0.0949
11	128.44	12911.3	0.0827
12	128.71	12938.0	0.0822
13	129.31	12998.2	0.0300
14	129.33	13000.5	0.0325
15	129.88	13055.5	0.0200
16	131.91	13259.9	0.0810
17	132.68	13337.0	0.0350
18	132.69	13338.5	0.0381
19	149.25	15002.5	0.0091
20	167.25	16812.3	0.0168

Figure 35 shows the aliphatic region of the spectra and the four carbons of the N-butyl chain at 12.92ppm, 19.78ppm, 31.15ppm and 39.14ppm.

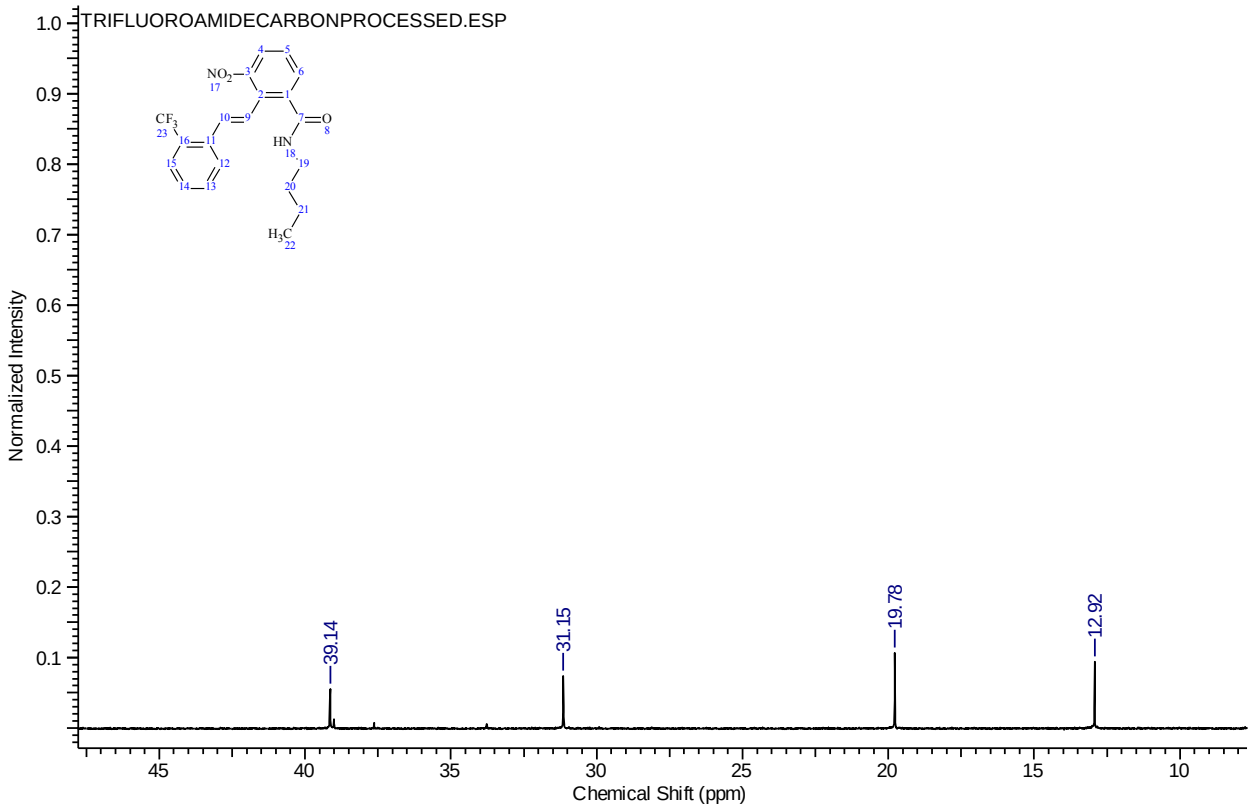

Figure 34: ^{13}C NMR Aliphatic region for 2-(2-(trifluoromethyl)styryl)-N-butyl-3-nitrobenzamide (2b)

The carbon spectra in Figure 36 show the aromatic region. The trifluoromethyl carbon is observed at 117.33ppm. The carbonyl carbon is observed at 167.26ppm and the carbon with the nitro functional group attached is observed at 149.25ppm. All aromatic ring carbons are observed in the region of 126-133ppm with those associated with the amide ring being more downfield. The carbons associated with the alkene are observed at 124.88ppm and 125.88ppm.

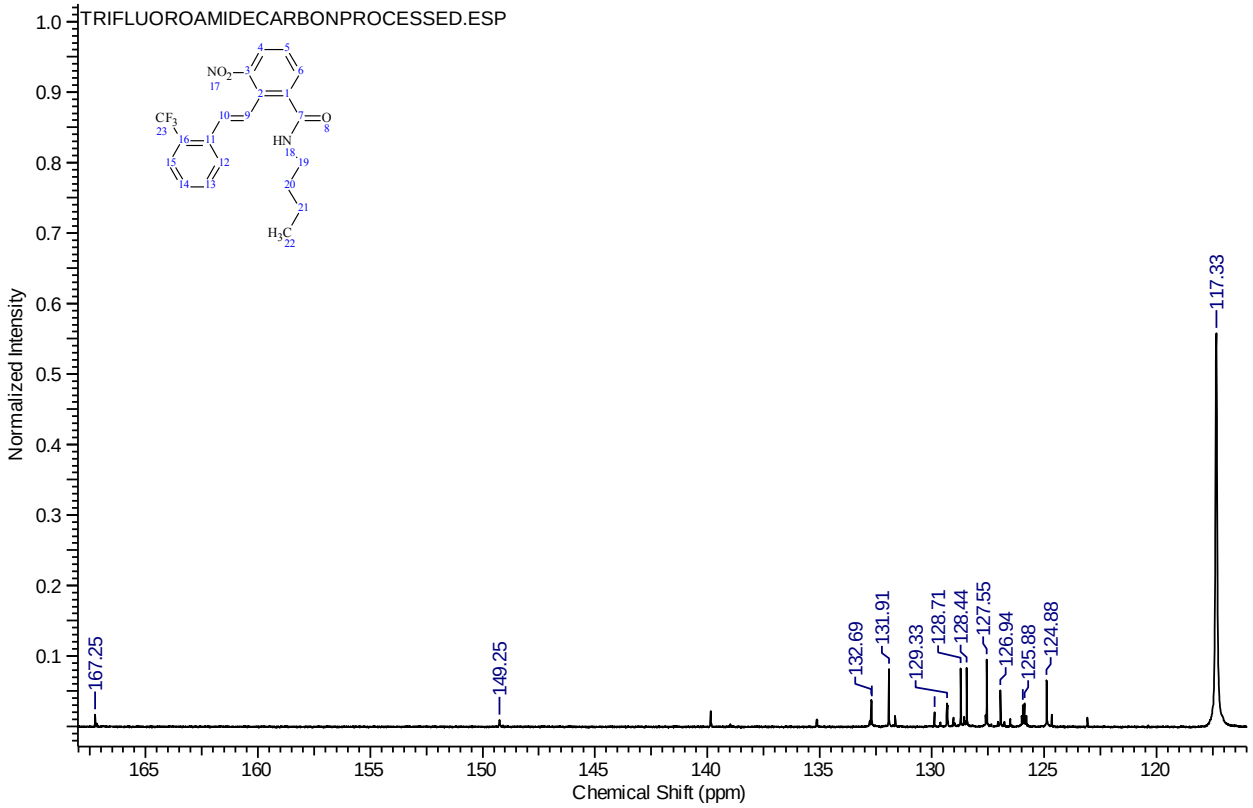

Figure 35: ^{13}C NMR Aromatic region for 2-(2-(trifluoromethyl)styryl)-N-butyl-3-nitrobenzamide (2b)

4.2.4 Discussion of FT-IR of Nitro-Styrenyl Amide: The FT-IR spectra for 2-(2-(trifluoromethyl)styryl)-N-butyl-3-nitrobenzamide (2b) is shown below. The large O-H stretch seen in the spectra for compound 2a is no longer seen in the amide derivative.

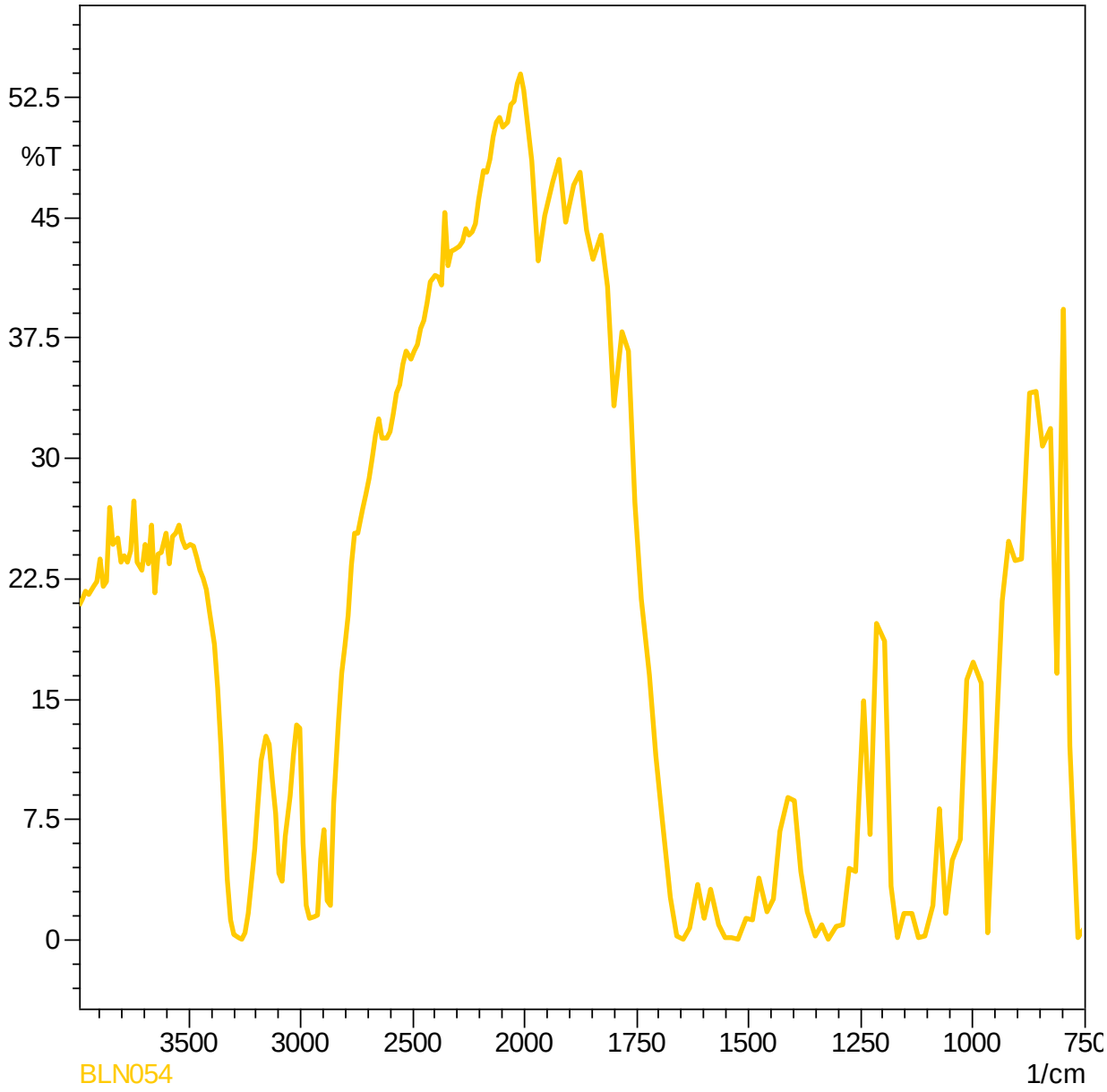

Figure 36: FT-IR Spectra of 2-(2-(trifluoromethyl)styryl)-N-butyl-3-nitrobenzamide (2b)

The smaller N-H stretch can be seen at 3300 1/cm. The N-H stretch also shows an overtone at 3150 1/cm. From 3000-2900 1/cm the C-N stretch can be seen. The Carbonyl stretch for the amide derivative is shown at 1670 1/cm.

4.3 Use of HPLC to Determine Purity of Compounds

High performance liquid chromatography (HPLC) can be used to determine purity and content of organic compounds. A pure compound will show a single peak at the expected elution time.

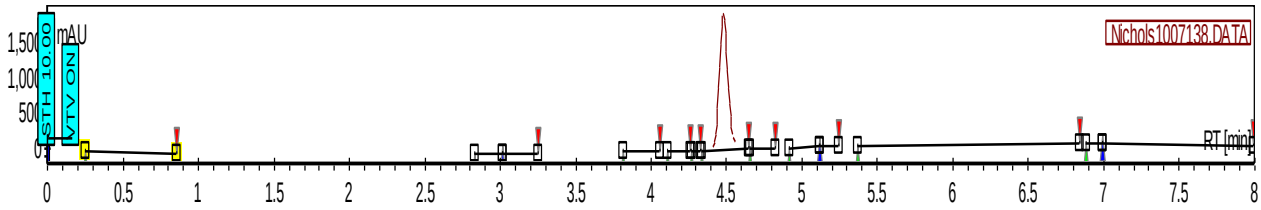

Figure 37: HPLC Chromatogram for 3-nitro-2-{(E)-2-[2-(trifluoromethyl)phenyl]ethenyl} benzoic acid (2a)

The chromatogram for compound 2a shows an elution time of 4.5 minutes.

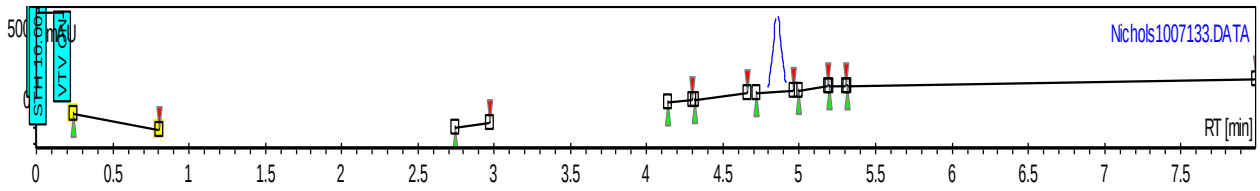

*Figure 38:*HPLC Chromatogram for 2-(2-(trifluoromethyl)styryl)-N-butyl-3-nitrobenzamide (2b)

The chromatogram for the amide derivative of compound 2a (compound 2b) shows an elution time of 4.9 minutes. The amide derivative should be expected to have a higher retention time due to the difference in mass and a stronger interaction with the absorption material. The amide derivative also shows a small impurity at 4.5 minutes which is most likely a small percentage of left over starting material.

4.4 Fluorine NMR Characterization of Compounds 2a and 2b

Fluorine NMR was also used to characterize compounds 2a and 2b due to the trifluoromethyl groups at the ortho position of each structure.

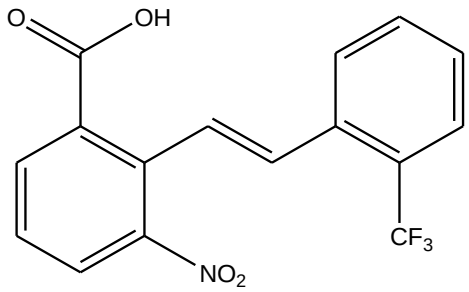

Figure 39: Structure of 3-nitro-2-{(E)-2-[2-(trifluoromethyl)phenyl]ethenyl} benzoic acid (2a)

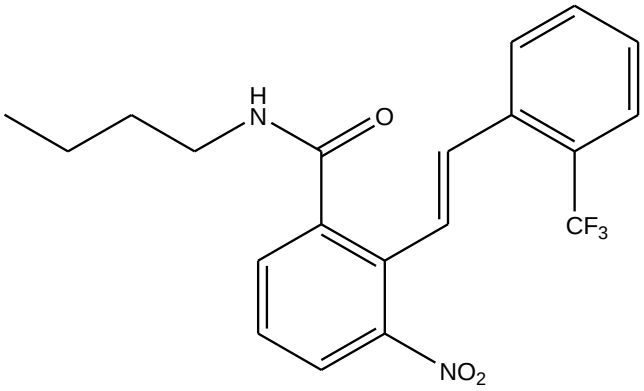

Figure 40: 2-(2-(trifluoromethyl)styryl)-N-butyl-3-nitrobenzamide (2b)

The fluorine NMR spectrum for compound 2a, Figure, shows a single peak for the trifluoromethyl group at -59.95ppm.

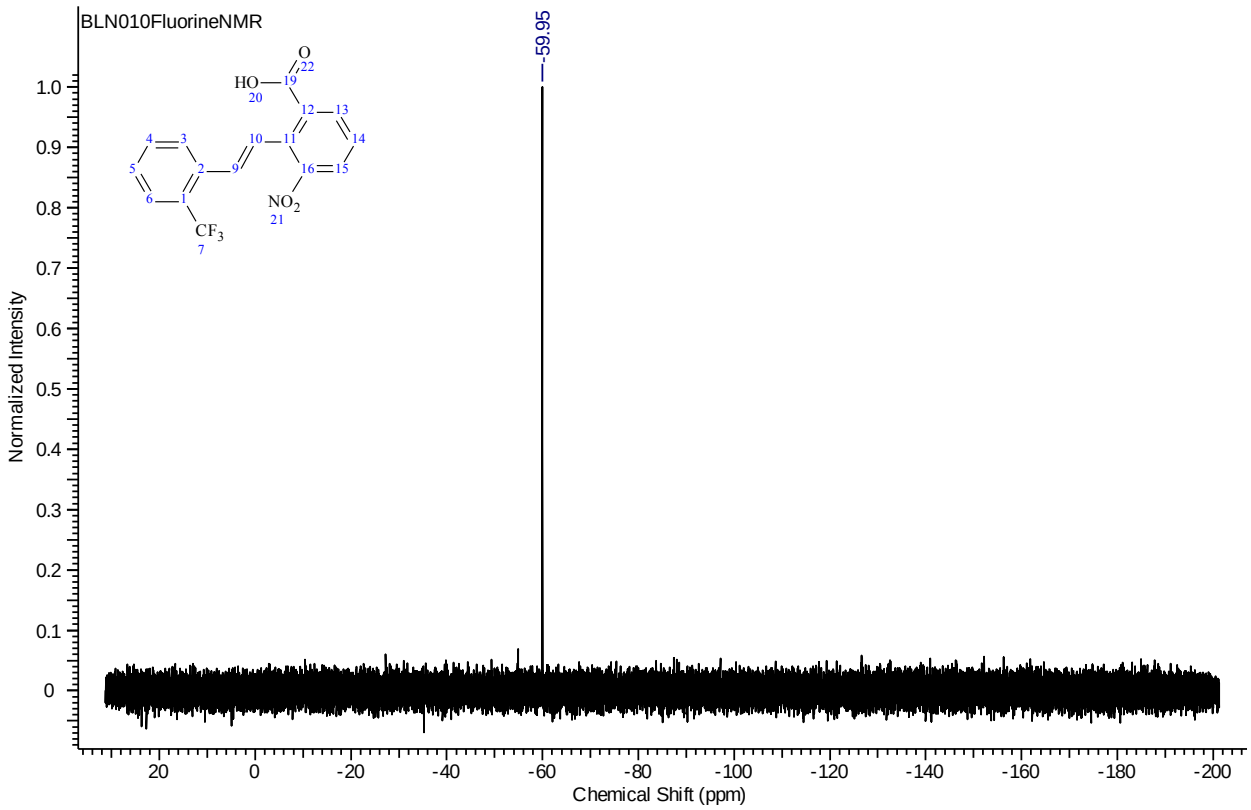

Figure 41: Fluorine NMR Spectra for 3-nitro-2-{(E)-2-[2-(trifluoromethyl)phenyl]ethenyl} benzoic acid (2a)

The spectrum for the fluorine NMR of compound 2b, shows two peaks at -59.70ppm and -59.75ppm. Only one peak is expected for this structure and the observation of two peaks suggests that either an impurity such as the acid chloride is present or that a resonance form of the product is also present in the product. A resonance form would show a slight difference in chemical shift for the trifluoromethyl group as observed in the spectrum.

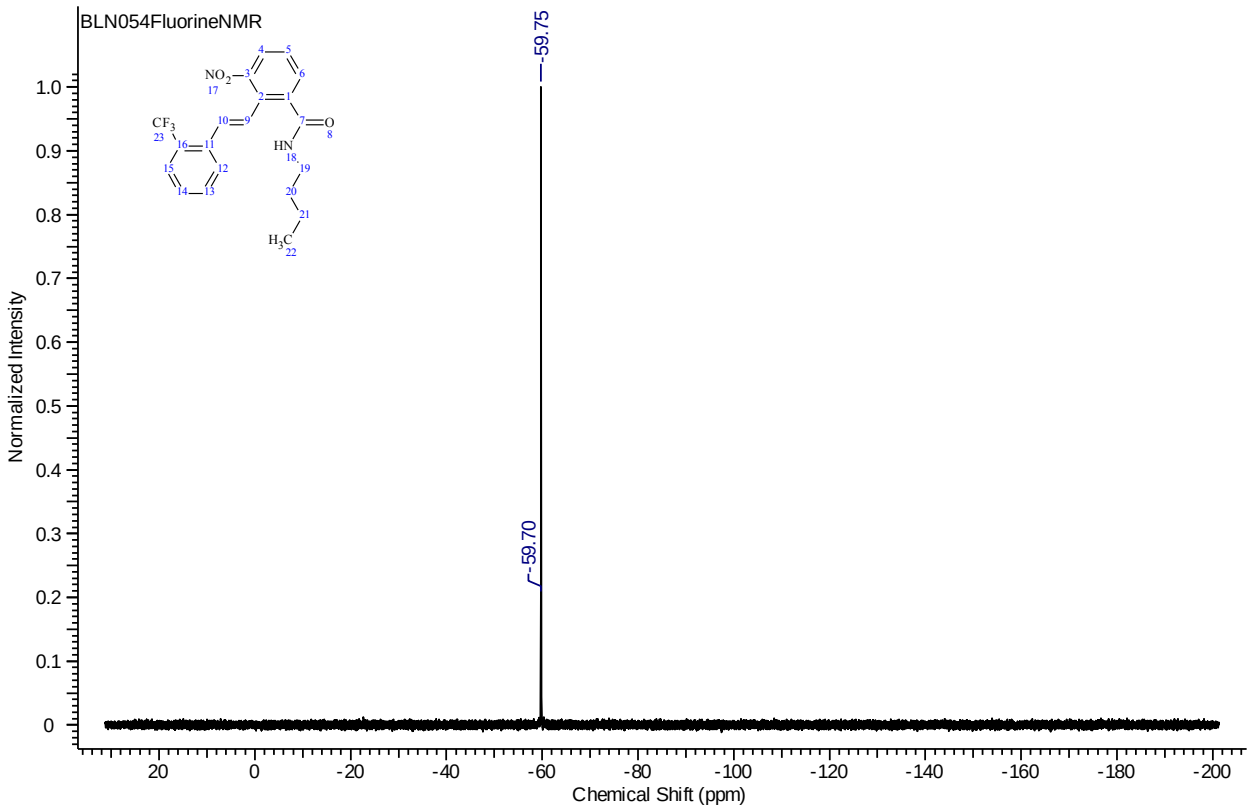

Figure 42: Fluorine NMR Aromatic region for 2-(2-(trifluoromethyl)styryl)-N-butyl-3-nitrobenzamide (2b)

4.5 Biological Analysis Using the NC-60 Cell Line Screening

The NCI60 anticancer drug screening program was developed by the US National Cancer Institute in the 1980s. The screen was developed in order to expand the scope of cancer drug discovery beyond leukemia models from transplantable murine neoplasms (Shoemaker, 2006). These previous modeled studies were not ideal for examining clinical activity and there was a need for a method to test solid human tumors. Researchers began with renal epithelial cells and found that they responded in vitro to anti-cancer drugs. Realizing that other tumor cell lines were needed as controls, panels of cell lines were created. These panels represent the nine major tumor types: leukemia, colon, lung, CNS (central nervous system), renal, melanoma, ovarian, breast and prostate (Shoemaker, 2006).

4.5.1 Testing Results for 2-[(E)-2-(4-chlorophenyl)ethenyl]-3-nitrobenzoic acid (3a):

The testing results for 2-[(E)-2-(4-chlorophenyl)ethenyl]-3-nitrobenzoic acid (3a) have been obtained from the National Institutes of Health. These results are summarized in the graph below, Figure 44. The diagram shows the effect of the compound on the growth rate for each cell line. The goal is to exhibit the lowest growth percent possible for the cancerous cells. These results are from a single dosage testing on the NCI60 cancer cell line. Compound 3a did not exhibit favorable results in the study. In each cell line tested, 3a neither slowed the growth of cancerous cells nor caused them to go into apoptosis. The best result came from the non-small cell lung cancer line HOP-92 which inhibited growth by 13.56%.

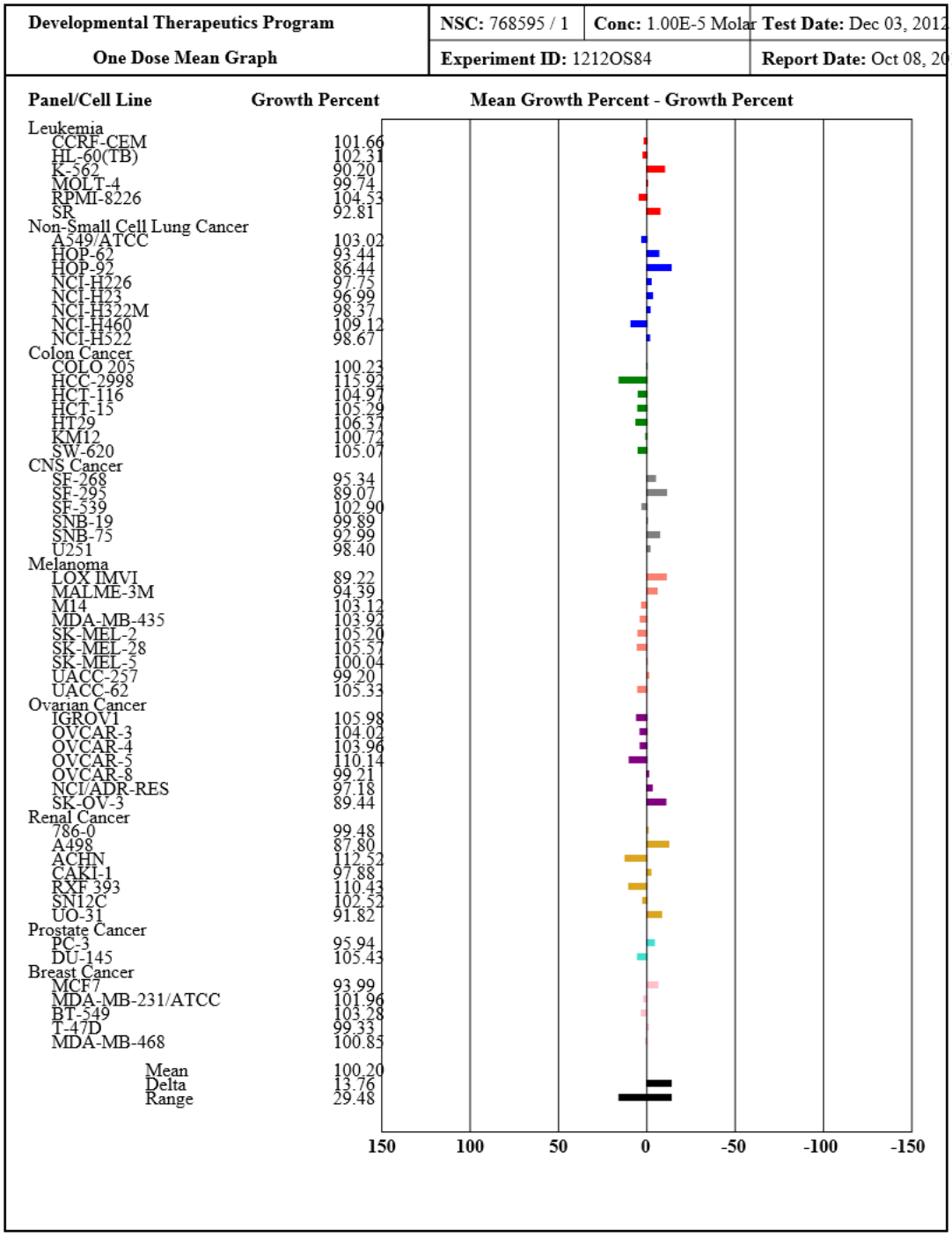

Figure 43: NCI60 Single Dose Test Results for Compound 3a

CHAPTER 5

Future Research

5.1 Conclusion and Future Work

The amide derivatives synthesized will undergo screening with the NCI60 cell line. The results of these studies will be used to determine a pattern of biological activity for the compounds. Additional amide derivatives will be synthesized and tested in order to establish the most accurate pattern. It is expected that the amide derivatives will show greater activity towards the cell lines than the carboxylic acid compounds have shown. It is also believed that the amide functionality should minimize the growth rate of the cancer cells.

In addition to the derivatives achieved with the N-butyl amine, compounds with other amine groups will also be synthesized for biological testing. The goal is to gain an understanding of the effect nitrostyrenyl amides have on the processes of cancer cell proliferation and apoptosis. Once a pattern is established it can be used to create better chemopreventives.

References

American Cancer Society. Cancer Facts & Figures 2013. Atlanta: American Cancer Society; 2013.

Chang, S., Na, Y., Shin, H. J., Choi, E., & Jeong, L. S. (2002). A short and efficient synthetic approach to hydroxy (E)-stilbenoids via solid-phase cross metathesis. *Tetrahedron Letters, 43*(41), 7445-7448. doi: http://dx.doi.org/10.1016/S0040-4039(02)01528-9

Gurpinar, E., Grizzle, W. E., Shacka, J. J., Mader, B. J., Li, N., Piazza, N. A., . . . Piazza, G. A. (2013). A novel sulindac derivative inhibits lung adenocarcinoma cell growth through suppression of Akt/mTOR signaling and induction of autophagy. *Mol Cancer Ther, 12*(5), 663-674. doi: 10.1158/1535-7163.mct-12-0785

Horvath, Z., Handler, N., Saiko, P., Madlener, S., Illmer, C., Murias, M., . . . Szekeres, T. (2004). 574 Comparative study of anticancer and apoptosis-inducing activity of stilbene derivatives in HL-60 human promyelocytic leukemia cells. *European Journal of Cancer Supplements, 2*(8), 174. doi: 10.1016/s1359-6349(04)80582-2

Juan, M. E. l., Wenzel, U., Daniel, H., & Planas, J. M. (2008). Resveratrol Induces Apoptosis through ROS-Dependent Mitochondria Pathway in HT-29 Human Colorectal Carcinoma Cells. *Journal of Agricultural and Food Chemistry, 56*(12), 4813-4818. doi: 10.1021/jf800175a

Kang, N. J., Shin, S. H., Lee, H. J., & Lee, K. W. (2011). Polyphenols as small molecular inhibitors of signaling cascades in carcinogenesis. *Pharmacology & Therapeutics, 130*(3), 310-324. doi: 10.1016/j.pharmthera.2011.02.004

Kuroda, Y., & Hara, Y. (1999). Antimutagenic and anticarcinogenic activity of tea polyphenols. *Mutation Research/Reviews in Mutation Research, 436*(1), 69-97. doi: 10.1016/s1383-5742(98)00019-2

Lee, S. K., Zhang, W., & Sanderson, B. J. S. (2008). Selective Growth Inhibition of Human Leukemia and Human Lymphoblastoid Cells by Resveratrol via Cell Cycle Arrest and Apoptosis Induction. *Journal of Agricultural and Food Chemistry, 56*(16), 7572-7577. doi: 10.1021/jf801014p

Liang, L., Tajmir-Riahi, H. A., & Subirade, M. (2007). Interaction of β-Lactoglobulin with Resveratrol and its Biological Implications. *Biomacromolecules, 9*(1), 50-56. doi: 10.1021/bm700728k

Likhtenshtein, G. (2010). *Stilbenes. applications in chemistry, life sciences and materials science*. WILEY-VCH Verlag GmbH & Co. KGaA, Weinheim.

Lion, C. J., Matthews, C. S., Stevens, M. F. G., & Westwell, A. D. (2005). Synthesis, Antitumor Evaluation, and Apoptosis-Inducing Activity of Hydroxylated (E)-Stilbenes. *Journal of Medicinal Chemistry, 48*(4), 1292-1295. doi: 10.1021/jm049238e

Liu, X., Yue, P., Zhou, Z., Khuri, F. R., & Sun, S.-Y. (2004). Death Receptor Regulation and Celecoxib-Induced Apoptosis in Human Lung Cancer Cells. *Journal of the National Cancer Institute, 96*(23), 1769-1780. doi: 10.1093/jnci/djh322

Mao, J. T., Roth, M. D., Fishbein, M. C., Aberle, D. R., Zhang, Z. F., Rao, J. Y., . . . Elashoff, D. (2011). Lung cancer chemoprevention with celecoxib in former smokers. *Cancer Prev Res (Phila), 4*(7), 984-993. doi: 10.1158/1940-6207.capr-11-0078

Mehta, N., Aggarwal, S., Thareja, S., Malla, P., Misra, M., Bhardwaj, T. R., & Kumar, M. (2010). SYNTHESIS, PHARMACOLOGICAL AND TOXICOLOGICAL

EVALUATION OF AMIDE DERIVATIVES OF IBUPROFEN. [Article]. *International Journal of ChemTech Research, 2*(1), 233-238.

Piazza, G. A., Keeton, A. B., Tinsley, H. N., Gary, B. D., Whitt, J. D., Mathew, B., . . . Reynolds, R. C. (2009). A novel sulindac derivative that does not inhibit cyclooxygenases but potently inhibits colon tumor cell growth and induces apoptosis with antitumor activity. [Research Support, N I H , Extramural]. *Cancer Prev Res, 2*(6), 572-580.

Rimando, A. M., & Suh, N. (2008). Biological/chemopreventive activity of stilbenes and their effect on colon cancer. [Research Support, N I H , Extramural Research Support, Non-U S Gov't Review]. *Planta Med, 74*(13), 1635-1643.

Sporn MB, Lippman SM. Agents for Chemoprevention and Their Mechanism of Action. In: Kufe DW, Pollock RE, Weichselbaum RR, et al., editors. Holland-Frei Cancer Medicine.6th edition. Hamilton (ON): BC Decker; 2003. Available from: http://www.ncbi.nlm.nih.gov/books/NBK12522/

Thomas Christian Lines. (2006). Patent No. 20120225833 A1. Washington, DC: U.S. Patent and Trademark Office.

Tsao, A. S., Kim, E. S., & Hong, W. K. (2004). Chemoprevention of Cancer. *CA: A Cancer Journal for Clinicians, 54*(3), 150-180. doi: 10.3322/canjclin.54.3.150

Appendix A

^{1}H NMR Spectra

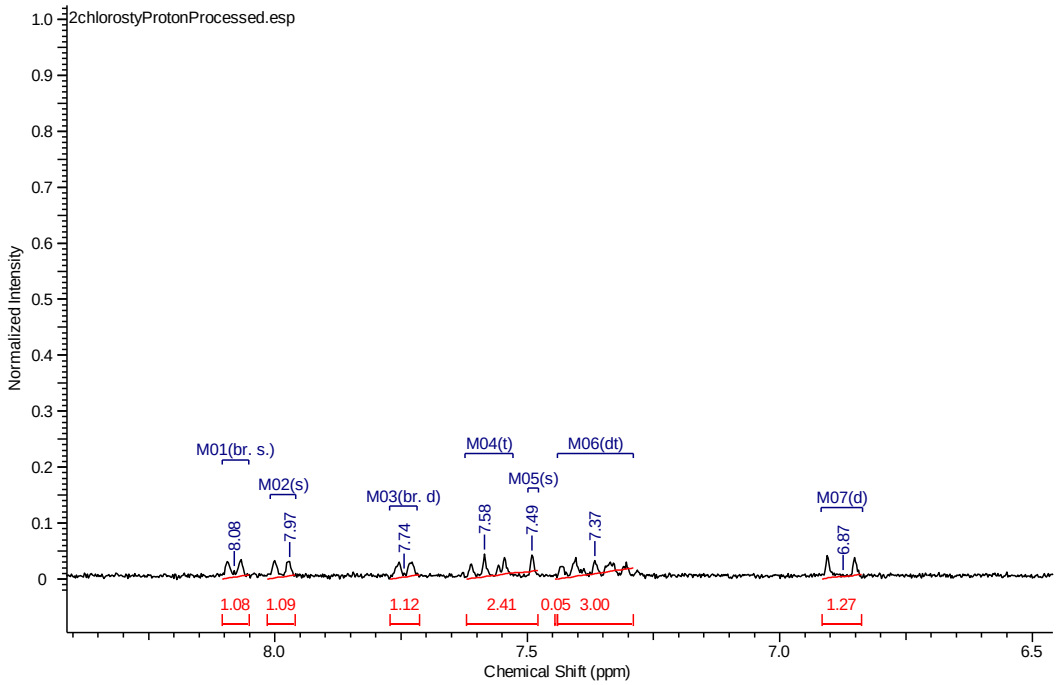

Figure 1.A: 2-[(E)-2-(2-chlorophenyl) ethenyl]-3-nitrobenzoic acid (1a)

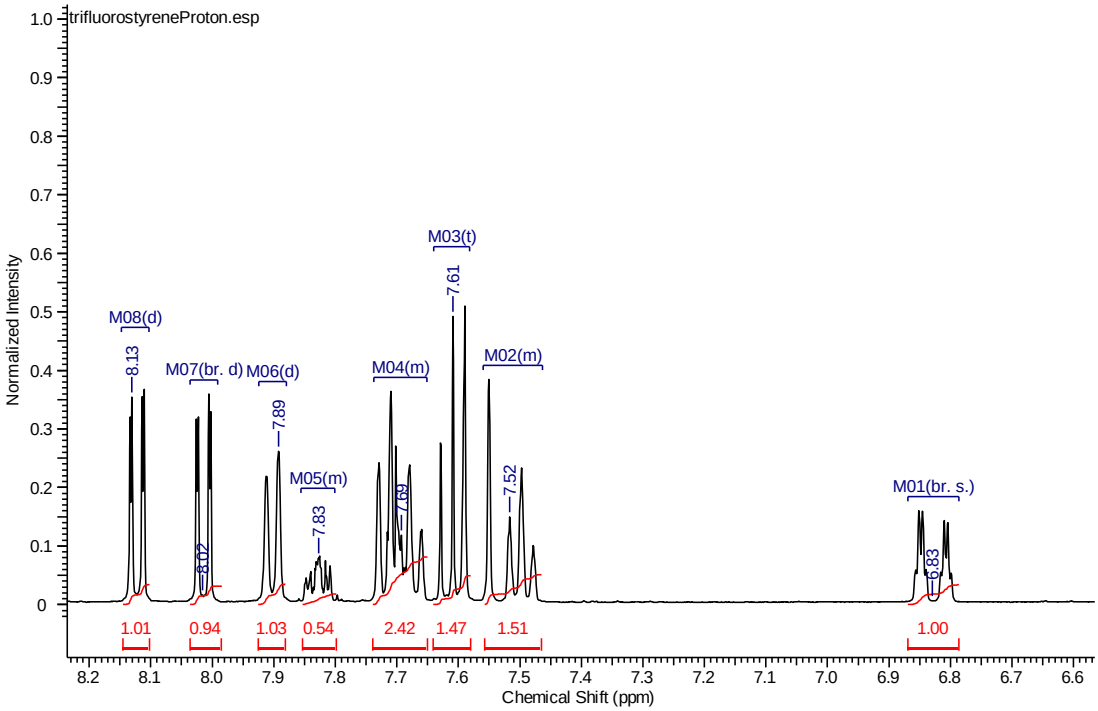

Figure 2.A: 3-nitro-2-{(E)-2-[2-(trifluoromethyl)phenyl]ethenyl} benzoic acid (2a)

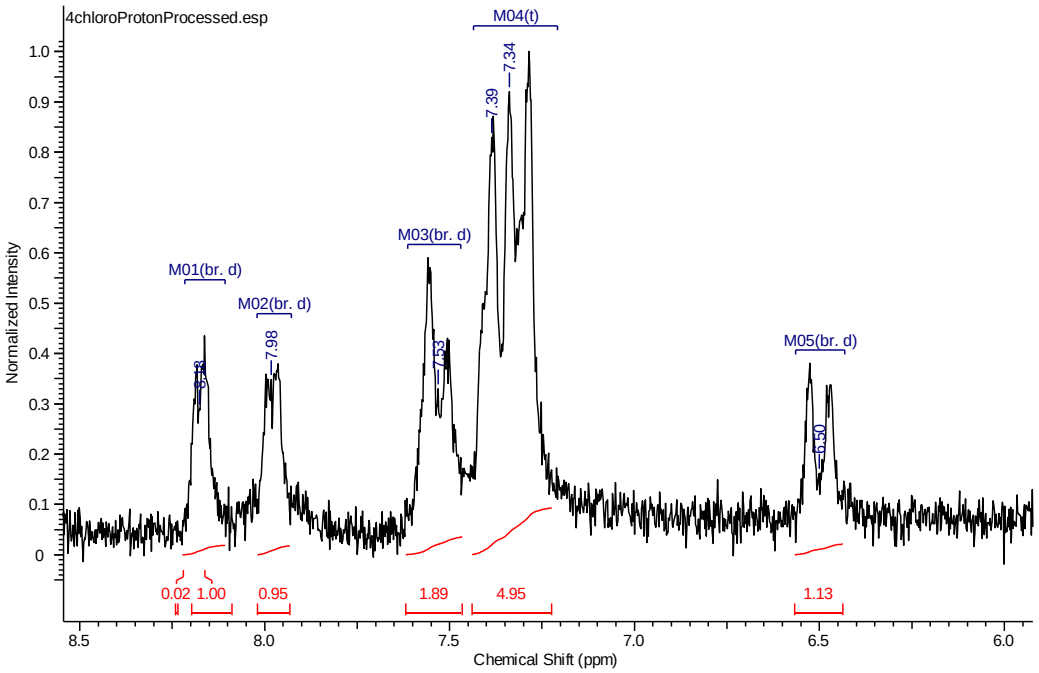

Figure 3.A: 2-[(E)-2-(4-chlorophenyl)ethenyl]-3-nitrobenzoic acid (3a)

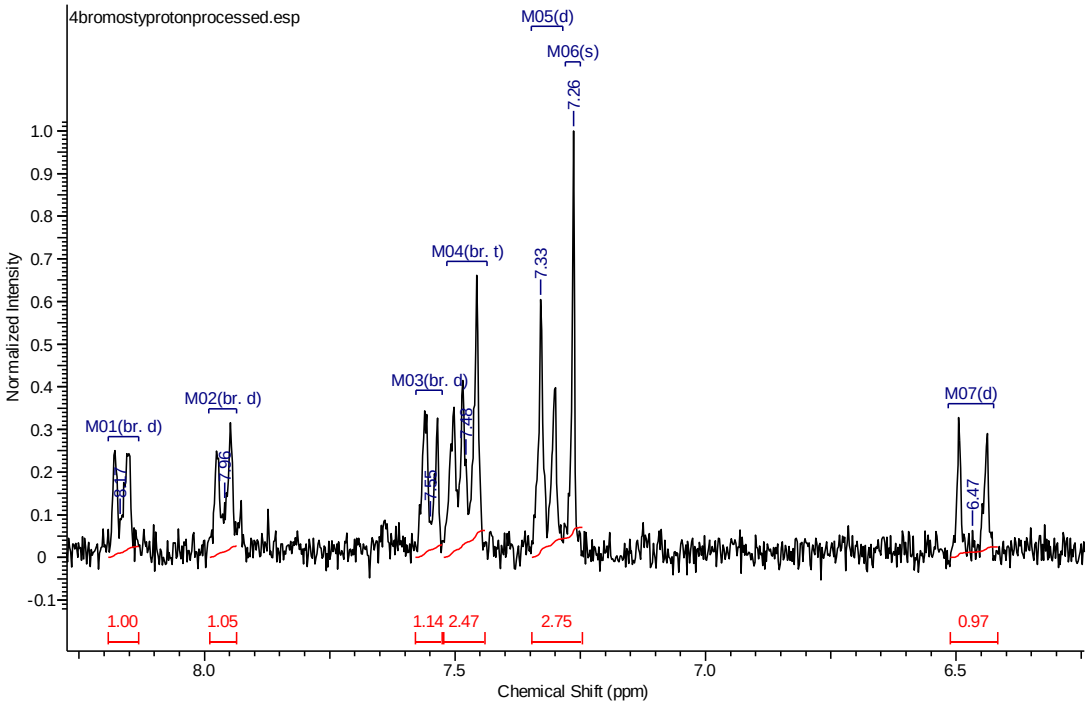

Figure 4.A: 2-[(E)-2-(4-bromophenyl) ethenyl]-3-nitrobenzoic acid (4a)

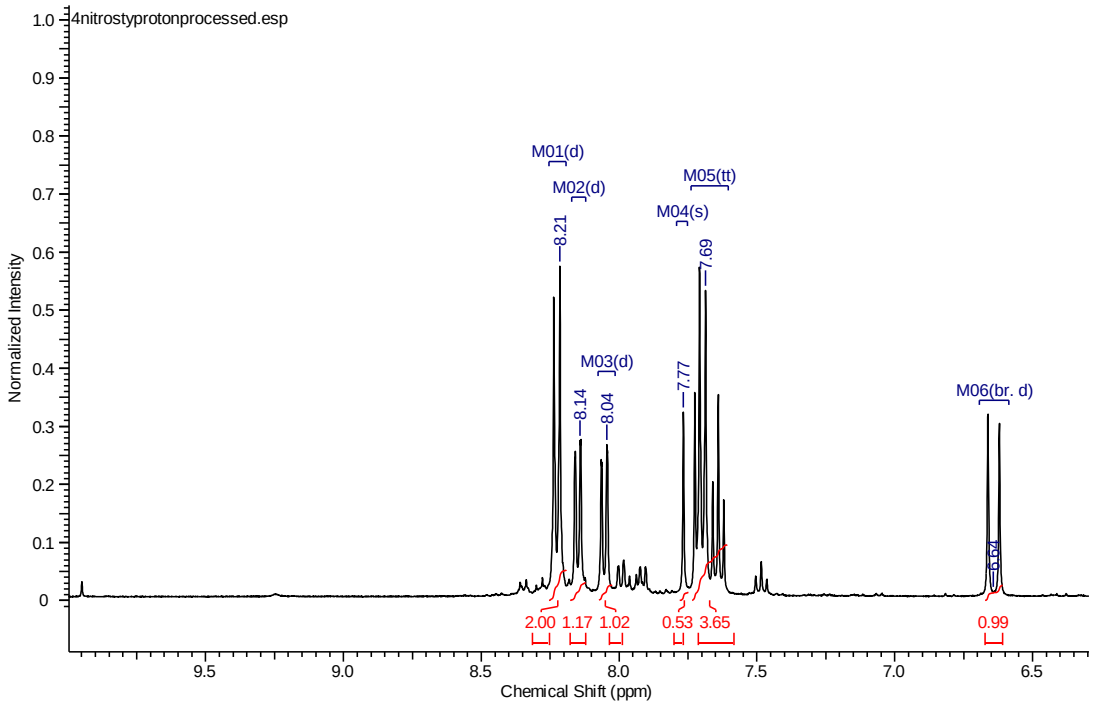

Figure 5.A: 2-[(E)-2-(4-nitrophenyl)ethenyl]-3-nitrobenzoic acid (5a)

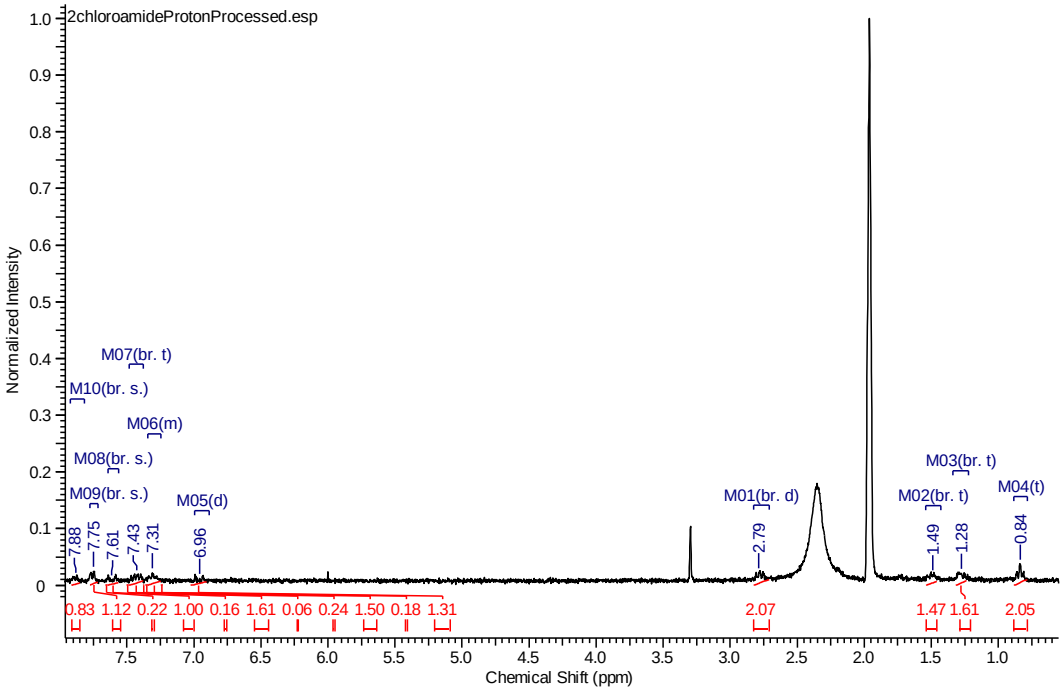

Figure 6.A: 2-(2-chlorostyryl)-N-butyl-3-nitrobenzamide (1b)

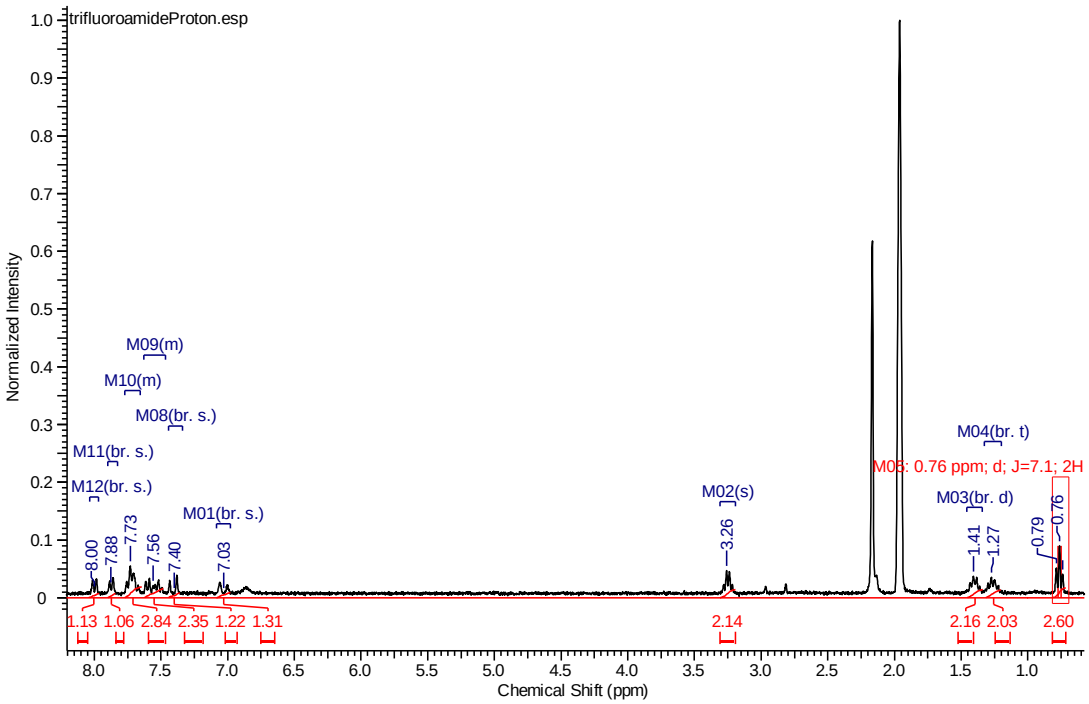

Figure 7.A: 2-(2-(trifluoromethyl)styryl)-N-butyl-3-nitrobenzamide (2b)

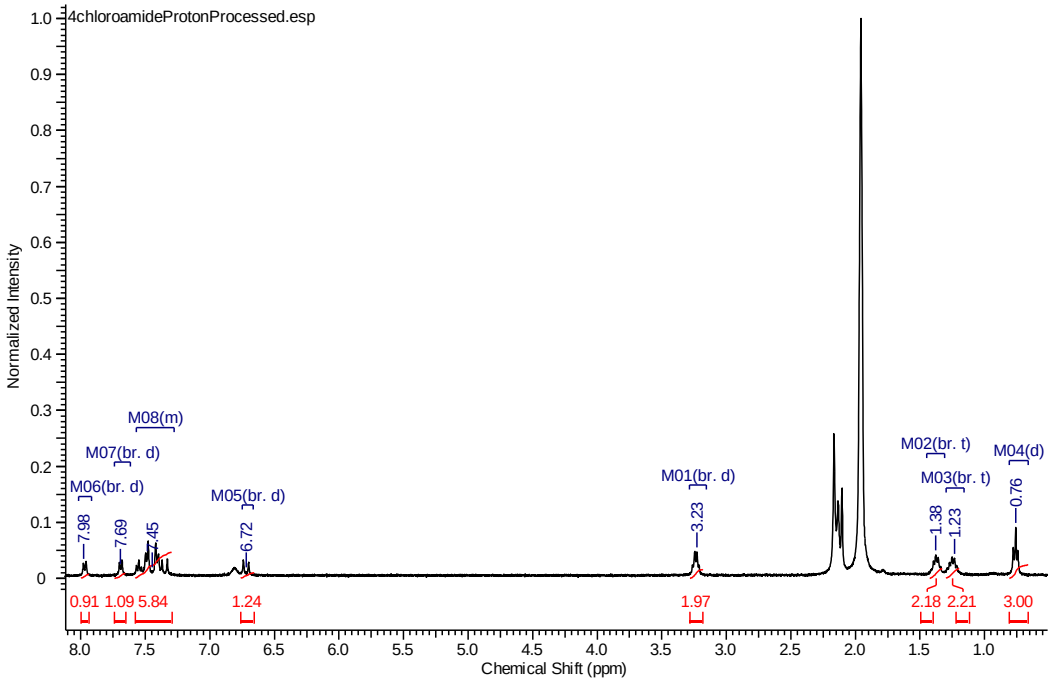

Figure 8.A: 2-(4-chlorostyryl)-N-butyl-3-nitrobenzamide (3b)

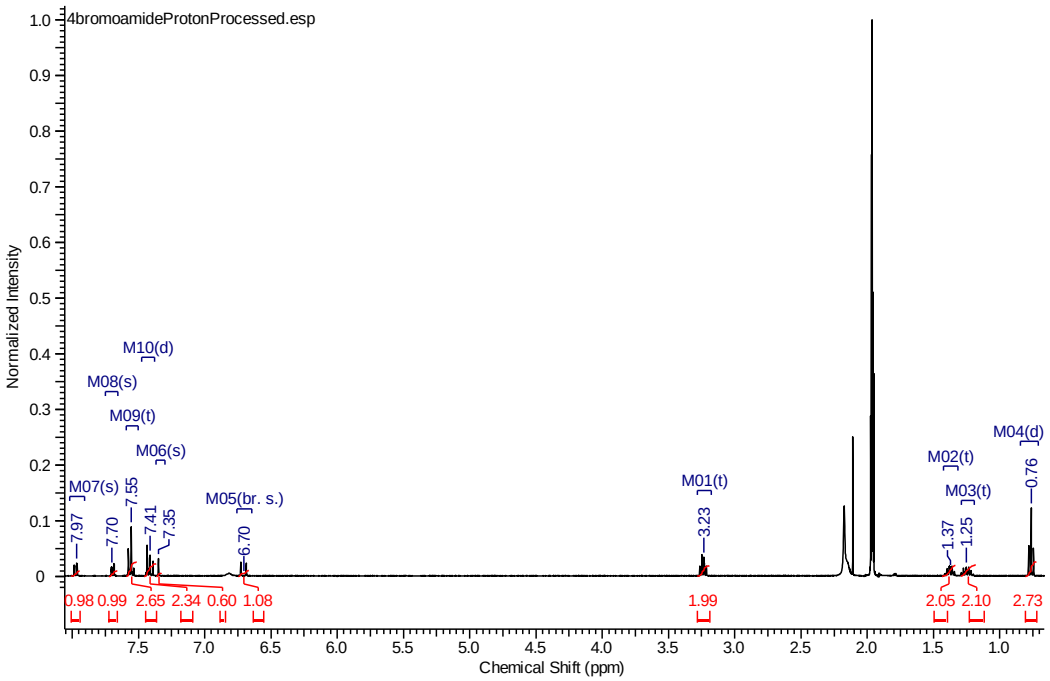

Figure 9.A: 2-(4-bromostyryl)-N-butyl-3-nitrobenzamide (4b)

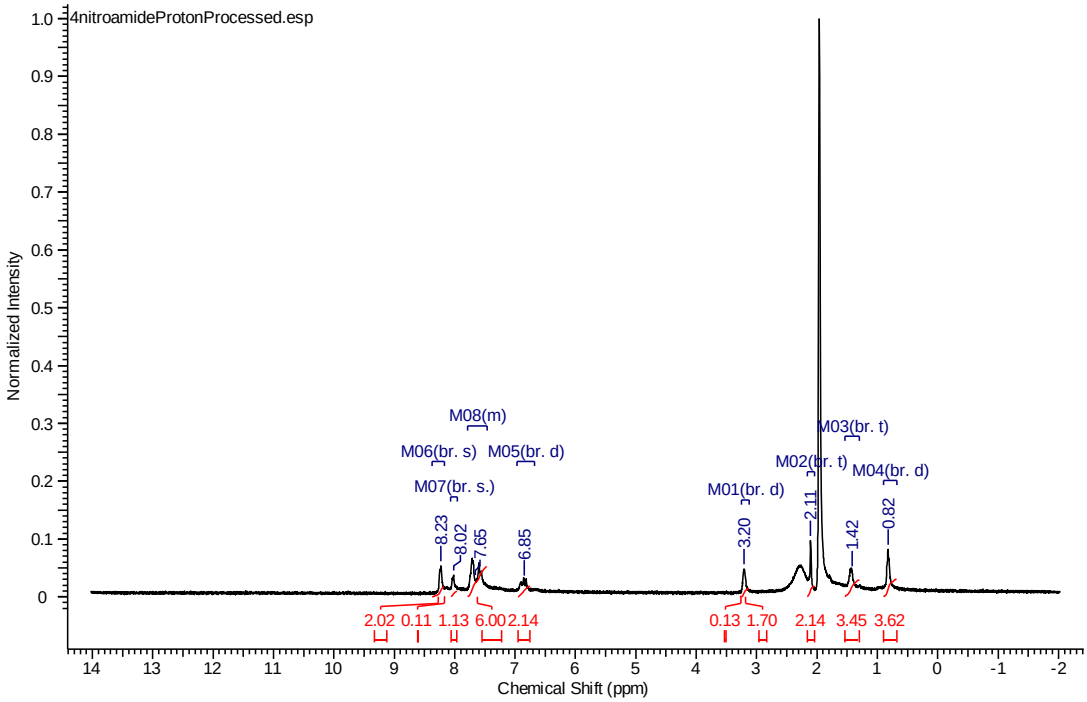

Figure 10.A: 2-(4-nitrostyryl)-N-butyl-3-nitrobenzamide (5b)

Appendix B

^{13}C NMR Spectra

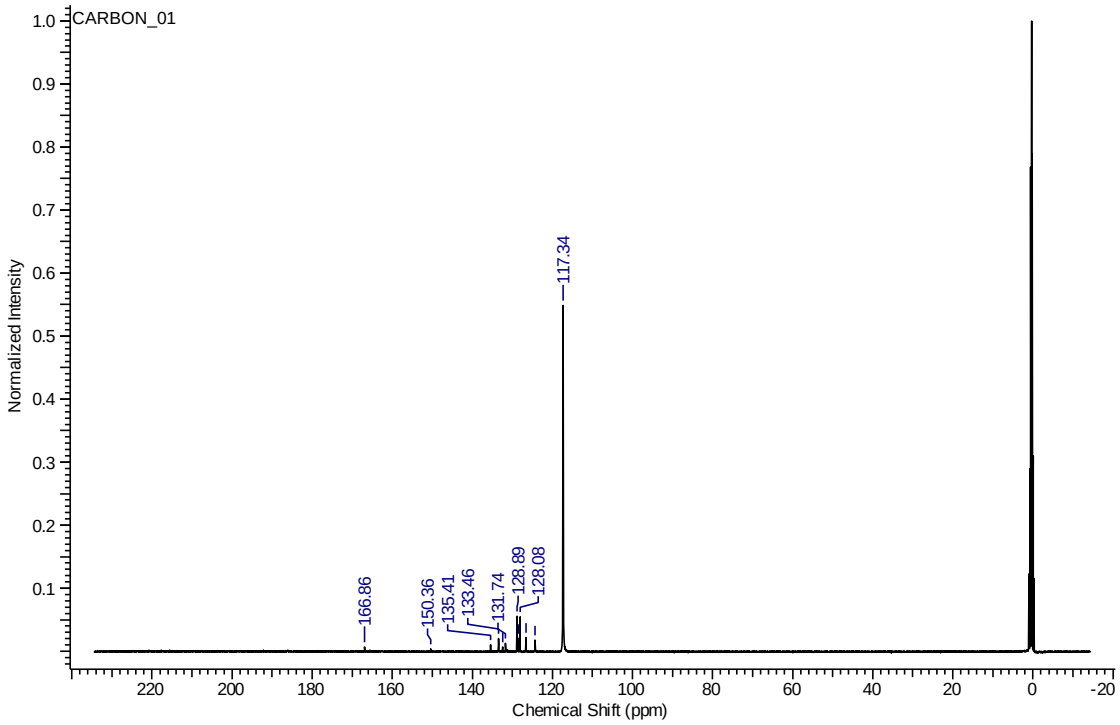

Figure 1.B: 2-[(E)-2-(2-chlorophenyl) ethenyl]-3-nitrobenzoic acid (1a)

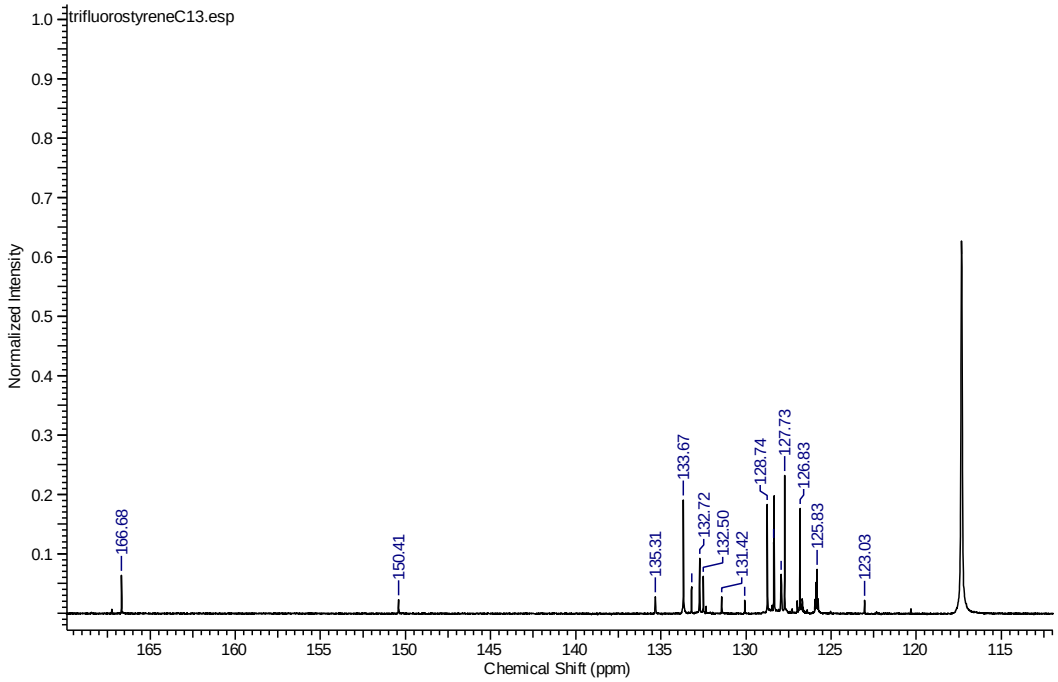

Figure 2.B: 3-nitro-2-{(E)-2-[2-(trifluoromethyl)phenyl]ethenyl} benzoic acid (2a)

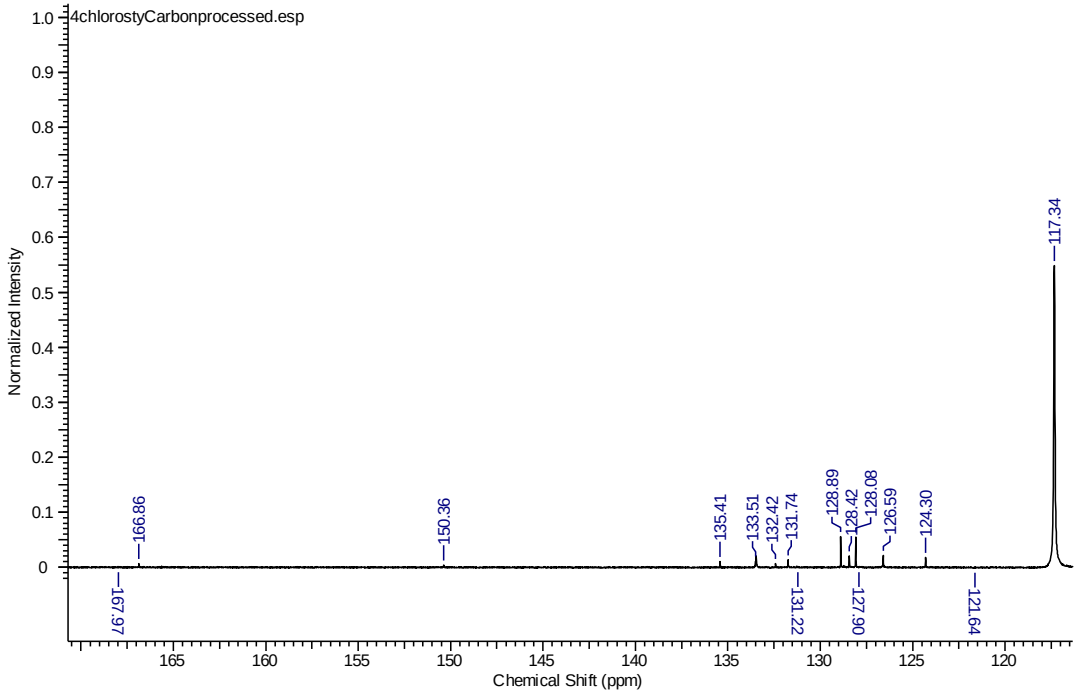

Figure 3.B: 2-[(E)-2-(4-chlorophenyl)ethenyl]-3-nitrobenzoic acid (3a)

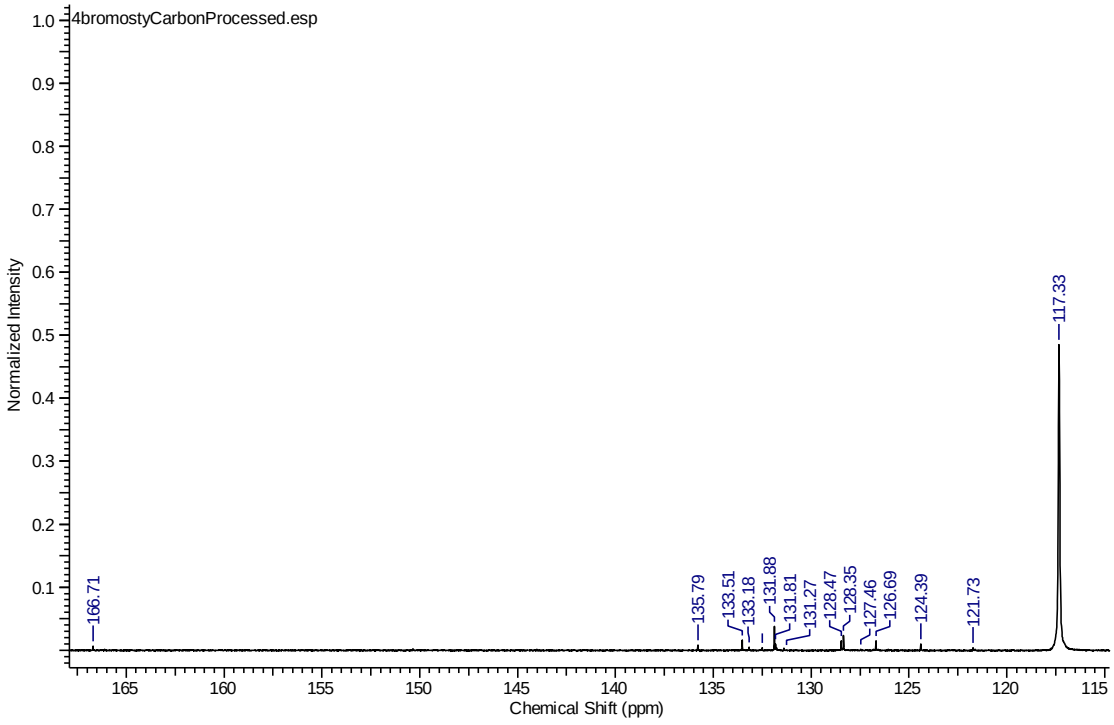

Figure 4.B: 2-[(E)-2-(4-bromophenyl) ethenyl]-3-nitrobenzoic acid (4a)

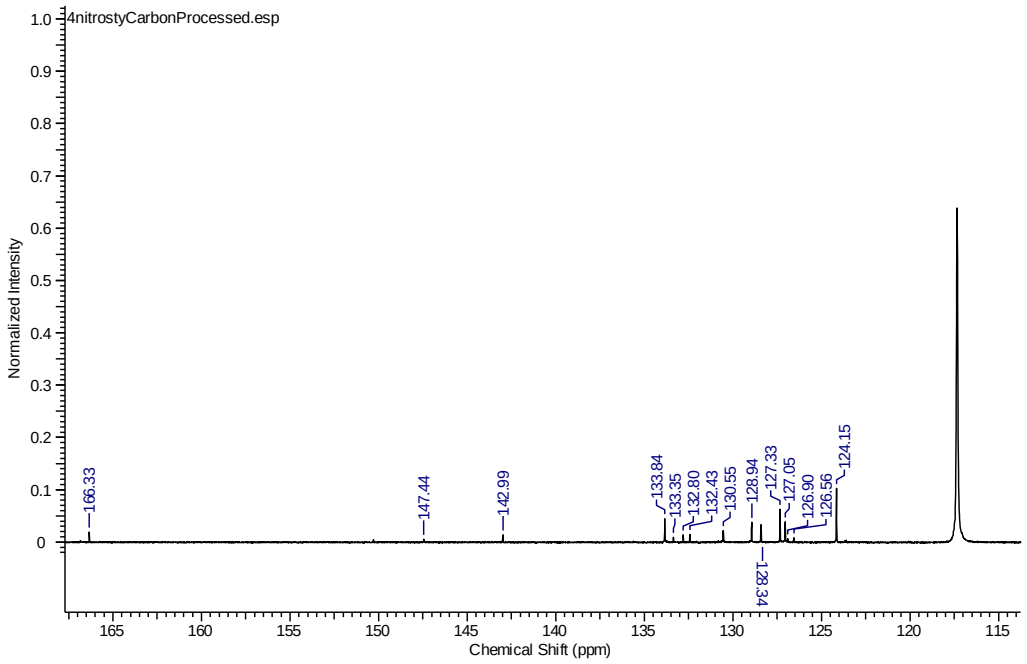

Figure 5.B: 2-[(E)-2-(4-nitrophenyl)ethenyl]-3-nitrobenzoic acid (5a)

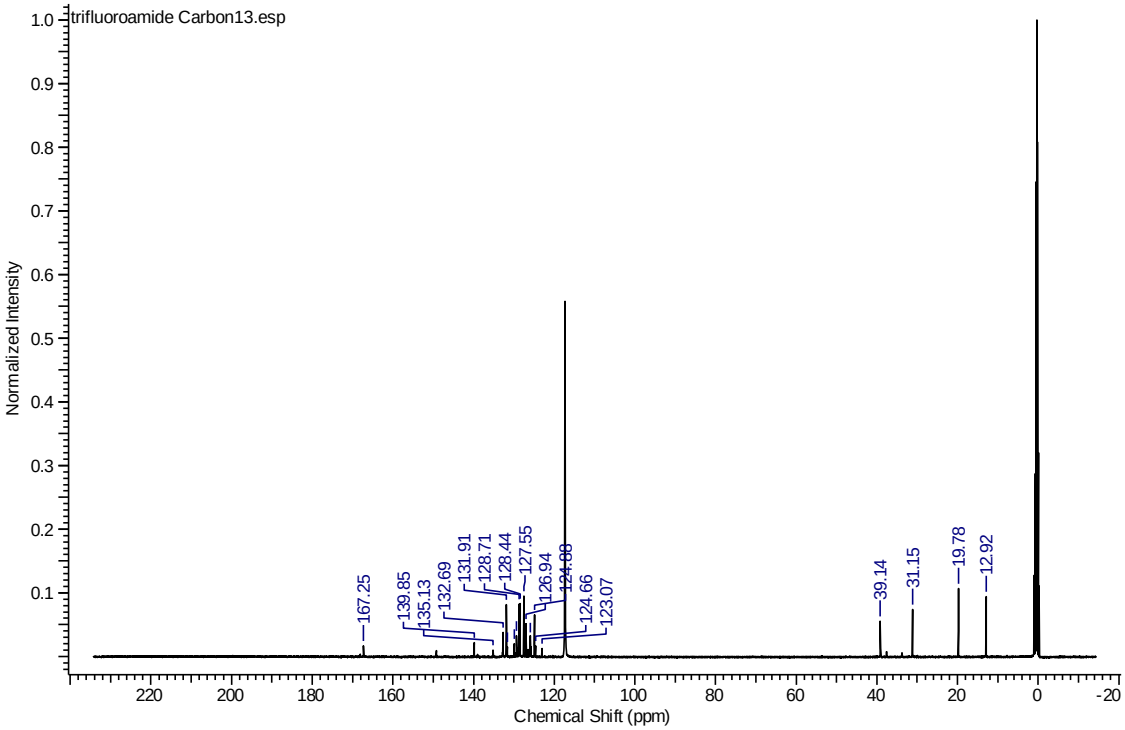

Figure 6.B: 2-(2-(trifluoromethyl)styryl)-N-butyl-3-nitrobenzamide (2b)

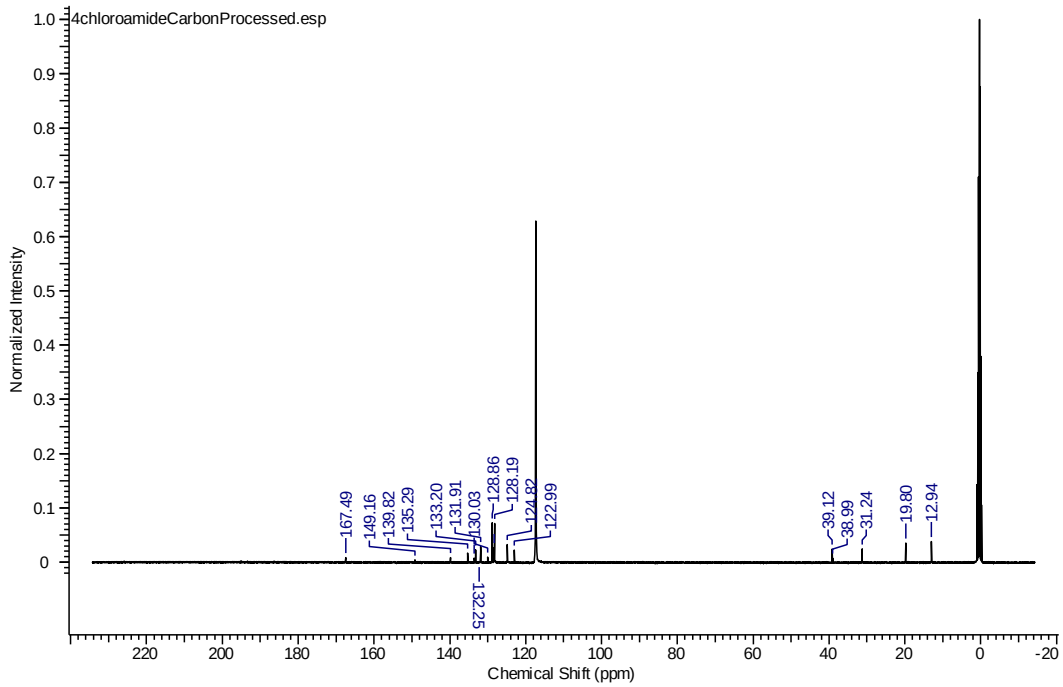

Figure 7.B: 2-(4-chlorostyryl)-N-butyl-3-nitrobenzamide (3b)

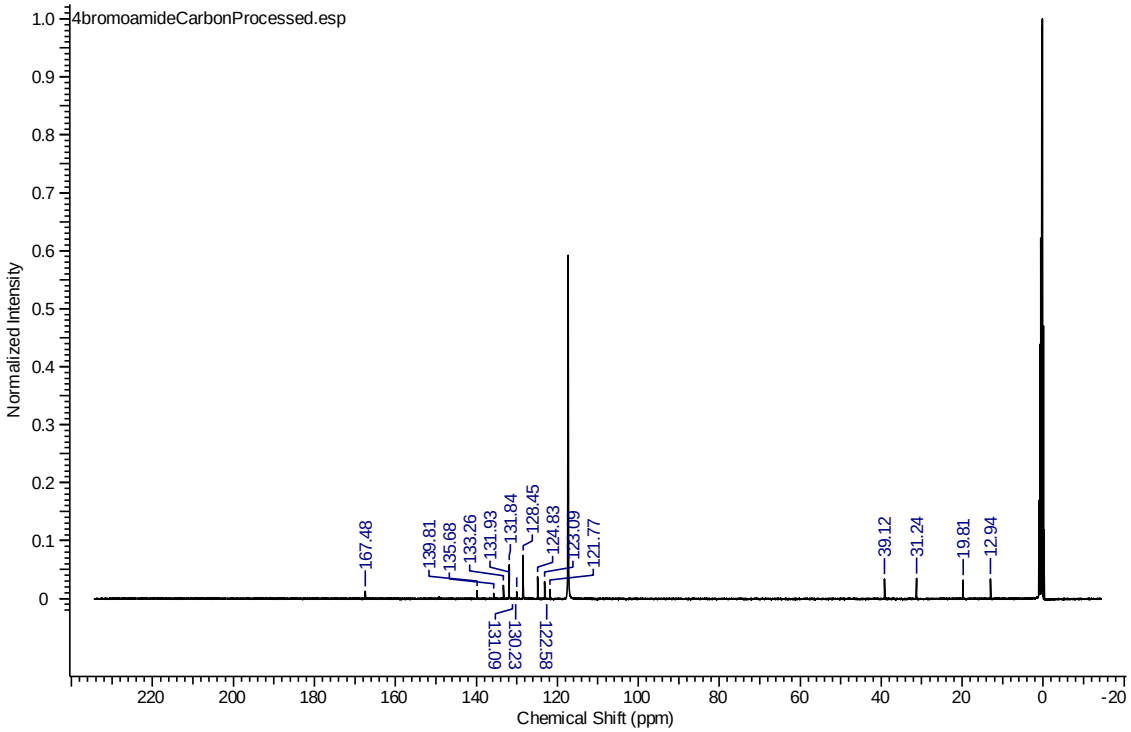

Figure 8.B: 2-(4-bromostyryl)-N-butyl-3-nitrobenzamide (4b)

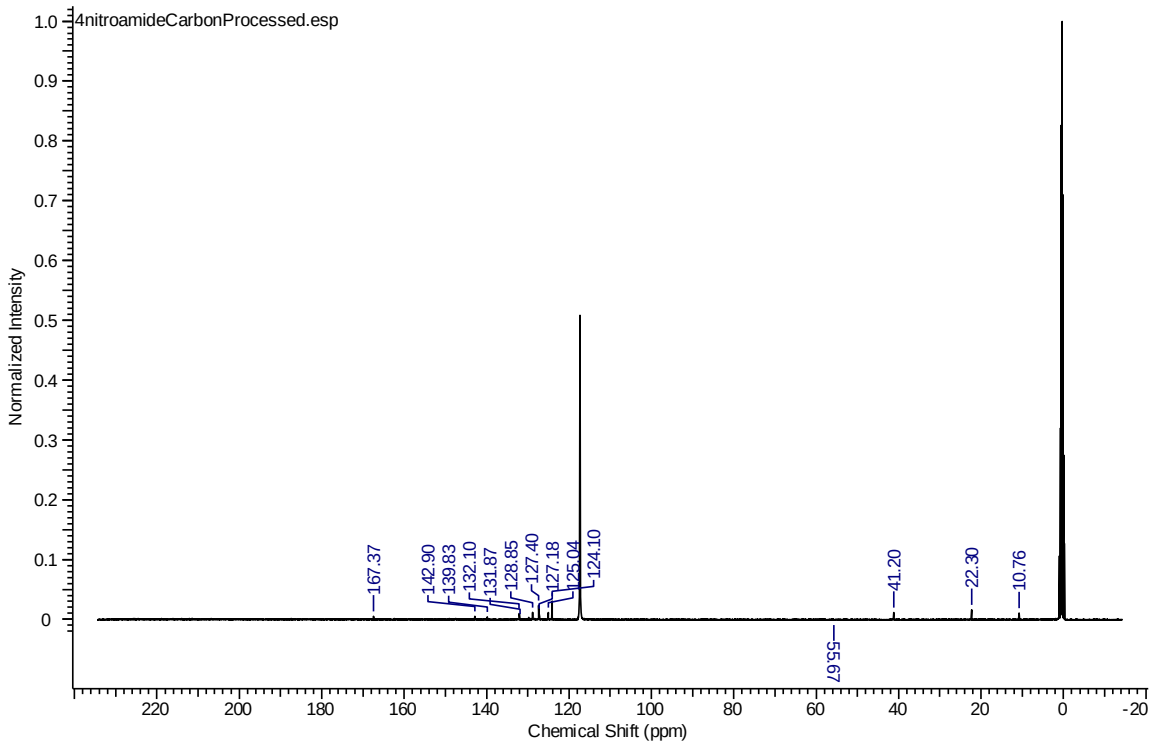

Figure 9.B: 2-(4-nitrostyryl)-N-butyl-3-nitrobenzamide (5b)

Appendix C

FT-IR Spectra

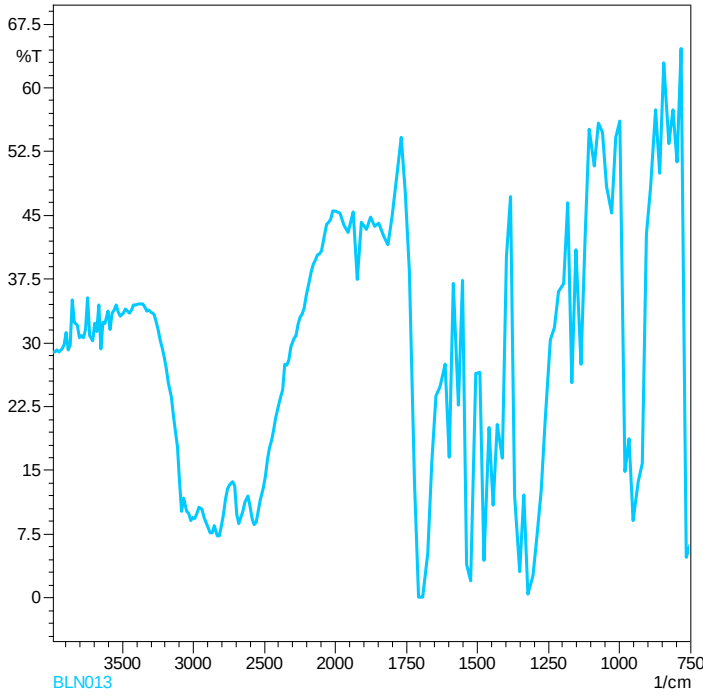

Figure 1.C: 2-[(E)-2-(2-chlorophenyl) ethenyl]-3-nitrobenzoic acid (1a)

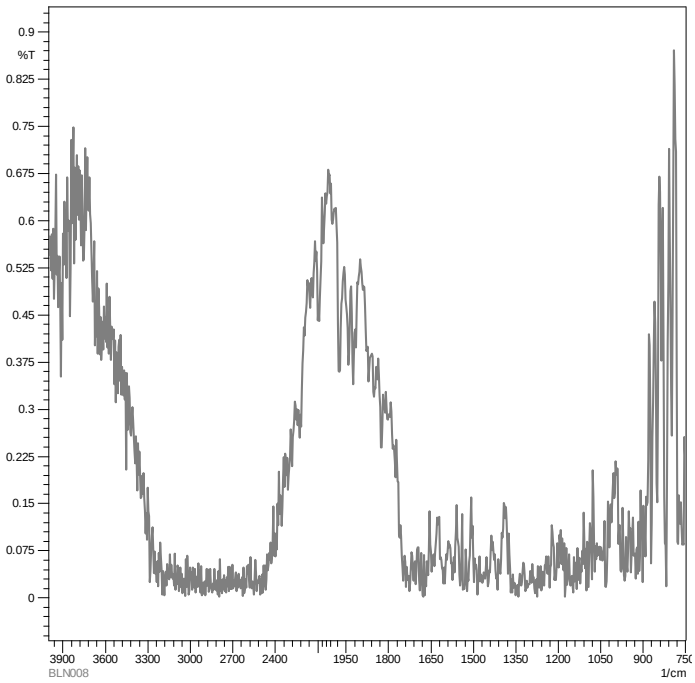

Figure 2.C: 3-nitro-2-{(E)-2-[2-(trifluoromethyl)phenyl]ethenyl} benzoic acid (2a)

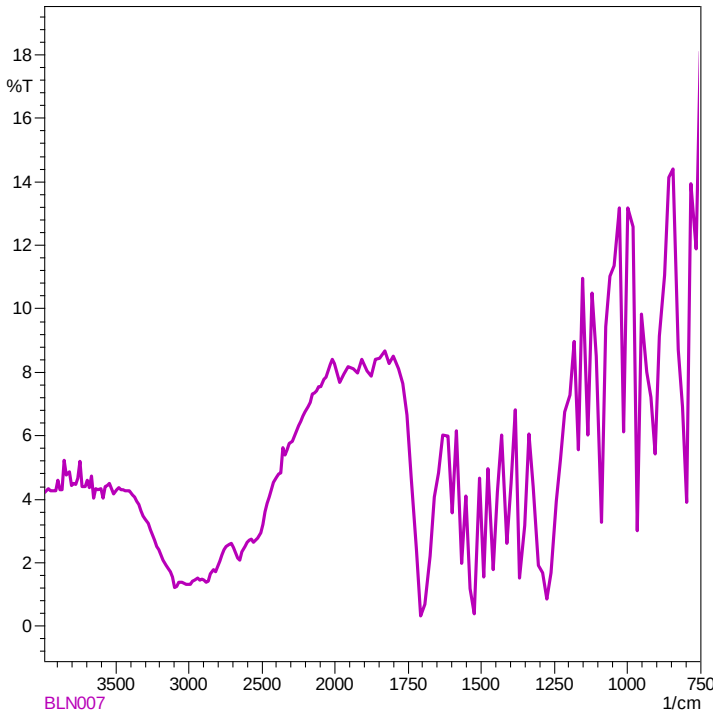

Figure 3.C: 2-[(E)-2-(4-chlorophenyl)ethenyl]-3-nitrobenzoic acid (3a)

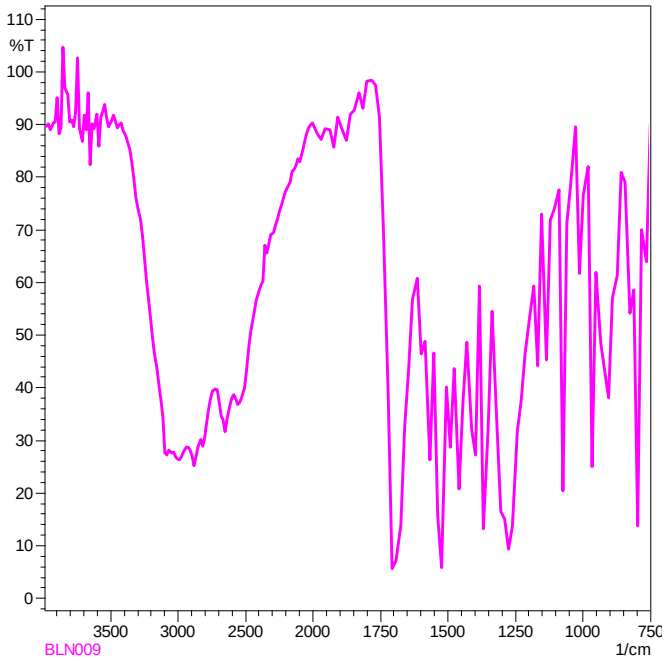

Figure 4.C: 2-[(E)-2-(4-bromophenyl) ethenyl]-3-nitrobenzoic acid (4a)

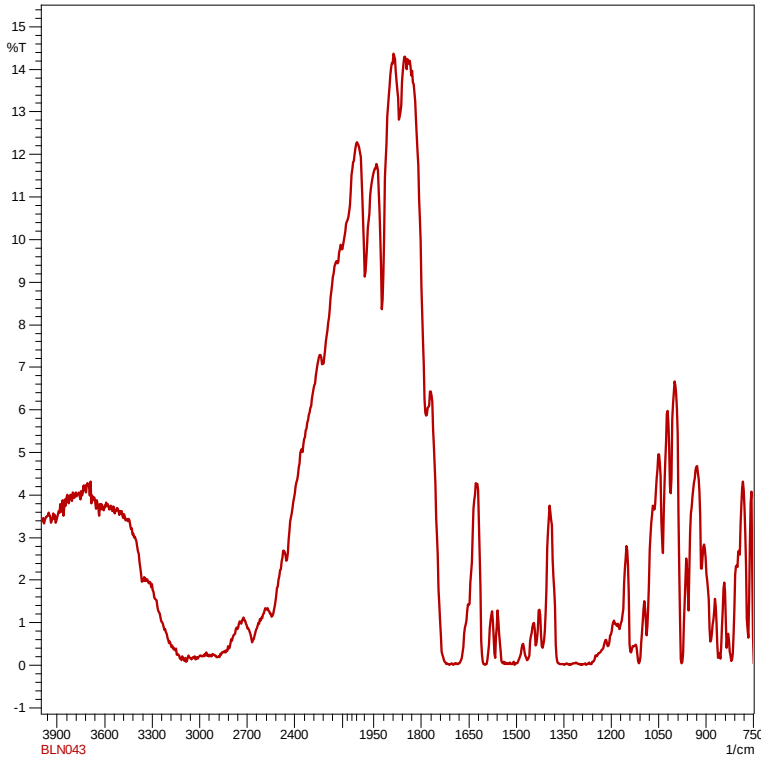

Figure 5.C: 2-[(E)-2-(4-nitrophenyl)ethenyl]-3-nitrobenzoic acid (5a)

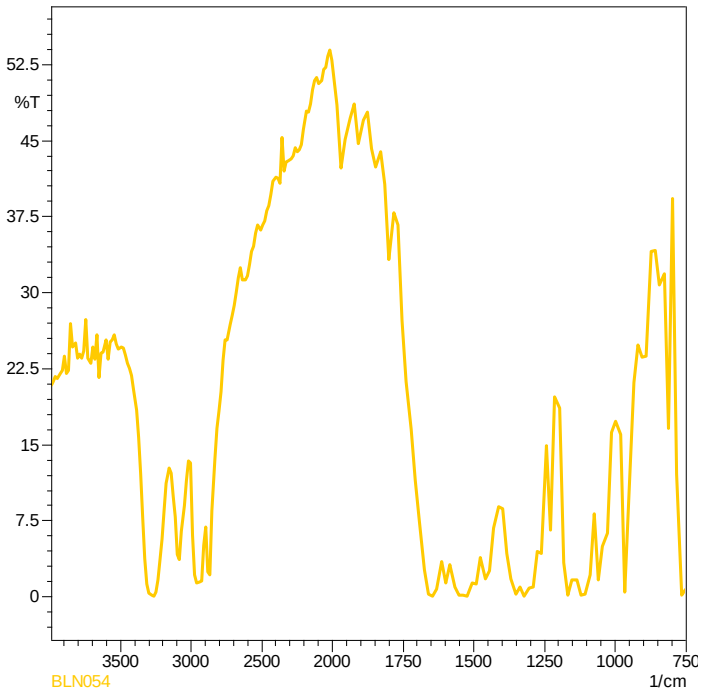

Figure 6.C: 2-(2-(trifluoromethyl)styryl)-N-butyl-3-nitrobenzamide (2b)

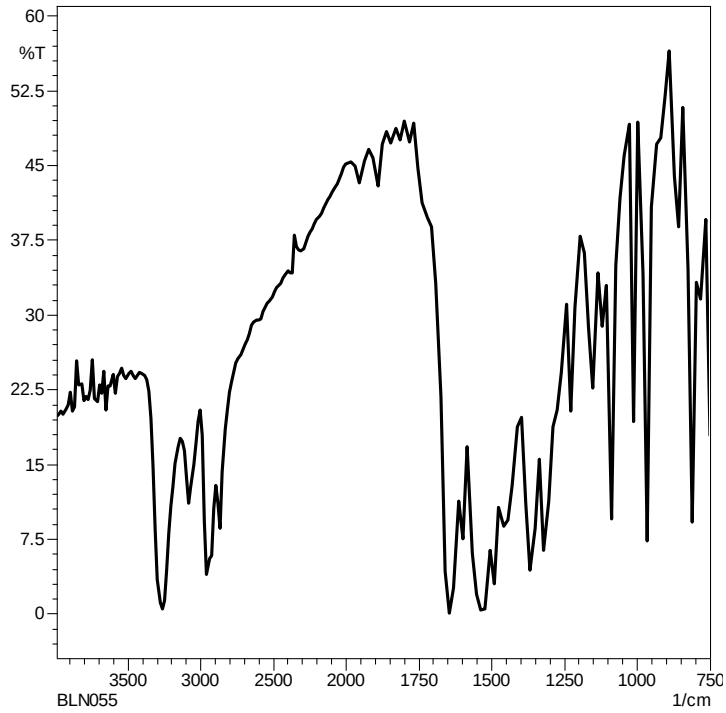

Figure 7.C: 2-(4-chlorostyryl)-N-butyl-3-nitrobenzamide (3b)

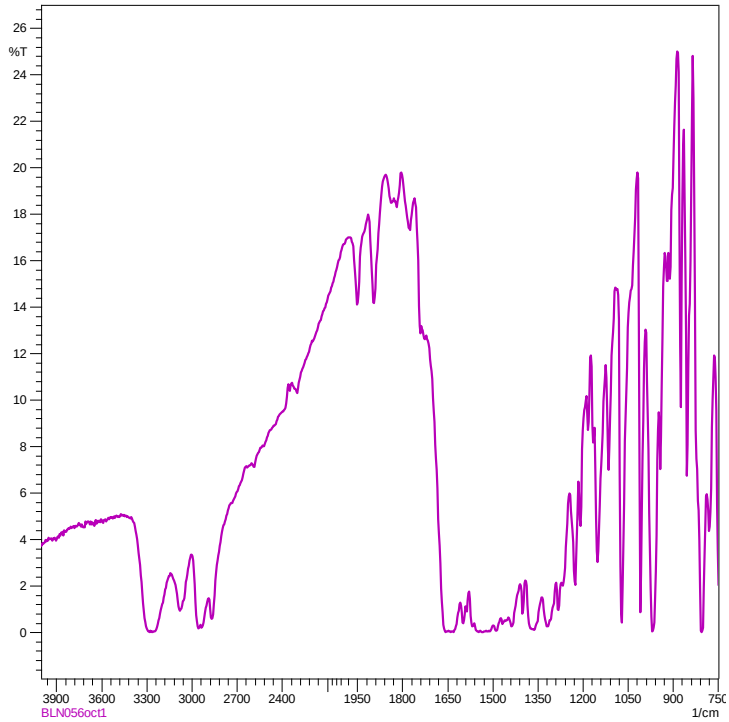

Figure 8.C: 2-(4-bromostyryl)-N-butyl-3-nitrobenzamide (4b)

Appendix D

HPLC Chromatograms

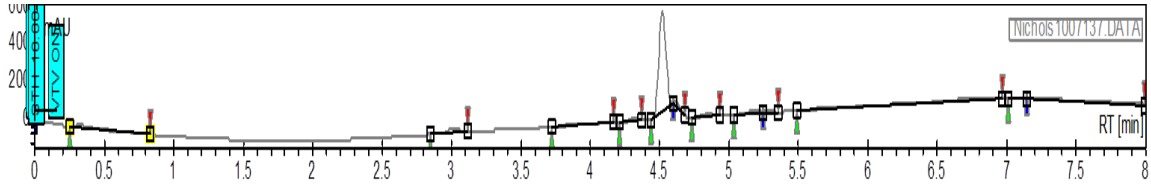

Figure 1.D: 2-[(E)-2-(2-chlorophenyl) ethenyl]-3-nitrobenzoic acid (1a)

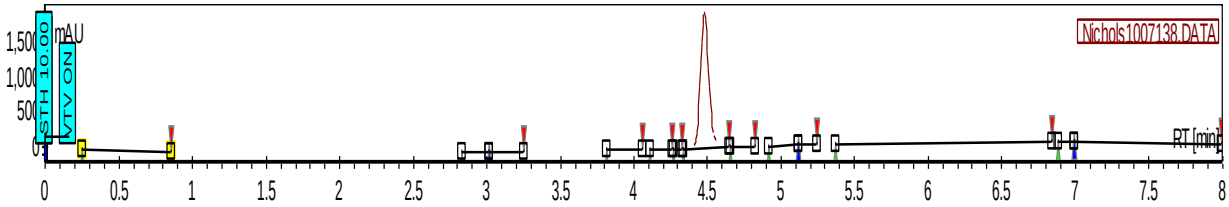

Figure 2.D: 3-nitro-2-{(E)-2-[2-(trifluoromethyl)phenyl]ethenyl} benzoic acid (2a)

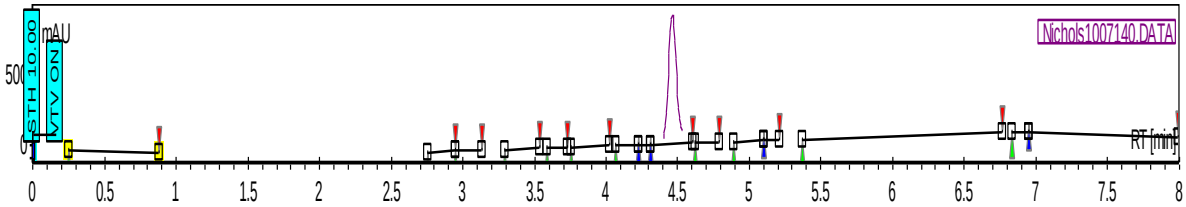

Figure 3.D: 2-[(E)-2-(4-chlorophenyl)ethenyl]-3-nitrobenzoic acid (3a)

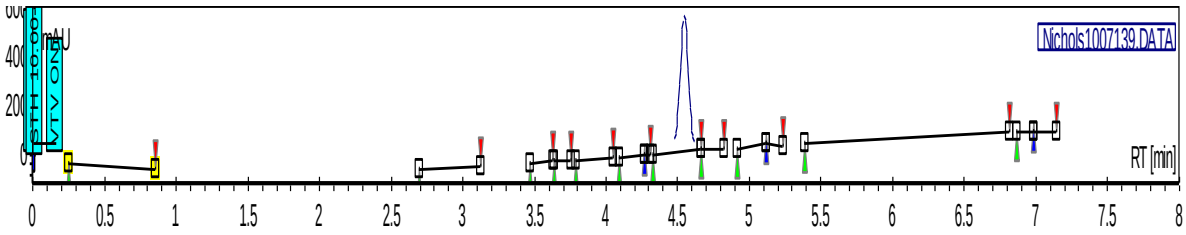

Figure 4.D: 2-[(E)-2-(4-bromophenyl) ethenyl]-3-nitrobenzoic acid (4a)

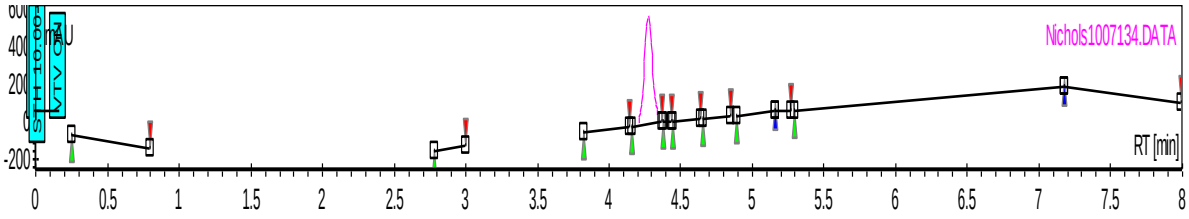

Figure 5.D: 2-[(E)-2-(4-nitrophenyl)ethenyl]-3-nitrobenzoic acid (5a)

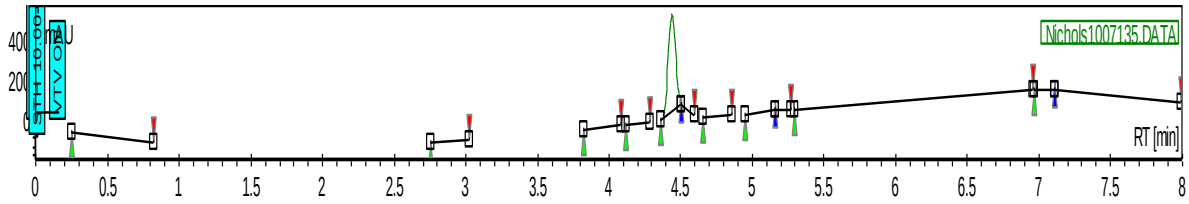

Figure 6.D: 2-(2-chlorostyryl)-N-butyl-3-nitrobenzamide (1b)

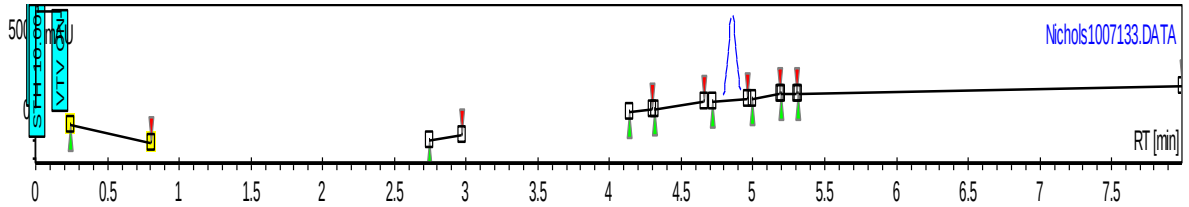

Figure 7.D: 2-(2-(trifluoromethyl)styryl)-N-butyl-3-nitrobenzamide (2b)

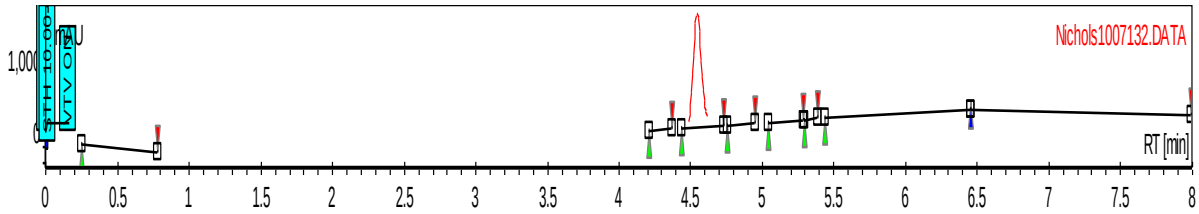

Figure 8.D: 2-(4-chlorostyryl)-N-butyl-3-nitrobenzamide (3b)

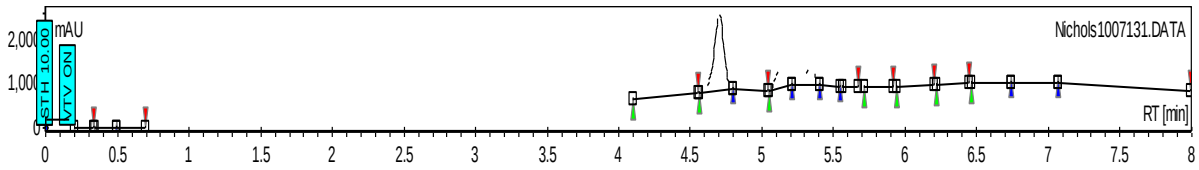

Figure 9.D: 2-(4-bromostyryl)-N-butyl-3-nitrobenzamide (4b)

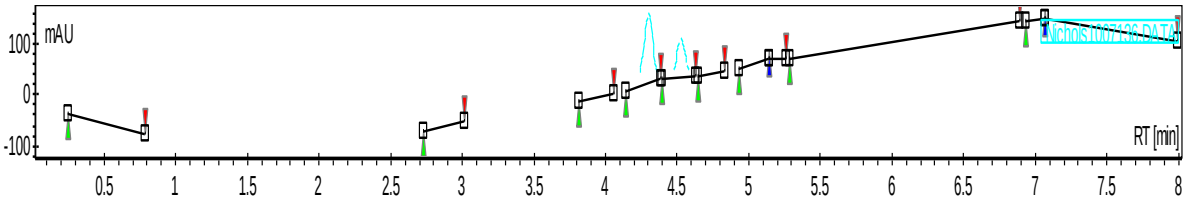

Figure 10.D: 2-(4-nitrostyryl)-N-butyl-3-nitrobenzamide (5b)